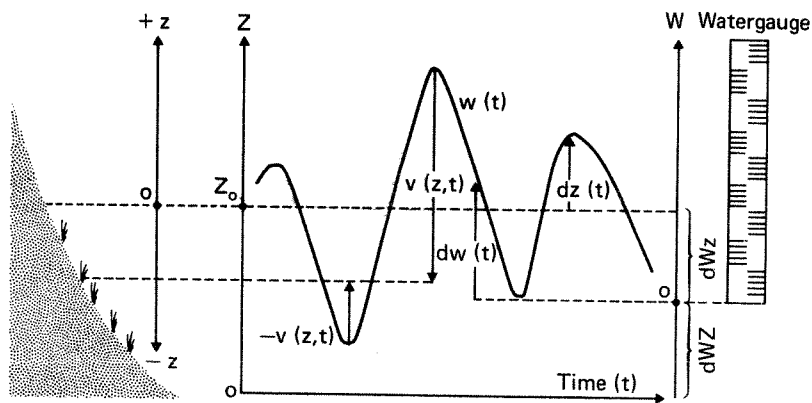OF–8162004

Regulation Impact on Submerged Macrophyte Communities in some Norwegian Lakes

Norwegian Institute for Water Research ⬤ NIVA

NIVA – REPORT

Norwegian Institute for Water Research ⬤ NIVA

Royal Norwegian Council for Scientific and Industrial Research

Report No.:	OF-8162004
Sub-No.:	
Serial No.:	1703
Limited distribution:	

Report title:	Date:
Regulation impact on submerged macrophyte communities in some Norwegian lakes	14.februar 1985
	Project No: OF-8162004

Author(s):	Topic group:
Rørslett, Bjørn	Geographical area:
	Number of pages (incl. app.) 119

Contractor:	Contractors ref. (or NTNF - No):
Norsk institutt for vannforskning	

Abstract:

The main results from a study of submerged macrophyte communities in regulated Norwegian lakes are summarized. Impact assessment is equivalenced to analysis of the vertical niche displacement, due to a fluctuating water level. Vertical niche size is shown to be limited by unfavourable physical environmental factors. Lower niche limits might be controlled by low-light induced mortality, whereas upper niche limits related to the extent of ice-scour. Statistical models of the environmental impact due to water-level fluctuations, and of the apparent underwater light field, are discussed.

4 keywords, Norwegian	4 keywords, English
1.	1. Macrophytes
2.	2. Statistics
3.	3. Impact assessment
4.	4. Regulated lakes

Project leader

For the Administration

Division leader

Norwegian Institute for Water Research   NIVA

OF-8162004

REGULATION IMPACT ON SUBMERGED MACROPHYTE COMMUNITIES IN SOME NORWEGIAN LAKES

TO LIV, ERLEND, AND GRO

‹ CONTENTS ›

The dissertation comprises the following five papers :

I   Rørslett,B.,Green,N.W.,Kvalvågnæs,K. 1978: Underwater stereophoto-
            graphy as a tool in aquatic biology.
            Aquat.Bot. 4: 73-81.

II   Rørslett,B. 1984a: Environmental factors and aquatic macrophyte
            response in regulated lakes - a statistical approach.
            Aquat.Bot. 19: 199-220.

III   Rørslett,B. 1984b: Statistics of the underwater light field.
            (manuscript)

IV   Rørslett,B. 1985a: Death of submerged macrophytes - actual field
            observations and some implications.
            Aquat.Bot. (in press)

V   Rørslett,B. 1985b: Regulation impact on submerged macrophytes
            in the oligotrophic lakes of Setesdal, South Norway.
            Verh.Int.Verein.Limnol. 22 (in press)

These papers are referred to by their Roman numerals (I-V) in the
text.

The dissertation papers (I-V) are presented in a separate appendix.

1 INTRODUCTION

The aims of the present study can be summarized as follows :

A) Develop sampling methods suitable for quantitative studies on submerged aquatic communities.

B) Establish a theoretical framework to assess lake regulation impact on niche size and spatial position by statistical methods.

C) Relate the response of the macrophytes to regulation-induced niche changes.

Some sixty percent of Norway's hydro-electric power potential has been developed so far (STATISTISK SENTRALBYRÅ 1983:12). On an area basis, lake regulations influence a major part of Scandinavian lakes. The regulation height of Norwegian reservoirs is commonly less than 10m. An estimated 23% is regulated less than 5m and some 22% is regulated 5-9.9m (STATISTISK SENTRALBYRÅ 1983:27).

There is a truly remarkable paucity of data on submerged macrophytes in regulated Scandinavian lakes. RØRSLETT (1980, V) summarized the scant data available. The true shore vegetation in regulated lakes is far better documentated (WASSEN 1966, NICKLASSON 1979, NILSSON 1981).

Based on qualitative field data only, BRAARUD (1928) reported negligible regulation impact on _Isoëtes lacustris_-dominated communities in the Norwegian lake Hurdalssjø (mean annual water-level range 3.6m, total range 5.3m). QUENNERSTEDT (1958) related changes in the vertical distribution of e.g. _Isoëtes lacustris_ to the annual water-level range in North Swedish lakes and reservoirs. An interesting case was the lake Gardiken, then unregulated, but with a wide natural water-level fluctuation of some 4m annually (5.7m annual maximum). This lake harboured some _Isoëtes lacustris_, allegedly with reduced performance and restricted vertical extension. NILSSON (1981) investigated the dynamics of littoral species in the subsequently regulated Gardiken (a substantial 20m nominal regulation height), and found no traces of the former submerged communities. Submergents survived, however, in the upstream located lake Övra Björkvattnet with a 5.9m nominal regulation height.

According to QUENNERSTEDT (1958), increasing the extent of regulation would eventually decrease the vertical distribution of e.g. isoetid species. The isoetid communities are the prevailing benthic primary producers in the mainly oligotrophic Scandinavian lakes (LOHAMMAR 1965, BRETTUM 1971, SAND-JENSEN 1978). Thus, any changes in isoetid performance due to regulation impact might have negative ecological implications.

The regulation impact affects the niche space of the species inhabiting the lake floors, resulting in structural and dynamic changes in the vegetation (cf. Fig.1 below).
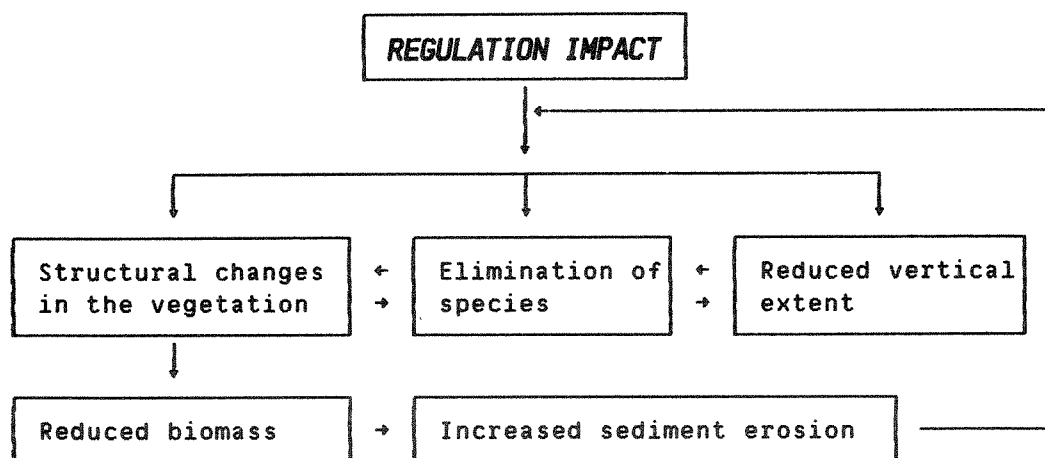

Fig. 1. The impact of a fluctuating water level invokes primarily the physical dimensions of the vegetation niche space, adversely affecting the dynamics and performance of the submerged communities. Increased sediment erosion from a declining vegetation coverage initiates a positive feed-back loop, thus enhancing the deterioration of macrophyte communities.

Quantitative assessment of regulation-induced impact on submerged macrophyte communities is impaired by the paucity and generally low spatial resolution of the currently available data. Hence, I initiated a research program directly addressing the spatial niche of the prevailing macrophytes in regulated, Norwegian lakes and reservoirs. The flow-chart for the response analysis in the niche space domain is outlined on Fig.2.
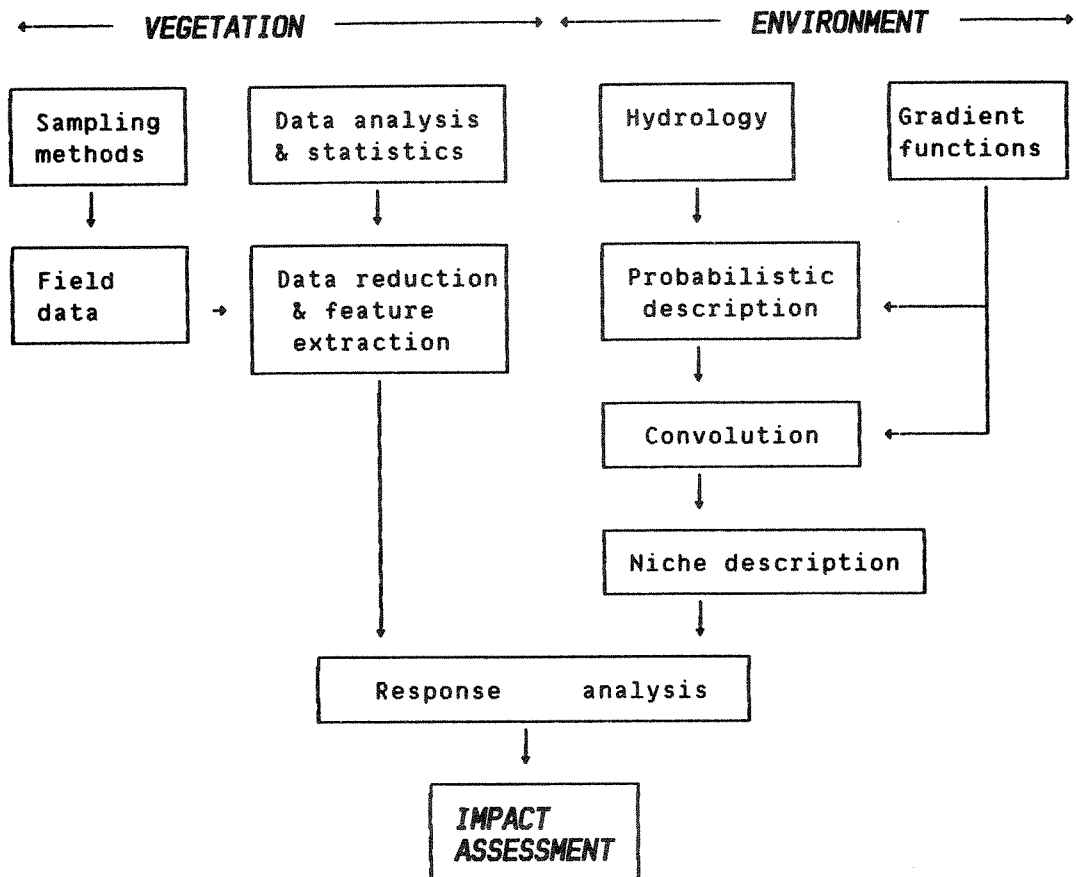
<----- **VEGETATION** -----> <----- **ENVIRONMENT** ----->

```
┌──────────┐    ┌──────────────┐    ┌──────────────┐    ┌──────────────┐
│ Sampling │    │Data analysis │    │  Hydrology   │    │  Gradient    │
│ methods  │    │& statistics  │    │              │    │  functions   │
└────┬─────┘    └──────┬───────┘    └──────┬───────┘    └──────┬───────┘
     │                 │                   │                   │
     ▼                 ▼                   ▼                   │
┌──────────┐    ┌──────────────┐    ┌──────────────┐          │
│ Field    │    │Data reduction│    │Probabilistic │◄─────────┤
│ data     │ →  │& feature     │    │description   │          │
│          │    │extraction    │    └──────┬───────┘          │
└──────────┘    └──────┬───────┘           │                  │
                       │             ┌──────────────┐          │
                       │             │ Convolution  │◄─────────┘
                       │             └──────┬───────┘
                       │                    │
                       │             ┌──────────────┐
                       │             │Niche descrip-│
                       │             │tion          │
                       │             └──────┬───────┘
                       │                    │
              ┌────────┴────────────────────┴──────┐
              │  Response      analysis            │
              └────────────────┬───────────────────┘
                               │
                      ┌────────────────┐
                      │ IMPACT         │
                      │ ASSESSMENT     │
                      └────────────────┘
```

Fig. 2. Conceptual framework for quantitative assessment of regulation impact on submerged macrophyte communites. The response analysis is in the niche space domain.

The research program addresses the factors influencing the niche space of the submerged macrophytes. To this end, I deliberately focused on the spatial description of the submerged communities, more than on the species within the communities. The selected approach to community description also is highly unsophisticated; thus I consider the community as no more than the observed species array within a small area of the lake floor. Hence, the 'community' term carries no phytosociological implications whatsoever.

2 STUDIED LAKES AND THEIR VEGETATION

During the years 1976-1982, I collected a substantial data base on the
vegetation, hydrology, morphometry, and hydrochemistry, of several
Norwegian lakes. Partially, this data base arose from various contract
works conducted by the Norwegian Institute for Water Research (NIVA,
Oslo). Lake descriptions and preliminary results are mainly published
in contract reports, hence it would be appropriate to shortly review
the main features of these lakes and their vegetatation here.

Initially, the data base encompassed 16 lakes. These lakes are listed
in Tab. 1 and their geographical location is indicated on Fig. 3
below. These lakes span a wide range of areas, altitudes, and nominal
extent of regulation. They are mainly clear-water, oligotrophic lakes.
One mesotrophic lake, Steinsfjord, deviates from the other lakes,
mainly due to a massive expansion of _Elodea canadensis_ (RØRSLETT _et
al._, 1984). Data from subsets of the data base are used in the
dissertation papers (II, III, IV, V). These subsets included only
lakes with available hydrological data, and where the vegetation data
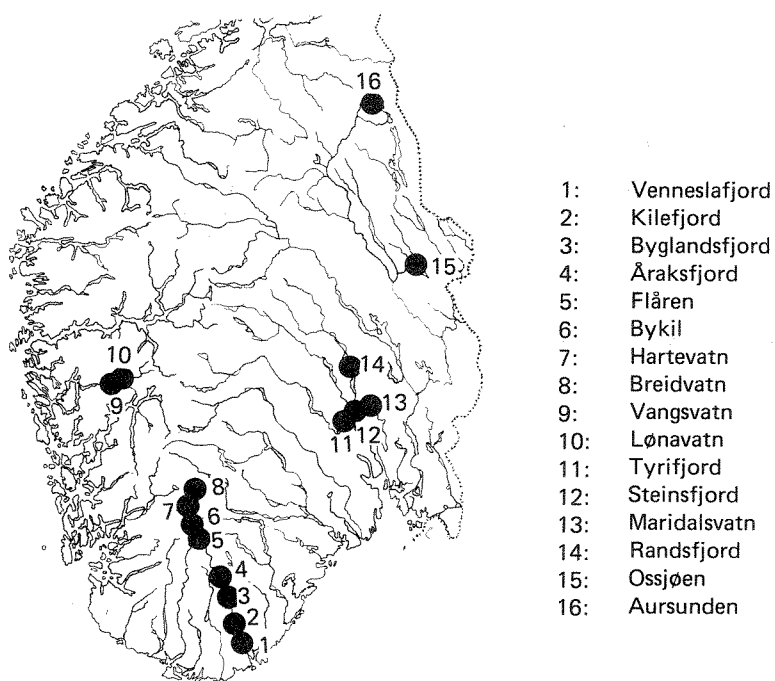were obtained by quantitative methods.

1:	Venneslafjord
2:	Kilefjord
3:	Byglandsfjord
4:	Åraksfjord
5:	Flåren
6:	Bykil
7:	Hartevatn
8:	Breidvatn
9:	Vangsvatn
10:	Lønavatn
11:	Tyrifjord
12:	Steinsfjord
13:	Maridalsvatn
14:	Randsfjord
15:	Ossjøen
16:	Aursunden

Fig. 3.   Geographical location of the investigated lakes
in Southern Norway.

Tab. 1.   Investigated lakes. Morphometric and hydrological
           data.

Lake	Alti-tude (m)	Area (km^2)	Lake type *	Regulation height ** (m)	Water-level range Annual mean (m)	max. (m)	Total *** (m)
Venneslafjord	38	1.7	UR	-	1.0		>1.0
Vangsvatn	46	8.0	UR	-	4.5	6.3	6.6
Tyrifjord	63	121.9	ST	1.0	2.0	2.9	3.5
Steinsfjord	63	13.9	ST	1.0	2.0	2.9	3.5
Lønavatn	77	3.0	UR	-	1.5		>2.0
Randsfjord	134	136.9	ST	3.0	2.9	3.9	4.2
Maridalsvatn	148	3.9	DW	2.0	1.1	1.3	1.6
Kilefjord	167	5.5	DR	1.5	2.0	2.9	3.2
Byglandsfjord	202	30.7	ST	5.0	3.6	4.9	5.9
Åraksfjord	203	11.2	ST	5.0	3.5	4.9	5.0
Flåren	274	1.4	WB	-	1.5		>1.5
Ossjø	435	45.2	ST	6.6	5.9	6.6	6.6
Bykil	500	1.0	DR	2.0	<1.0		<1.0
Aursunden	689	44.0	ST	5.9	5.5	6.1	6.1
Hartevatn	757	6.0	ST	7.0	6.4	7.3	7.8
Breidvatn	897	3.1	ST	2.5	3.0	3.5	3.5

*) Reservoir/lake types:
   UR= nominally unregulated   DR= damping reservoir
   ST= storage reservoir   WB= weir basin
   DW= drinking water reservoir

**) Nominal regulation height as licensed by Norwegian authorities

***) Total within-lake range for all years 1945-1982

Tab. 2. Optical and hydrochemical data from the investigated lakes.

LAKE	k_{PAR} m^{-1}	Secchi depth m	pH	Conductivity mS m^{-1}	HCO$_3$ meq m^{-3}	P mg m^{-3}	N mg m^{-3}
Venneslafjord	0.36	8-10	5.2-5.8	1.1-2.2	80	6	180
Vangsvatn	0.46	5-9	5.9-6.5	0.9-2.1		9	180
Lønavatn	-	5-9	5.9-6.5	0.9-1.7		6	170
Tyrifjord	0.53	5-10	7.0	3.2	180	7	400
Steinsfjord	0.58	2-7	8.4	9.0	610	11	250
Randsfjord	0.54	4-9	7.0	3.8		5	450
Maridalsvatn	0.46	5-8	6.8	2.8	85	5	410
Kilefjord	0.35	9-12	5.2-5.8	1.1-1.7	45	7	190
Byglandsfjord	0.34	9-21	5.8-6.0	1.0-1.2	40	2	130
Åraksfjord	0.32	9-23	5.8-6.1	1.0-1.1	40	<2	140
Flåren	0.60	>4	5.7-6.3	1.1-2.8	50	5	150
Ossjøen	0.80	3-7	6.3	1.9	90	7	280
Bykil	0.37	9-12	5.6-6.3	0.9-1.4	40	4	140
Aursunden	0.45	6-10	7.25	3.3	320	5	250
Hartevatn	0.46	7-13	6.0-6.4	0.9-1.3	70	4	120
Breidvatn	0.29	10-18	6.2-6.6	0.9-1.1	70	3	140

Comments: Compiled from data obtained by the Norwegian Institute for Water Research (NIVA) from 1976 to 1982. Data from central lake sites.

k_{PAR} Estimated by averaging over all observations and depths for each site, using best-fit models as advocated in (III). Lake Steinsfjord value dropped to 0.54 when data from 1983-84 were included.

Secchi: Observed range given
depth

Others: Observed range given for small data series, otherwise median values.

The vegetation data were acquired along two different lines of approach.

The species present in a lake were assessed mainly by examination of drift material in near-shore areas, and floristic inventory of a 200m shore-line, at one to a maximum of twelve sites in each lake. A representative range of sites was selected, spanning from strongly exposed habitats to sheltered bays. Special attention was paid to the in- and outflow areas in larger lakes.

The quantitative distribution of vegetation in the vertical gradient was studied by means of underwater stereophotography (I). A quadrat size of $0.25m^2$ was used throughout. At any site, photographic sampling was depth-stratified random, and the vertical sampling density exceeded the pre-assigned minimum of 20 samples m^{-1} within the vegetated zone, whenever possible. Often a far higher sampling density was employed, up to a maximum of ~ 100 samples m^{-1}.

The site locations were pre-assigned before field work commenced, by a table of random numbers used as site coordinates. Once a set of potential sites were drawn, a stratified subset of sites spanning the exposure gradient was selected. This scheme could be followed only for the larger lakes, however. Cost expenditure and the need for access by road prevented the realization of a truly stratified random sampling scheme for all lakes in the Setesdal valley.

The observed species are listed in Tab. 3. The helophytes in general have negligible occurrence, and are not given in the table. Major helophytes are _Equisetum fluviatile_, _Carex rostrata_ (Otra lakes), while other _Carex_ species, e.g. _C. acuta_, and _C. aquatilis_, prevail in the Southeastern lakes. Tall helophytes, e.g. _Phragmites australis_, are confined to lake Steinsfjord.

The isoetids total 13 species. Six major species are present in nearly all lakes, viz. _Eleocharis acicularis_, _Isoëtes echinospora_, _Isoëtes lacustris_, _Juncus bulbosus_, _Ranunculus reptans_, and _Subularia aquatica_.

The total number of species per lake ranged from 10 to 37, while the number of permantly submerged species in each lake ranged from 0 to 29 (Tab. 3).

Tab. 3. Aquatic species found in the investigated lakes.
'o' = not permanently submerged
'●' = also found below lowest water level

Isoetids

Species/lake no.	1	2	3	4	5	6	7	8	9	10	11	12	13	14	15	16
Alopecurus aequalis	-	o	o	o	o	o	o	-	-	o	-	o	-	o	-	-
Crassula aquatica	-	o	o	o	o	o	-	-	-	-	-	-	-	-	-	-
Elatine hydropiper	-	-	-	o	o	o	-	-	-	-	-	-	-	-	-	-
Eleocharis acicularis	●	●	●	●	●	●	●	●	o	o	●	o	o	o	o	●
Isoetes echinospora	●	●	●	●	●	●	●	●	●	●	●	o	o	o	o	●
Isoetes lacustris	●	●	●	●	●	●	●	●	●	●	●	-	●	●	-	●
Juncus bulbosus	●	●	●	o	o	o	●	●	●	●	●	o	●	o	o	o
Limosella aquatica	-	o	o	o	o	o	-	-	-	-	-	-	-	-	-	-
Littorella uniflora	●	●	●	●	●	●	●	●	-	-	-	-	-	-	-	-
Lobelia dortmanna	●	●	●	●	●	●	●	●	-	-	-	-	-	-	-	-
Peplis portula	-	-	-	●	o	o	-	-	-	-	-	-	-	-	-	-
Ranunculus reptans	●	●	●	●	o	●	●	o	o	o	o	o	●	o	o	o
Subularia aquatica	o	o	o	●	o	●	o	o	o	o	o	o	●	o	o	o

Species/lake no.	1	2	3	4	5	6	7	8	9	10	11	12	13	14	15	16

Elodeids

Species/lake no.	1	2	3	4	5	6	7	8	9	10	11	12	13	14	15	16
Callitriche autumnalis	-	-	-	●	●	●	-	-	-	-	-	-	-	-	-	-
Callitriche hamulata	●	●	●	●	-	●	●	●	o	o	●	o	●	?	-	o
Callitriche verna	o	o	o	o	o	o	o	o	o	o	o	o	●	o	o	o
Chara spp.	-	-	-	-	●	-	-	-	-	-	-	-	-	●	-	-
Elodea canadensis	-	-	-	●	●	●	-	-	-	-	-	-	-	-	-	-
Myriophyllum alternifl	●	●	●	●	●	●	●	-	-	-	●	-	●	●	-	-
Myriophyllum verticill	-	-	-	●	--	-	-	-	-	-	-	-	-	-	-	-
Najas flexilis	-	-	-	-	●	-	-	-	-	-	-	-	-	-	-	-
Nitella confervacea	-	-	-	-	●	-	-	-	-	-	-	-	-	-	-	-
Nitella opaca/flexilis	●	●	●	●	●	●	●	●	●	●	-	-	-	-	●	●
Potamogeton alpinus	-	-	-	●	●	●	-	-	-	-	-	-	-	-	-	-
Potamogeton berchtold.	-	-	●	--	●	-	-	-	-	-	-	-	-	-	-	-
Potamogeton crispus	-	-	-	-	●	-	-	-	-	-	-	-	-	-	-	-
Potamogeton gramineus	-	-	-	●	●	●	-	-	-	-	-	-	-	-	-	-
Potamogeton obtusif.	-	-	-	●	-	-	-	-	-	-	-	-	-	-	-	-
Potamogeton panormit.	-	-	-	-	●	-	-	-	-	-	-	-	-	-	-	-
Potamogeton perfoliat.	-	-	-	●	●	●	-	-	-	-	-	-	-	-	-	-
Potamogeton x nitens	-	-	-	●	●	-	-	-	-	-	-	-	-	-	-	-
Ranunculus conferv.	-	-	-	-	●	-	-	-	-	-	-	-	-	-	-	-
Ranunculus peltatus	-	●	●	●	●	●	-	-	-	-	-	-	-	●	-	-
Utricularia intermedia	●	-	●	●	-	-	-	●	-	-	-	-	-	-	-	-
Utricularia minor	●	-	-	●	●	●	●	●	●	●	●	-	-	-	-	●
Utricularia ochroleuca	●	-	-	●	-	●	-	●	●	●	●	-	-	-	-	-
Utricularia vulgaris	●	●	●	●	●	●	●	●	●	●	●	-	-	-	-	-

Species/lake no.	1	2	3	4	5	6	7	8	9	10	11	12	13	14	15	16

<u>Tab. 3.</u>   (continued)
        Aquatic species found in the investigated lakes.
          'o'= not permanently submerged
          '●'= also found below lowest water level

Species/lake no.	1	2	3	4	5	6	7	8	9	10	11	12	13	14	15	16

Nymphaeids

	1	2	3	4	5	6	7	8	9	10	11	12	13	14	15	16
Nuphar lutea	−	−	−	●	−	●	●	−	−	−	−	−	−	−	−	−
Polygonum amphibium	−	−	−	●	●	●	−	−	−	−	−	−	−	−	−	−
Potamogeton natans	−	●	●	●	●	●	●	−	−	−	−	−	−	−	−	−
Sagittaria sagittif.	−	−	−	o	o	o	−	−	−	−	−	−	−	−	−	−
Sparganium angustif.	●	●	●	o	o	o	●	●	●	●	●	o	●	o	o	o
Sparganium hyperboreum	−	−	−	−	−	−	−	−	−	−	−	−	−	o	−	−
Sparganium minimum	−	−	−	−	−	o	o	−	−	−	−	−	−	o	−	−

Species/lake no.	1	2	3	4	5	6	7	8	9	10	11	12	13	14	15	16

Lemnids

Lemna minor	−	−	−	●	●	−	−	−	−	−	−	−	−	−	−	−

Others

	1	2	3	4	5	6	7	8	9	10	11	12	13	14	15	16
Fontinalis spp.	−	●	●	−	−	−	−	−	−	−	−	−	−	−	−	●
Sphagnum spp.	●	●	●	−	−	−	−	●	●	●	●	o	●	−	●	●
Spongilla cf.lacustris	●	●	●	●	−	●	●	●	●	●	●	−	●	−	●	●

Species/lake no.	1	2	3	4	5	6	7	8	9	10	11	12	13	14	15	16
Species no. total	19	22	24	37	37	33	20	18	15	16	15	10	12	15	10	14
" " submerged	17	17	19	29	26	23	16	15	10	10	12	0	10	4	3	8

Lake no.

1=Venneslafjord	2=Vangsvatn	3=Lønavatn	4=Tyrifjord
5=Stensfjord	6=Randsfjord	7=Maridalsvatn	8=Kilefjord
9=Byglandsfjord	10=Åraksfjord	11=Flåren	12=Ossjøen
13=Bykil	14=Aursunden	15=Hartevatn	16=Breidvatn

3 SUMMARIES OF DISSERTATION PAPERS

(I): Stereophotography as a tool in aquatic biology

Quantitative sampling of submerged macrophyte communities in general is time-consuming and inefficient. Photography, however, provides a means to acquire such data fairly rapid and larger sampling regions can be accessed within reasonable time.

The paper (I) describes the technical details of a SCUBA diver-operated stereophotographic system, based upon 35mm cameras. The system uses dual cameras to produce high-quality stereophotographic images of a $0.25m^2$ quadrat.

Some unique advantages of photographic sampling should be pointed out:

- an instantaneous record of the sampled area and prime data is combined by the processed image.
- the data, as photographic images, may be conveniently stored, analysed and re-analysed when the need arises.
- the community spatial relationships are preserved, and can be reconstructed in optical methods for measurement purposes.

The paper demonstrated the general validity of the photographic sampling approach. We also showed that loss of information was negligible provided the species present did not form a closed canopy, which precisely would be the normal case of submerged macrophyte communities dominated by isoetids. In fact, we pointed out that the increased sampling area compared to ordinary grab samplers would enhance the detection probability of small-grown, delicate species.

(II): Environmental factors and aquatic macrophyte response in regulated lakes - a statistical approach

The major environmental gradient in any lake correlates with depth. Plants are distributed across this vertical gradient according to niche preferences. Neglecting within-lake gradients, the spatial niche projects on to segments of the vertical gradient. Thus the niche description simplifies to the spatial coordinates of the vertical dimension, and the associated point-time probability distribution of environmental factors.

In regulated lakes, it is necessary to distinguish between depth and relative elevation, i.e., spatial position in the vertical gradient. Depth is the height of water overlaying the plants at any time, thus the instantaneous value may be nil.

The basic idea underlying (II) is very simple:

> Given the probability distribution of the water levels, all factors can be related to the spatial position in the vertical environmental gradient

The optimal depth and elevation datum is shown to be the median water level. The datum provides for translation of the probability distribution function (pdf) of the water levels, p_v, such that

> Expected value of a gradient function
>
> = Convolution of function by pdf p_v

It can be shown that this represents a mapping from a Lagrangian into a Eulerian coordinate system. The paper (II) considers only (weakly) stationary stochastic processes, and as such represents a first-order approximation to the statistics of environmental factors.

The selected approach leads to a number of interesting consequences. In the z-domain (Eulerian coordinates), the time-averaged Lagrangian (depth) functions are vertically displaced depending upon the pdf p_v. The impact of regulation is assessed by recomputing any gradient function convolution with a Dirac delta-function pdf.

Depth in its time-averaged sense is <u>not equivalent</u> to relative elevation when the water level fluctuates throughout time. The magnitude of the discrepancy is generally large in shallow waters, where many species attain peak performance. The bias occurring when depth is used in lieu of vertical position, can be evaluated analytically for known pdf's p_v. For a sinusoidal water level fluctuation, the bias peaks at the median water level. Lake data demonstrated significant bias over the entire vertical gradient.

Environmental stress factors, e.g., ice-scour, influence aquatics over a much larger part of the vertical gradient with a variable water level. The exact vertical distribution of the factor depends critically on the pdf p_v. Thus, lakes with closely similar ranges of water level fluctuations can show quite different vertical distributions. Factors operating through threshold statistics are most adversely influenced by a time-varying water level. Using a simplified statistical model, this is demonstrated for subsurface irradiance.

In general, regulation impact results in a compressed vertical niche. Simultaneously, the potential niche is shifted into deeper waters. Vegetation data from nine oligotrophic, regulated Norwegian lakes show significant correlation to the reduced vertical niche defined by ice-scour and threshold irradiance. Water-level schedules determine the actual vegetational response; thus, the total probability distribution of water levels should replace the regulation height or mean annual range of water level variation in an analysis of response features.

(III): Statistics of the underwater light field

Subsurface irradiance is a major environmental factor influencing the submerged macrophyte communities in freshwater lakes. The underwater light field is highly variable in space and time. The inherent variability of the light field renders the statistical analysis of potential macrophyte-light relations difficult. However, once a statistical description is established, hypotheses of macrophyte response to the light factor can be formulated and tested.

In a previous paper (II), the vertical attenuation coefficient was assumed to follow a Normal law. This paper (III) extends the statistical analysis. Based upon the Normality assumption, the light field can be shown to follow a Lognormal law at any depth. The expectation and variance have closed-form expressions for a stationary water level. The stochastic description enables the definition of derived functions, e.g., the expected duration and intensity of the underwater light field below any selected threshold value. The impact of a fluctuating water level can be assessed as well, using the convolution method outlined in (II). In this case, neither expected light intensity nor its variance can be expressed in closed form.

The Normality assumption is justified initially by the Central Limit Theorem, since the scattering and absorption of subsurface irradiance is caused by several partially independent factors. Using a large data base of light measurements from Norwegian lakes, the paper demonstrates this assumption to hold in general for field data. The studied lakes were mainly oligotrophic. The two productive lakes included did fit the Normality model, however.

(IV): Death of submerged macrophytes - actual field observations and some implications

This paper addresses macrophyte death incidents observed in the lakes Tyrifjord and Steinsfjord. The spatial distribution of rooted, dead macrophytes was obtained by photographic sampling.

Sudden death of a macrophyte differs from the normal seasonal growth-senescence pattern. Whenever the mortality rate exceeds the re-generation capacity, population performance and dynamics are adversely affected. Submerged macrophytes inhabit a hostile environment, and might easily succumb to prolonged periods of unfavorable environmental conditions. Two hypotheses are put forward in (IV):

  i) Environmental-induced mortality can regulate the spatial performance, i.e., the niche extent.

  ii) A species' susceptibility increases with the life-span length.

These hypothetical assertions were tested by various statistical methods.

Identifiable sudden death incidents occurred in less than 5% of the samples (N=3257). The major species in the submerged communities of each lake generally prevailed in these incidents.

Sufficient data points for the dominating isoetid Isoëtes lacustris at two exposed Tyrifjord sites enabled a statistical analysis of death incidents within the vertical gradient. Mortality rate increased sharply towards the lower limit of the zone colonized by I.lacustris. This would be expected if the control factor had an exponential depth distribution. Using log-transformed mortality rates, neither depth nor expected light intensity proved efficient in modelling the observed spatial mortality distribution, however.

An alternative approach, based upon a theoretical dose-response model with an implicit critical threshold irradiance, resulted in a highly significant relation (R^2 =95.8%, P<0.001) between probit-transformed mortality and a hazard function derived from light threshold statistics.

(V): Regulation impact on submerged macrophytes in the oligotrophic lakes of Setesdal, South Norway

This paper reports the vegetational details of seven oligotrophic lakes in the Otra watercourse, Setesdal valley (South Norway). These lakes have closely similar hydrochemistry, and all are highly transparent with Secchi-disc readings from 10 to 23m. The nominal regulation heights are 2.0 to 7.0m.

Macrophyte communities were dominated by isoetid species; <u>Isoëtes lacustris</u>, <u>I. echinospora</u>, and <u>Littorella uniflora</u>. Helophytes had negligible occurrence in five of the seven lakes. The number of submerged species declined significantly with increasing lake altitude, and also with extent of regulation. When only permantly submerged species were included, the species richness correlated only to regulation extent.

Submerged macrophytes divided into shallow-, intermediate- and deep-water species. Community distribution, using time-averaged depths, in the vertical gradient correlated significantly to the extent of ice-scour and threshold irradiance probability. Increasing regulation heights successively eliminated the shallow- and intermediate-water species, thus, only a deep-water community of <u>Nitella</u> cf. <u>flexilis</u>, bryophytes (mainly <u>Sphagnum subsecundum</u>) and freshwater sponges (<u>Spongilla</u> cf. <u>lacustris</u>) survived in the most heavily regulated lake. Perennial isoetids, mainly <u>Isoëtes lacustris</u>, did occur to a water-level range exceeding 3.6m annual mean and 5.9m total, however.

4 CONCLUDING DISCUSSION

The present study demonstrated some important facts regarding the lakes impacted by man-made water-level schedules and their vegetation.

Firstly, the main environmental gradient of all lakes related to the vertical spatial gradient, confirming the assertion put forward in HUTCHINSON (1975:408 et seq.). Thus, niche description <1> simplifies to the evaluation of the potential factors within segments of this gradient.

The necessity of discerning vertical position of a submerged community from its occurrence depth became apparent, however. The vertical position can be measured directly in the field, whereas the depth associated with this point in space can only be derived from computations based upon statistics of the water-level fluctuations. This important distinction is stressed in (II). Put simply, this is the key to regulation impact assessment. With any depth-related environmental factor, its expectation at some position in the vertical gradient implies a mapping from a Lagrangian (or moving coordinate) system into an Eulerian, or fixed-coordinate system. This mapping is obtained as a convolution integral (II).

Secondly, the vertical distribution of the submerged communities in the studied lakes followed easily generalized patterns. This distribution is a doubly-exponential decline below the depth of peak abundance, thus indicating a common limiting factor for all species (RØRSLETT 1983, IV, V). Deep-water community patchiness induces heavy rippling of the vertical distribution curves. This is a major feature, obtainable by the enhanced spatial resolution provided for by the photographic sampling method (I).

<1>   Unfortunately, the concepts of 'niche' and 'habitat' are ambiguous and confused in the literature (cf. WHITTAKER et al. 1973, CHRISTIANSEN & FENCHEL 1977, ALLEY 1982, AARSSEN 1984). Partly, this ambiguity stems from a failure to recognize that any real (i.e., existing) niche implies a spatial (or habitat) aspect, thus, delineation of 'habitat' from 'niche' cannot apply spatial criteria only.

Thirdly, niche space description involved mainly the physical dimensions of the environment ambient to the submerged species. Thus, niche space for the dominant species Isoëtes lacustris could be defined by two separate factors, viz. ice-scour (upper spatial limit) and thresholding light intensity (lower spatial limit).

A fluctuating water level induces environmental stochasticity with any depth-related and depth-varying factor, as seen from the literally fixed point of view of a submerged community. Spectral analysis of the water-level time series demonstrated the significance of low-frequent fluctuation patterns (RØRSLETT 1983, V). All lakes analyzed by this method had dominant annual spectral peaks ($f=1$ yr^{-1}). Frequencies up to $f=4$ yr^{-1} accounted for 80% or more of total variance of these time series. Thus, perennial species would be exposed to a clearly repeating annual pattern of water-level changes.

According to some recent ecological theories, e.g., CHRISTIANSEN & FENCHEL (1977), increased environmental stochasticity would lead to wider ecological niches for the impacted species. This hypothesis was not supported by my study. Spatial niche extent of the submerged species generally decreased in the strongly regulated lakes. Concomitantly, the niche was displaced towards deeper waters (II, V). Partly, this could be caused by a restricted niche space, due to environmental factors operating through thresholds. In (IV), the importance of thresholding light intensity was demonstrated for Isoëtes lacustris. A fluctuating water level would augment the probability of encountering critical thresholds at vertical positions corresponding to fringe habitats, thus, mortality rates would be expected to increase sharply in such areas (IV).

The species richness in the studied lakes <1> related to three factors, viz. altitude, lake area, and extent of regulation. Thus, a multiple linear regression had a coefficient of determination (R^2) 81.8% (P<0.01). Regression coefficients showed species richness to be positively related to lake area, and negatively related to altitude and extent of regulation. The regression equation was:

$$S = 20.53 - 1.96 \ \Delta W - 0.012 \ H + 0.075 \ A$$

<1>   Excluding the meso-eutrophic lake Steinsfjord.

where S = number of submerged species
       ΔW = mean annual range of water-level (m)
       H = Lake altitude   (m a.s.l.)
       A = Lake area (km^2)

In all lakes, again with Steinsfjord as an exception, the submerged communities had one to three strongly prevailing species, regardless of the actual size of the lake species pool. Thus, species richness _per se_ might not be that important parameter in a description of lake vegetation, when oligotrophic Scandinavian lakes are concerned. I consider this observation to justify the initial emphasis on a total community description. Furthermore, since the isoetid _Isoëtes lacustris_ proved to be the outstanding species in nearly all my lakes, regulation impact assessment might, to a first-order approximation, be based upon niche space analysis for solely that particular species.

The vertical niche displacement, due to regulation impact, can be estimated from the weighted mean spatial position, or characteristic depth D_c <1> , of the submerged communities. In the studied lakes, within-lake variation of the characteristic depth was insignificant (RØRSLETT 1983). The regression equation relating D_c to the regulation extent was:

$$Log_{10} (D_c) = 0.28 + 0.12 \; \Delta W$$

where ΔW = mean annual range of water-level (m)

Although highly statistically significant (P<0.001), the demonstrated relationship between D_c and regulation extent clearly cannot be extrapolated outside the observed range of regulation heights. This relationship pertains to the total submerged community, and does not account for niche displacements of individual species. Actually, by mapping estimated niche boundaries of _Isoëtes lacustris_ onto the regression relationship, (II) demonstrated the niche extent of this species to be rather weakly related to the range of water-level fluctuations in the studied lakes. Its niche size would be predictable, however, were the probability distribution of the water-level schedule used rather than the mean fluctuation range.

<1>   Depth applied in its time-averaged sense, i.e., the expected height of the water column overlaying the community (cf. II, V).

Furthermore, the general trend towards communities dominated by stoneworts and bryophytes in the strongly impacted lakes urgently needs positive corroboration. My data showed that such communities prevailed in Hartevatn, a lake nominally regulated 7.0m. As to the fate of these species in lakes regulated 10m or more, nothing is known. It should be pointed out, however, that such excessively regulated lakes could harbour weakly developed communities of annual isoetids and amphiphytes, e.g., from the genera _Eleocharis_, _Ranunculus_, _Callitriche_ and _Sparganium_. Such communites have been reported from Norwegian lakes regulated 9-25m (RØRSLETT 1980, JOHANNESSEN _et al._ 1984). Their spatial extent and production is negligible compared to the unregulated lake, however.

Impact assessment initially was a major aim for this study. The changes in niche size for the submerged species would likely be an important indication of such impact. Based upon the niche boundary relations for _Isoëtes lacustris_ reported in (II,IV,V), the niche displacement and compression for this species would be obtainable for any lake with given water-level schedule. An example of the niche size prediction would be the lakes Aursunden and Ossjøen. These lakes are nominally regulated 5.9 and 6.6m, respectively, and their draw-down patterns are closely similar. Spatial extent of the _Isoëtes lacustris_ niche in Aursunden is estimated at 5 and 2m for the pre- and post-regulation situation, respectively. The corresponding estimates for the lake Ossjøen are 2.5 and 0m. Lake Aursunden indeed harbours a submerged community with thriving _Isoëtes_, while this species is completely lacking in Ossjøen.

ACKNOWLEDGEMENTS

REFERENCES

AARSEN, L.W. 1984: On the distinction between niche and competitive
ability: implications for coexistence theory.
Acta Biotheor. 33: 67-84.

ALLEY, T.R. 1982: Competition theory, evolution, and the concept of
an ecological niche. Acta Biotheor. 31: 165-180.

BRAARUD, T. 1928: Den høiere vegetasjon i Hurdalssjøen.
Nyt Mag. NatVidensk. 83: 9-47.

BRETTUM, P. 1971: Fordeling og biomasse av Isoetes lacustris og
Scorpidium scorpioides i Øvre Heimdalsvatn, et høyfjellsvann
i Sør-Norge. Blyttia 29: 1-12.

CHRISTIANSEN, F.B. & FENCHEL, T.M. 1977: Theories of Populations in
Biological Communities. Springer-Verlag, Berlin, 144 pp.

HUTCHINSON, G.E. 1975: A Treatise on Limnology. III: Limnological
Botany. Wiley & Sons, New York, 660 pp.

JOHANNESSEN, M. et al. 1984: A/S Bleikvassli Gruber. Kjemiske og bio-
logiske undersøkelser i Kjøkkenbukta og Store Bleikvatn.
Norwegian Institute for Water Research, Report O-82121, 39 pp.

LOHAMMAR, G. 1965: The vegetation of Swedish lakes. Acta Phytogeogr.
Suec. 50: 28-48.

NICKLASSON, A. 1979: Konsekvenser ur naturvårdssynspunkt av vatten-
ståndsförändringar i oligotrofa sydsvenska sjöar.
Statens Naturvårdsverk PM 1185 (1979), 123 pp.

NILSSON, C. 1981: Dynamics of the shore vegetation of a North Swedish
hydro-electric reservoir during a 5-year period.
Acta Phytogeogr. Suec. 69: 1-94.

QUENNERSTEDT, N. 1958: Effects of water level fluctuation on lake
vegetation. Verh. Intern. Verein. Limnol. 13: 901-906.

RØRSLETT, B. 1980: Reguleringsvirkninger på høyere vegetasjon i norske innsjøer. <u>Norsk inst. vannforskn. Årbok 1979</u>: 27-31.

RØRSLETT, B. 1983: Tyrifjord og Steinsfjord. Undersøkelse av vann-vegetasjon 1977-1982. <u>Norwegian Institute for Water Research</u>, Report O-7800604, 300 pp.

RØRSLETT, B., BERGE, D. & JOHANSEN, S.W. 1984: Mass invasion of <u>Elodea canadensis</u> in a mesotrophic, South Norwegian lake - impact on water quality. <u>Verh. Intern. Verein Limnol.</u> 22 (in press)

SAND-JENSEN, K. 1978: Metabolic adaption and vertical zonation of <u>Littorella uniflora</u> (L.)Aschers. and <u>Isoetes lacustris</u> L. <u>Aquat. Bot.</u> 4: 1-10.

STATISTISK SENTRALBYRÅ 1983: Naturressurser 1982. (Norwegian nature resources 1982. In Norwegian). <u>Central Bureau of Statistics of Norway</u>, Report 83/1: 1-62.

WASSÉN, G. 1966: Gardiken. Vegetation und Flora eines lappländischen Seeufers. <u>K.Sv.Vetenskapsakad. Avh.Naturskyddsärend</u>. 22.

WHITTAKER, R.H., LEVIN, S.A. & ROOT, R.B. 1973: Niche, habitat and ecotope. <u>Amer. Naturalist</u> 107: 321-338.

STEREOPHOTOGRAPHY AS A TOOL IN AQUATIC BIOLOGY

BJØRN RØRSLETT, NORMAN W. GREEN and KNUT KVALVÅGNÆS

Norwegian Institute for Water Research, P.O. Box   333, Blindern, N-Oslo 3 (Norway)

(Received 14th March 1977)

ABSTRACT

Rørslett, B., Green, N.W. and Kvalvågnæs, K., 1978. Stereophotography as a tool in
aquatic biology. *Aquat. Bot.,* 4: 73—81.

The details of an underwater stereophotographic system is outlined. This system is
based on 35mm cameras, using high-resolution colour film. A modular construction enables
adaption of the photographic system to a wide range of applications. Interfaced to a com-
puterised data base, the system offers quick and fairly accurate information feedback on
the investigated biological communities. Objects down to about 0.5mm natural size are
detectable. Spatial relationships and the state of the organisms are easily documented. By
time-lapse photography, changes in aquatic communities, e.g. due to pollution impacts,
may be well monitored.

INTRODUCTION

In studying aquatic communities, there is a continual demand for methods
offering quick and accurate information feedback. Most methods loose some
biological detail in the attempt to sample a larger region. In addition, they
may be inefficient or too time-consuming (Lundälv, 1971). Photography,
however, provides a means by which this demand may be satisfied.

Some advantages of photography should be pointed out. An instantaneous
record of the sampled area and prime date is combined by the processed
image. The data, as photographic images, may be conveniently stored,
analysed and re-analysed when the need arises. Thus, for example, spatial
relationships of a community structure can easily be reconstructed in optical
models. Time-lapse photography allows for population studies without inter-
ferring with the organisms themselves. Species identification is often made
easier by stereoscopic interpretation. Stereophotography enables measure-
ments of object co-ordinates in the three-dimensional model, thus providing
quantitative parameters such as distances and volumes. Productivity may be
estimated using empirically determined relationships between biomass and
linear measurements.

The Norwegian Institute for Water Research carries out extensive investi-
gations of lakes, rivers and coastal waters. We have initiated photographic

74

techniques in this connection, applying stereophotography to studies on marine hard-bottom benthos and freshwater macrophytes.

METHODS

Stereophotography of test quadrats

A layout of the stereophotographic equipment used is shown in Fig. 1. This system is an extension of that described by Lundälv (1971), but adaptable to land work as well.

The basic module is a double reference frame of brass which is welded together in the shape of a box $0.5 \times 0.5 \times 0.1$ m. At each corner, there are extended arms where accessory parts can be attached. The frame is painted yellow and has grid markers at 2 cm intervals. Calibration points are also provided for use in photogrammetric analysis. An adjustable camera platform is mounted to the reference frame by means of four solid brass rods held parallel to each other by tight-fitting collars and cross-going pins. Accessory equipment to be mounted to the reference frame would include colour and gray scales, clock, depth gauge, thermometer and a blank plate where pertinent information can be written. All of this would be captured by the cameras. The clock, in particular, guarantees matching the separate photographs of a stereopair.

The underwater buoyancy of the stereophotographic unit may be trimmed by exchangeable floats. On very soft, muddy bottoms the reference frame is prevented from sinking into the sediment by the attachment of plastic plates (see Fig. 1). In addition, these plates temporarily keep turbid water, a result of contact with the muddy bottom, out of the area to be photographed.

Photographic equipment

In underwater photography, turbidity can greatly diminish image crispness and resolution. A wide-angle lens is needed in order to get closer to the subject, but still cover a large area. We have used two mechanical synchronized 35mm cameras, Nikonos III, with 15 mm f/2.8 UW-Nikkor lenses. The lenses are factory calibrated in order to match in focal length, thus ensuring geometric accuracy in the stereomodel.

A constant light source is provided by a Rollei E36RE electronic flash in underwater housing with an external light sensor. For maximum image sharpness, we use high-resolution colour film (Eastman Kodak 2483 Photomicro-

Fig. 1. Layout of the stereophotographic equipment, partially disassembled, used in underwater photography. The basic parts consist of: double reference frame of brass (a), camera platform (b), brass rods (c), colour and gray scales (d), clock (e), depth gauge (f), compass (g), thermometer (h), note plate (i), floats (j), soft bottom plates (k), 35 mm cameras with lenses (l), synchronizing arm (m), flash in underwater housing (n) and light sensor (o).

75

l

m

j

h

d

o   b

c

n

j

i

j

c

g

d

e   f

a

j

k

k
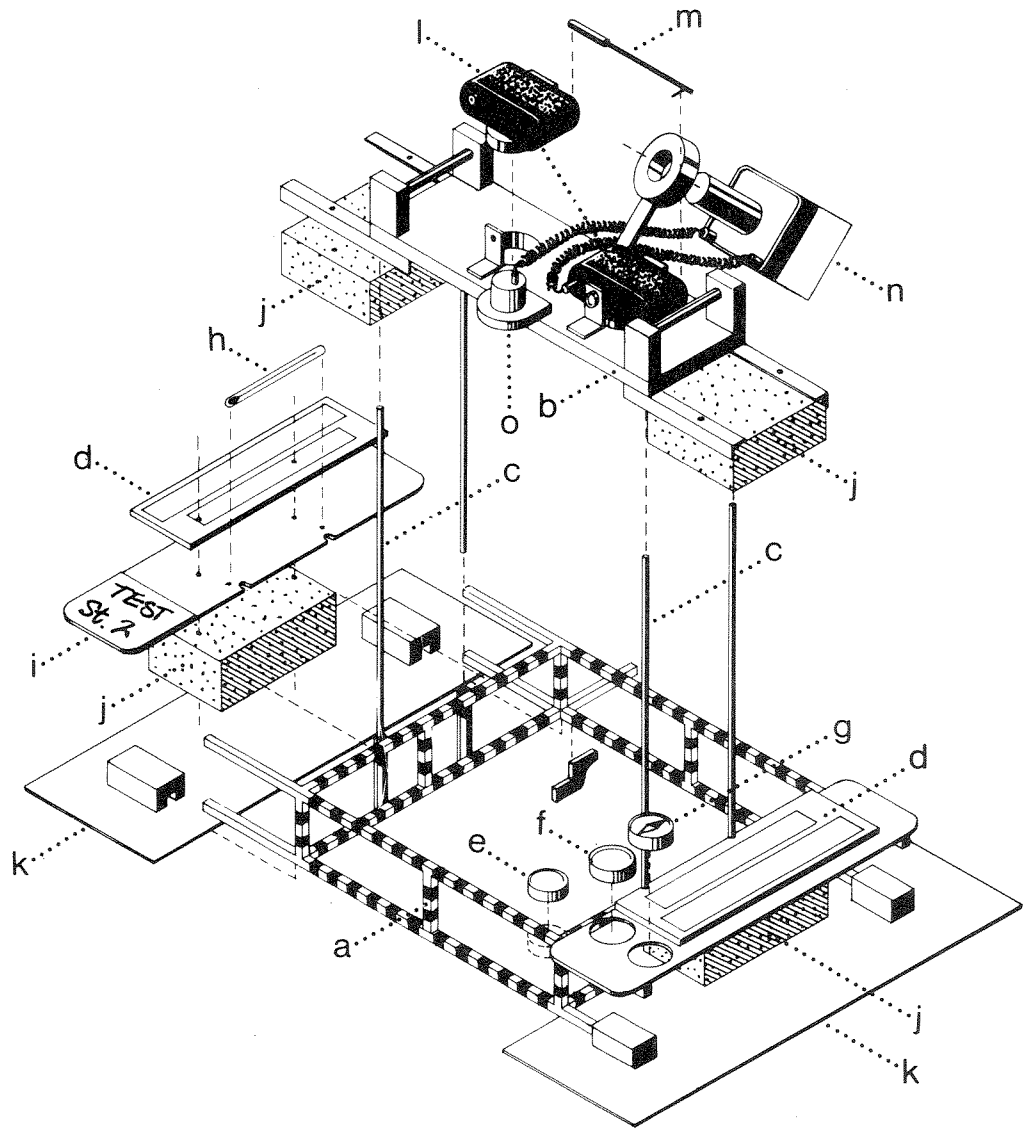
76

graphy). The film colour balance is adjusted by Wratten filters on the flash and may be controlled against the colour scales.

For terrestrial applications, another camera platform is mounted on the reference frame. Here we use motor-driven Nikons equipped with 20 mm f/4 Nikkor lens. In this case, infrared false-colour film (Eastman Kodak Infrared Ektachrome) is appropriate, enhancing differentiation of foliage.

The image scale for underwater and land photography is approximately 1:22 at the upper reference frame. Examined at 12—20 times magnification, this scale allows for discrimination of objects down to about 0.5 mm size.

Time-lapse photography

Monitoring of test quadrats is easily made by repeated photographic coverage if reliable means of sample area labelling exists.

On subsurface soft bottoms, we have used plastic shafts with an angled profile. The shaft is pounded into the mud leaving only a coloured end with the quadrat identification over the sediment surface. Such stakes can easily be
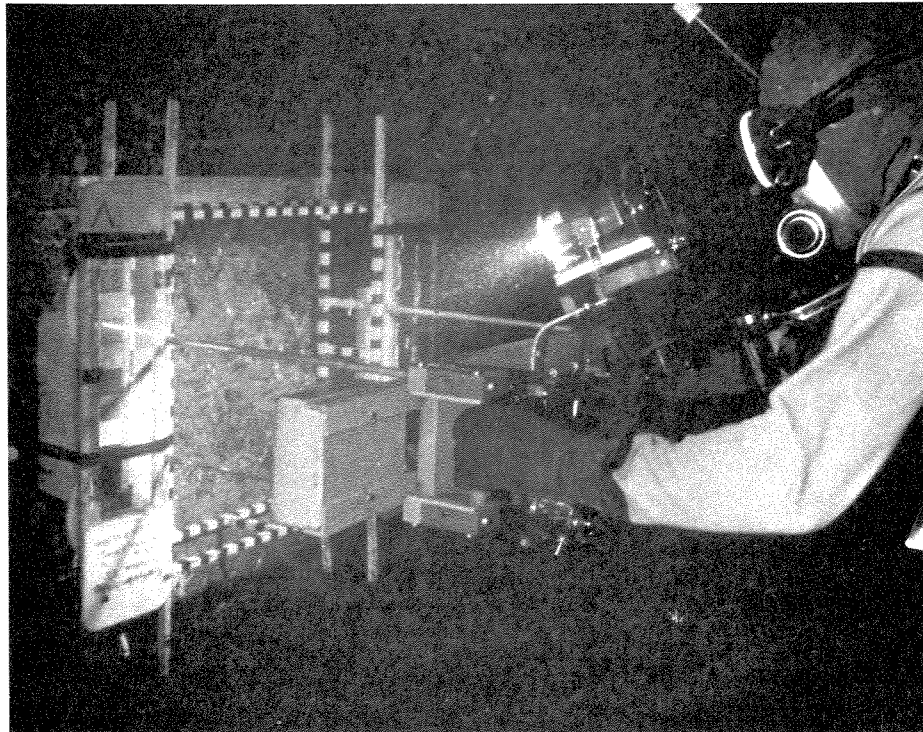
Fig. 2. A SCUBA diver operating the stereophotographic outfit in a marine hard-bottom community.

77

relocated and photographed in a specified corner of the reference frame, thus capturing approximately the same area each time.

More accurate means can be applied on hard substrates where plastic dowels are placed into drilled holes. A rigid rod is mounted between the dowels and has fixed stop points for the reference frame. Thus data can be accumulated covering exactly the same area. A diver operating the stereo-photographic outfit is shown on Fig. 2.

DATA ACQUISITION AND PROCESSING

The speed of photographic data acquisition enables a thorough coverage of biological features at the studied localities. A trained SCUBA diver would obtain up to five stereopairs per minute when working along predetermined transects in lakes and rivers. The operating schedule on the hard-bottom localities, being less flexible, results in a somewhat lower photographic work-rate.

The wealth of information presented by the stereopairs necessitates a scheme for handling the input data flow. A "quick-look" analysis based on photointerpretation profiles the salient features. Time-consuming photo-grammetric analysis may then concentrate on selected applications. Measurements of spatial distances are performed in a small stereocomparator, following the analytical procedure of Torlegård and Lundälv (1974).

Photointerpretation results include lists of identified species, counts of individuals if appropriate, and cover estimates by means of a grid overlaying the stereomodel. Actual depth values are read from the depth gauge on the reference frame and related to the mean water level. Species names given by eight-letter mneumonic codes are entered into a computerised data base together with image identification, ground co-ordinates and photointerpretation results. While diving, the operator communicates with the surface crew through an underwater telephone. His vocal observations are taped on a portable tape-recorder and later added to the data base.

The data set may then be manipulated by computer, giving species frequencies, diversity indices and coverage as functions of the adjusted water depth. This first-time analysis can provide valuable information of biological features, as exemplified by Fig. 3.

DISCUSSION

Efficiency of sampling based on photography

The advantages of photographic sampling would be considerably less if too many details were lost on the photography. We have tested this by stereophotography on a species-rich shore community using false-colour infrared film. Fifty test quadrats were photographed and their species content assessed in the field. The stereopairs were independently evaluated, the mean

78
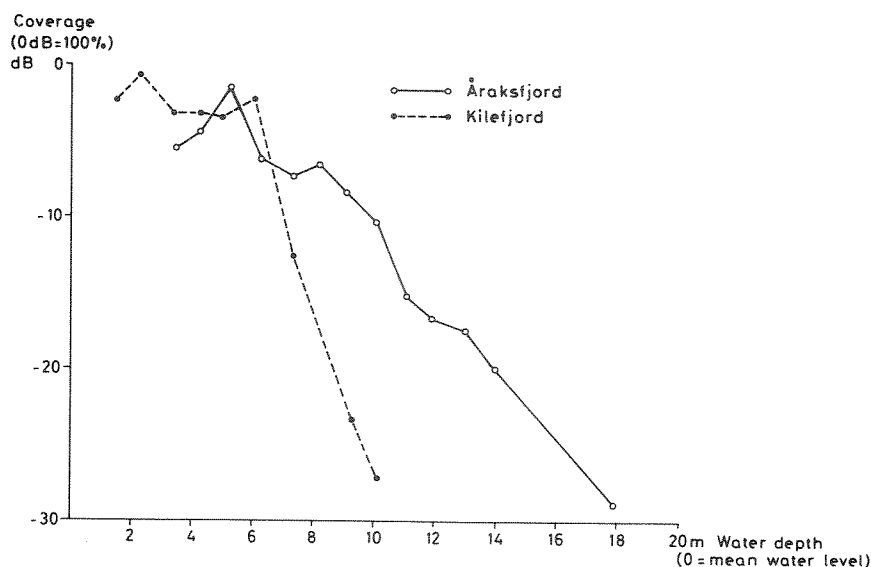
Fig. 3. Depth distribution of macrobenthic coverage in two clearwater Norwegian lakes based on photographic data collected in August 1976. These lakes, situated in the Setesdal valley of South Norway, have transparencies exceeding 10 m and are regulated for hydroelectrical power plants. In both lakes, coverage maximum corresponds with the position of a littoral shelf, as pointed out by Spence (1976). The coverage decline in Lake Åraksfjord (—2 dB/m) corresponds roughly to vertical light attenuation, whereas the presence of a steep underwater slope in Lake Kilefjord is reflected by a faster decrease with depth (—6 dB/m).

evaluation time per stereopair being roughly equal to the time used in the field. The results show no significant difference in the assessment of prominent species (e.g. *Alisma plantago-aquatica* L.), whereas small-growing species such as *Elatine hydropiper* L. was significantly more often found $(\chi^2 = 4.0, P < 0.05)$ by photointerpretation.

Patchiness in the distribution of submergent communities is evident (Fig. 4) and complicates statistical treatment of the data. This difficulty may be lessened by increasing the number of stereopairs taken.

The sparseness of deep-water vegetation (see Fig. 3) indicates that photography by divers is likely to be more efficient than conventional grab methods. For example, the maximum probability of observing *Utricularia minor* L. at its depth limit (13 m in the lake Åraksfjord, South Norway) is estimated to be 3×10^{-3} based on our sample size. Only 3 out of 1000 hauls at this depth would be expected to contain *U. minor* if the grab sampled quadrats the size of our reference frame. A smaller grab size may well lower the probability of occurrence by an order of magnitude.

Data from some 20 lake stations, collected in 1976, show macrophytes to be regularly present in the depth range 10—18 m. The angiosperms *Elodea*

79
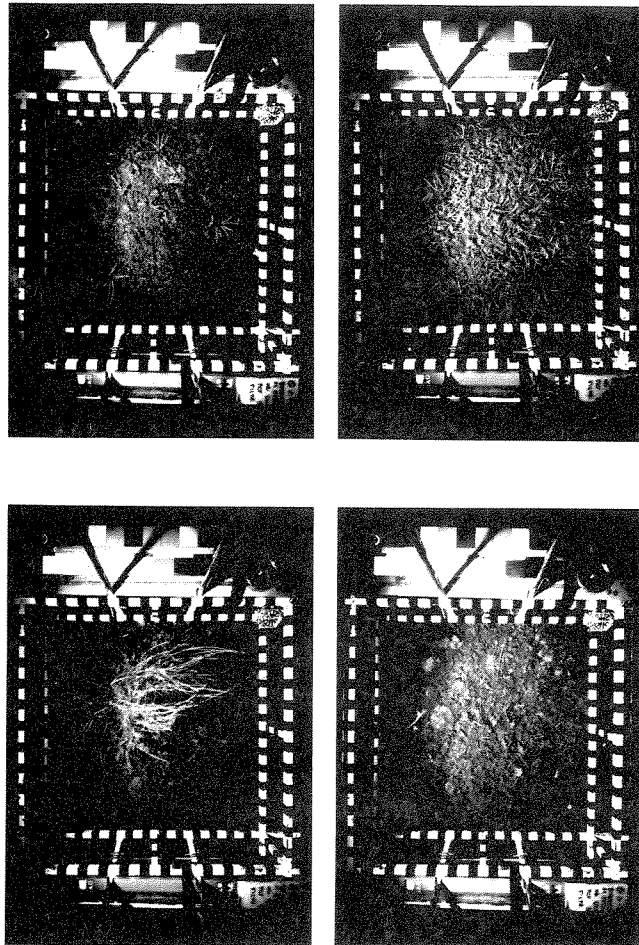
Fig. 4. Patchiness in the submerged vegetation from the oligotrophic Lake Byglandsfjord (Setesdal valley, South Norway). The photography, randomly selected within a five-minute interval of the diving session, all originate from a littoral shelf at four meters depth. The plant carpet is mostly *Isoëtes echinospora* with scattered individuals of *I. lacustris* and *Juncus bulbosus*.

canadensis Michx. and *Utricularia minor* penetrate to depths of 10—13 m whereas the stonewort *Nitella* cf. *flexilis* (L.) C. Ag. was observed in 15—18 m depth. Mosses and freshwater sponges (*Porifera: Spongillidae*), however, constitute most deep-water communities at our stations.

The values for *E. canadensis* and *U. minor* expand the depth range colonized by angiosperms according to Hutchinson (1975). Moreover, the photography documents the active growth of these deep-water angiosperms. The spatial information provided by stereophotography allows for easy differentiation of

80

living and moribound states of the plants. Such information is easily lost with grab sampling.

Limitations of the photographic approach

The stereophotographic method, in its present version, cannot easily cope with a number of situations commonly encountered in the field. Some practical problems are

(1) excessive water turbidity, reducing image contrast and resolution,

(2) very rough substrates,

(3) photography in very shallow waters (<1 m depth),

(4) identification of very small species, species needing microscopic examination, or species with extremely similar appearance (e.g. some forms of *Isoëtes lacustris* L. and *I. echinospora* Durien),

(5) occurrence of larger organisms within the sampled quadrat, as they may obscure the view of smaller forms, and

(6) plants with elongated or trailing shoots, such as many species of *Potamogeton, Ranunculus* and *Sparganium.*

Although other photogrammetric principles, for example convergent stereophotography, may overcome some of these problems, the photographic approach is obviously restricted in its application potential. The commonly unproductive Norwegian inland waters, however, are very often explorable by the photographic techniques.

The same situation holds for marine benthic fauna, according to our limited experience.

CONCLUSIONS

Despite the limitations previously outlined, stereophotography offers a versatile tool for the aquatic biologist. We have found this method to be rapid and accurate in use. The amount of biological information contained in the data enables a quantitative evaluation of the observations made.

The profit of time-lapse capabilities in underwater photography will be fully reaped in the future monitoring of our reference stations.

ACKNOWLEDGEMENTS

81

REFERENCES

Hutchinson, G.E., 1975. A Treatise on Limnology. Vol. 3. Limnological Botany. Wiley, London and New York, 660 pp.

Lundälv, T.L., 1971: Quantitative studies on rocky-bottom biocoenoses by underwater photogrammetry. A methodological study. Thalassia Jugosl., 7: 201—208.

Spence, D.H.N., 1976: Light, zonation and biomass of submerged freshwater macrophytes. In: E.A. Drew, J.N. Lythgoe and J.D. Woods (Editors), Underwater Research, Academic Press, London, New York and San Francisco, 1976, 430 pp.

Torlegård, A.K.I. and Lundälv, T.L., 1974: Underwater analytical system. Photogramm. Eng., 40: 287—293.

ENVIRONMENTAL FACTORS AND AQUATIC MACROPHYTE RESPONSE IN REGULATED LAKES — A STATISTICAL APPROACH

BJØRN RØRSLETT

Norwegian Institute for Water Research, P.O.B. 333, Blindern, N-Oslo 3 (Norway)

(Accepted for publication 23 February 1984)

ABSTRACT

Rørslett, B., 1984. Environmental factors and aquatic macrophyte response in regulated lakes — a statistical approach. *Aquat. Bot.*, 19: 199—220.

In regulated lakes, it is necessary to distinguish between depth and relative elevation. Depth is the height of water overlaying the plants at any time, thus the instantaneous value may be nil. The optimal "depth" and elevation datum is shown to be the median water level. However, depth in its time-averaged sense is *not equivalent* to relative elevation when the water level fluctuates throughout time. The magnitude of the discrepancy is generally large in shallow waters.

Environmental stress factors, e.g. ice-scour, influence aquatics over a much larger part of the "depth" gradient with a variable water level. Factors operating through threshold statistics, e.g. subsurface irradiance, are most adversely influenced by a time-varying water level. In general, regulation impact results in a compressed vertical niche. Simultaneously, the potential niche is shifted into deeper waters. Vegetation data from nine oligotrophic, regulated Norwegian lakes show significant correlation to the reduced vertical niche defined by ice-scour and threshold irradiance. Water-level schedules determine the actual vegetational response; thus the total probability distribution of water levels should replace the regulation height or mean annual range of water level variation in an analysis of response features.

INTRODUCTION

Environmental factors potentially influencing aquatic macrophytes are often functionally related to the water depth (Sculthorpe, 1967; Hutchinson, 1975). Pertinent examples are: subsurface irradiance, hydrostatic pressure, temperature, turbulence, and sediment particle size. Neglecting successional effects, potential plant sites in a lake are spatially fixed and stationary in time (cf. Stanley et al., 1976). In most lakes, however, the water level itself is fluctuating throughout time. Scandinavian lakes situated in larger watersheds have natural wide fluctuations, with annual water-level variations of 2—5 m. Lakes regulated for hydro-electric power production often have regulation heights exceeding 5 m. Nearly one-half of the Norwegian reservoirs is regulated at 10 m or more (Statistisk Sentralbyrå, 1983, p. 27).

200

The vertical distribution of submerged macrophyte communities in reg-
ulated lakes is clearly influenced by the annual water level amplitude
(Quennerstedt, 1958; Wassén, 1966; Nilsson, 1981; Rørslett, 1983, 1984).
The response details, however, differ significantly between lakes (Rørslett,
1984). Communities of isoetids, generally the main benthic producers in the
oligotrophic lakes of Norway, are thriving in some lakes with water-level
variations exceeding 6 m, but may be largely lacking in closely similar lakes
with smaller annual fluctuations. The cause of such phenomena has a major
bearing on the planning of regulation schemes, in order to minimize the
ecological impact of the scheme.

The depth concept relates to the vertical extent, or dimension, of a water
layer, as seen downwards from the current water surface. Equivalently, this
equals the height of the water layer above the bottom. The vertical extent of
water overlaying a submerged plant population in regulated lakes is obvi-
ously a time-dependent variable. Consequently, the impact of depth-related
environmental factors also changes throughout time.

This paper focuses on a statistical description of "depth", and environ-
mental factors related to "depth", when the water level fluctuates in time.
The approach selected is to describe the fluctuations in a time-fixed co-
ordinate system, using the probability density of instantaneous deviations of
water level from the coordinate datum levels. Any environmental factor may
then be functionally related to the time-fixed vertical levels.

The general validity of this approach is demonstrated, based upon environ-
mental and vegetational data from regulated lakes in Norway. In particular,
the close relationship between the statistically described environmental
factors and vegetational response is outlined. Vegetation distribution pat-
terns are broadly described, aiming at the salient response features con-
sidered characteristic for low-to-intermediate altitude, oligotrophic, reg-
ulated lakes in Norway. The regulation impact is deliberately exemplified by
physical factors, because the invoked stress on the aquatic ecosystem is
bound to be of a mainly physical nature.

MATERIAL AND METHODS

Study area and field data

The statistical approach is discussed with vegetation and water-level data
from nine selected Norwegian lakes. The location of the lakes is indicated on
Fig. 1, and some pertinent data on the water-level variations are given in
Table I.

The evaluation of a lake's trophic state is based on extensive biological
and hydrochemical investigations carried out by the Norwegian Institute for
Water Research (NIVA) from the 1970's onwards. All lakes are more or less
oligotrophic, with nominal regulation height ranging from 1.5 up to 7.0 m.
Regulations for hydro-electric power purposes date back to the 1950's, or in

201

some cases even earlier. Thus, any post-regulation transient phenomena can be ruled out. One lake (Vangsvatn) is unregulated, but has a naturally wide annual fluctuation in water level.

Submerged vegetation was sampled by means of under-water stereo-

1: Vangsvatn
2: Tyrifjord
3: Randsfjord
4: Maridalsvatn
5: Kilefjord
6: Byglandsfjord
7: Åraksfjord
8: Hartevatn
9: Breidvatn
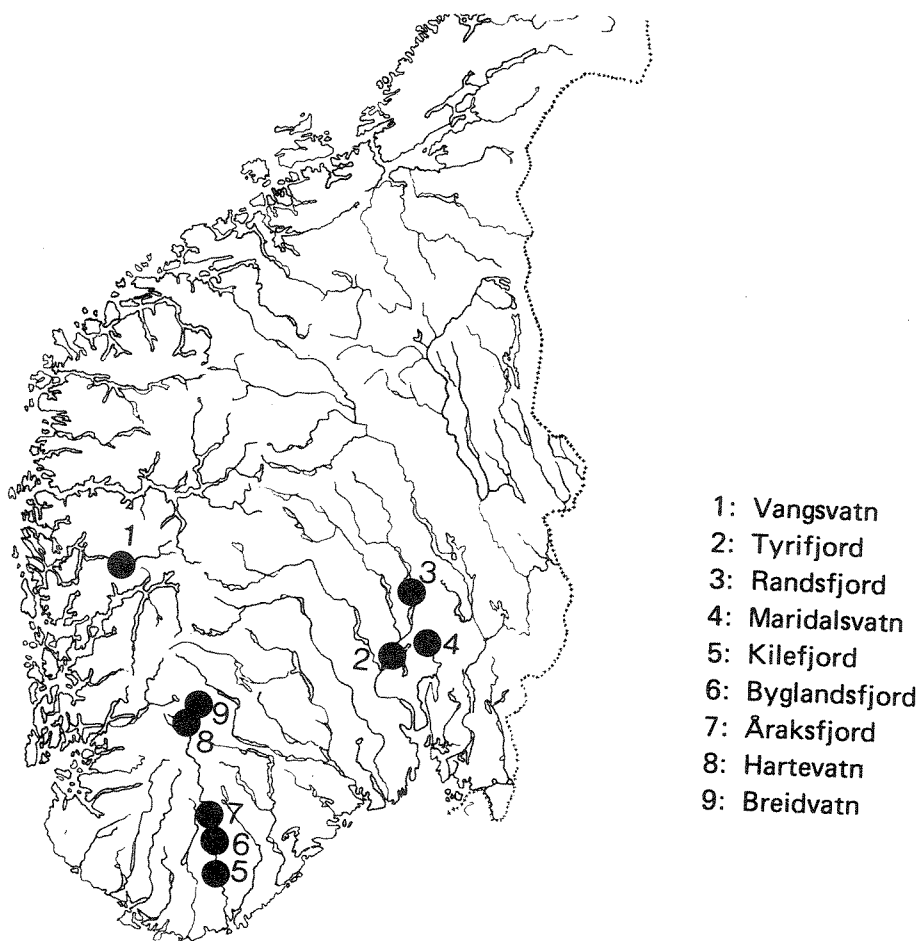
Fig. 1. Location of the nine investigated lakes (South Norway).

photography (Rørslett et al., 1978), with quadrat size 0.25 m². Coverage of species was determined by a nested grid method (Rørslett, 1983), with statistical relative accuracy within ± 20% for cover exceeding 0.1%, and within ± 30% for very low cover in the 0.001—0.1% range. A total of some 3800 photographic samples was obtained from 36 sites during the years 1976—81. Preliminary analysis revealed a close relationship between community depth distribution and site exposure, thus only data from the most strongly exposed sites are considered here for between-lake comparisons.

202

TABLE I

List of the lakes studied

Lake	Altitude (m a.s.l.)	Area (km²)	Regulation height[1] (m)	Water level amplitude (m)		Total range[2]
				Annual		
				Mean	Max.	
Vangsvatn	46	8.0	—	4.5	6.3	6.6
Tyrifjord	63	121.9	1.0	2.0	2.9	3.5
Randsfjord	134	136.9	3.0	2.9	3.9	4.1
Maridalsvatn	148	3.9	2.0	1.1	1.3	1.6
Kilefjord	167	5.5	1.5	2.0	2.9	3.2
Byglandsfjord	202	30.7	5.0	3.6	4.9	5.9
Åraksfjord	203	11.2	5.0	3.5	4.9	5.0
Hartevatn	757	6.0	7.0	6.4	7.3	7.8
Breidvatn	897	3.1	2.5	3.0	3.5	3.5

[1] Nominal regulated height (m) as licensed by Norwegian authorities.
[2] Maximal annual range (m) during the years 1945—1978.

Further details on vegetation and convolution smoothing of depth distribution curves are found in Rørslett (1983, 1984).

Subsurface photosynthetic available radiation (PAR, 350—700 nm) was measured with a Li-Cor LI-185 Quantum meter and sensor LI-192S (Lambda Instruments, Inc.) intermittently during the months May—October. Estimation of vertical attenuation coefficients was performed by a proprietary computer program, using a non-linear least squares fitting method.

Water-level data from the lakes were obtained from official gauges monitored by the Norwegian Water Resources and Electricity Board (NVE, Oslo). Daily measurements of water levels were used whenever available. Statistics for water levels were computed for the years 1945 to 1978—81.

Statistical description of water-level fluctuations

The major environmental gradient in any lake correlates with depth (Hutchinson, 1975). Plants are distributed across this vertical gradient according to niche preferences. Neglecting within-lake gradients, the spatial niche projects on to segments of the vertical gradient. Thus, the niche description simplifies to the spatial coordinates of the vertical dimension, and the associated point-time probability distribution of environmental factors.

Regulation impact should be assessed from a "plant's point of view", i.e. with stationary spatial coordinates for individuals, and time-varying extent of water overlaying the plants.

The coordinate system adopted is shown in Fig. 2, and the corresponding relations between the water level and vertical scales are given in Table II. Coordinate axes are oriented positively upwards, except for instantaneous

203

deviations of water level, which are positive downwards in order to conform with common usage of "depth".

Representing the time series of water levels as a continuous random variable $W = w(t)$, the cumulative probability distribution function (cdf) is

$$P_W(w) = \text{Prob} \ (w(t) \leqslant w)$$
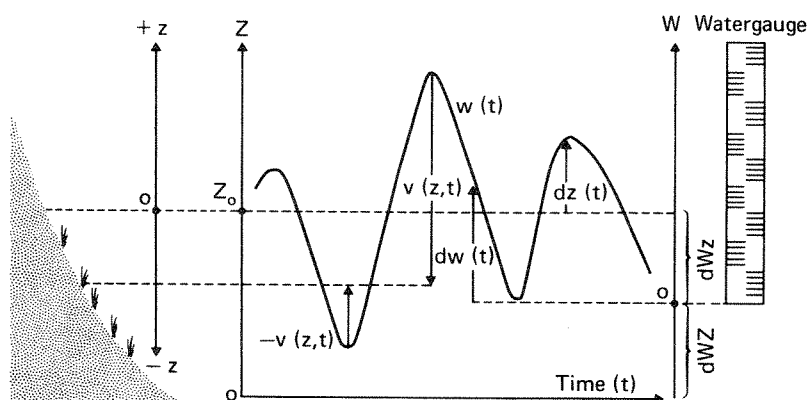
Fig. 2. Coordinate system used to describe the time statistics of a changing water level, related to spatially fixed plant sites. Refer to Table II for a definition of symbols.

TABLE II

Relations between z-, Z- and W-scales. Base scale is z-scale, cf. Fig. 2

Item (cf. Fig. 2)	Relationship
Translocations	
Water level scale into Z-coordinate (elevation)	$Z = W + \mathrm{d}WZ$
Z-coordinate into local z-scale	$z = Z - Z_0 = W + \mathrm{d}Wz$
Instantaneous variables	
Water level	$w(t) = \mathrm{d}w(t) + \mathrm{d}WZ$
Deviation of water level	$\mathrm{d}z(t) = w(t) - Z_0$
re: time-fixed zero point	$= \mathrm{d}w(t) - \mathrm{d}Wz$
Deviation of water level	$v(z,t) = \mathrm{d}z(t) - z$
re: z-scale	
Depth re: z-scale	$\mathrm{d}(z,t) = \begin{cases} v(z,t) & v \geqslant 0 \\ 0 & v < 0 \end{cases}$

Assuming a "smooth", i.e. differentiable, cdf, the corresponding probability density function (pdf) is

$$p_W(w) = \frac{\mathrm{d}P(w)}{\mathrm{d}w}$$

thus

204

$$P_W(w) = \int\limits_{-\infty}^{w} p_W(u)\,\mathrm{d}u$$

Assume the z-scale datum, i.e. Z_0, to be known. As shown in Table II, the z- and W-scales differ only by a translocation constant $\mathrm{d}Wz$. Thus, the pdf $p_v(z)$ of instantaneous deviations of water level in the z-scale is

$$p_v(z) = p_W(z + \mathrm{d}Wz)$$

and the cdf's are related as

$$P_v(z) = P_W(z + \mathrm{d}Wz)$$

The cdf is preferably estimated from daily water-level data, spanning at least 10—15 years of measurement. The cdf $P_W(w)$ may be recognized as the "water level duration" curve of hydrology, with a rotation of axes and labelling the cumulative probability as percentage of time.

Translocation into the z-scale depends on the datum level Z_0. Noting the fundamental ecological difference between the aquatic and the terrestrial environment (Hutchinson, 1975), the datum should optimalize the delineation between these contrasting environments throughout time. This is equivalent to a 2-state classification (Aquatic:Terrestrial) of the total Z-scale gradient.

The 2-state classification of the Z-scale is based on mutually exclusive events, and is easily found by application of probability theory.

The event $E_1 = "Z < Z_0"$ implies $(Z \in$ Aquatic$)$
and $E_2 = "Z \geqslant Z_0"$ implies $(Z \in$ Terrestrial$)$
The associated probabilities are obviously

$$p(E_1) = \text{Prob } (w(t) > Z_0) = 1 - P_W(Z_0)$$

$$p(E_2) = \text{Prob } (w(t) \leqslant Z_0) = P_W(Z_0)$$

$$p(E_1) + p(E_2) = 1$$

with a minimum classification error in the case of

$$p(E_1) = p(E_2)$$

or $P_W(Z_0) = 1/2$

Thus, the optimal datum Z_0 is the median water level. This datum can also be shown to maximize classification information (entropy) by information theory (Rørslett, 1983).

Based on the datum Z_0, the vertical distribution of macrophytes along the Z-scale is easily described in the time-fixed z-coordinate system (cf. Fig. 2). This ensures, for example, that limits of depth extension for any species in a lake are (approximately) stationary in time, regardless of the actual water level at sampling time.

205

A generalized z-level function

Let $H(z,t)$ be any function of environmental factors in the vertical gradient, possibly discontinuous across the water surface $(v(z,t) = 0)$. Then

$$H(z,t) = h(v) = \begin{cases} f(v) & \text{if } v \geqslant 0 \\ g(v) & \text{if } v < 0 \end{cases} \tag{1}$$

and $v = \mathrm{d}z(t) - z$ (Fig. 2)

Assuming a weakly stationary process, the statistics of $H(z,t)$ are obtained by time-averaging. The time-averaged mean, or expectation of $H(z)$ is directly obtained as

$$E(H(z)) = \int_{-\infty}^{+\infty} \int_{-\infty}^{+\infty} H(z-u,t)p_v(u,t)\mathrm{d}t\,\mathrm{d}u$$

$$= \int_{-\infty}^{+\infty} H(u)p_v(z-u)\mathrm{d}u \tag{2}$$

$$= \int_{-\infty}^{+\infty} h(z-u)p_v(u)\mathrm{d}u \qquad *$$

i.e. as the time-domain convolution by the pdf of the instantaneous deviations from the reference datum. The proof of eqn. (2) follows directly from the definition of the expectation of a random variable, noting that $v = u - z$. Equation (2) is valid even with a time-stationary water level, in this case the pdf $p_v(z)$ degenerates into a Dirac spike centered at $z = 0$.

The variance of $H(z)$ is from (2)

$$\mathrm{Var}(H(z)) = E(H^2(z)) - E(H(z))$$

$$= \int_{-\infty}^{+\infty} (H(u) - E(H(z)))^2 p_v(z-u)\mathrm{d}u \tag{3}$$

$$= \int_{-\infty}^{+\infty} H(u)^2 p_v(z-u)\mathrm{d}u - E(H(z))^2$$

In general, $\mathrm{var}(H(z)) \neq \mathrm{var}(H(-z))$. The exception is with any linear and continuous function, as evident from eqn. (1).

Special functions

Based upon eqn. (1), the vertical distribution of environmental factors is given by substitution of the f- and g-functions into eqn. (2).

- -

*) last line should read

$$\int_{-\infty}^{+\infty} h(u-z)\, p_v(u)$$

206

A special case of eqn. (2) is the actual mean depth $D(z)$, which from Table II is given by

$$D(z) = E(\mathrm{d}(z)) = \int\limits_{-\infty}^{+\infty} \max(u - z, 0) p_v(u) \mathrm{d}u \tag{4}$$

The mean depth $D(z)$ re z-scale is always different from $|z|$ (except in the rare case of a constant water level), and the magnitude of this difference depends on the pdf $p_v(z)$. Furthermore, $D(z)$ is always greater than zero for all levels not exceeding the maximal water level observed.

The implication is that depth in its time-averaged sense is *not equivalent* to relative elevation, even with elevation datum located at the median water level.

From $D(z)$, the mean hydrostatic pressure at any z-level $P(z)$ is

$$P(z) = K(Z_0) + a D(z) \tag{5}$$

K = pressure at Z_0, approx. 1 Atm.

a = pressure coefficient, approx. 0.1 Atm. m^{-1} water

Thus, hydrostatic pressure equals the mean depth $D(z)$ in its ecological information value.

Ice-scour stress at draw-down $IS(z)$ may be estimated from the pdf $p_{v;\mathrm{winter}}(z)$ by a time-domain convolution as

$$IS(z) = \int\limits_{-\infty}^{+\infty} b(u - z) p_{v;\mathrm{winter}}(u) \mathrm{d}u \tag{6}$$

with the "box" function $b(u)$ defined by

$$b(u) = \begin{cases} 1 & \text{if } -0.1 d_{\mathrm{ice}} \geqslant u \geqslant 0.9 d_{\mathrm{ice}} \\ 0 & \text{otherwise} \end{cases}$$

By normalizing $IS(z)$ to unity, $IS(z)$ estimates the probability of ice scour at any z-level. Ice thickness d_{ice} is preferably a mean for the ice-covered period.

The regulation impact on the actual subsurface light regime is complex. The following presentation aims at the salient features, and uses a much simplified statistical model.

Subsurface irradiance in general follows an exponential law, which as a time-function of z-levels is conveniently described by

$$I(z,t) = I_0(t) H(z,t) \tag{7a}$$

$$i(z,t) = I(z,t)/I_0(t) \tag{7b}$$

with

207

$$H(z,t) = \begin{cases} \exp\left(-Kv(z,t)\right) & v(z,t) \geqslant 0 \\ 1 & \text{otherwise} \end{cases}$$

I_0 = Irradiance immediately below the water surface
K = Random variable, distributed Normal (k,s^2)
$\quad k$ = mean vertical coefficient of attenuation (ln-units m^{-1})
$\quad s$ = standard deviation of K

The available subsurface irradiation at any depth correlates to the photosynthesis activity of submerged macrophytes. There is some evidence that underwater light controls the lower vertical range of macrophytes through the probability of critical threshold levels (Rørslett, 1983, 1984).

The threshold probabilities are easily related to fluctuating water level by eqns. (2) and (7a,b). As a first approximation, the regulation impact on relative threshold intensities, r, is outlined. Seeking the probability $(i(z) \leqslant r)$, eqn. (7b) is simplified to

$$\ln i(z,t) = -Kd(z,t) \tag{8}$$

which demonstrates that the random variable

$$\frac{\ln i(z,t) + kd(z,t)}{sd(z,t)}$$

is distributed normal $(0,1)$. Noting that $\ln i(z,t) = 0$ for $d(z,t) = 0$, the threshold probability is obtained as

$$\text{Prob } (i(z) \leqslant r) = \int_{-\infty}^{0} G\left(\frac{k|u| + \ln r}{s|u|}\right) p_v(z-u) du \tag{9}$$

where $G()$ is the Gaussian integral

$$G(t) = (2\pi)^{-1/2} \int_{-\infty}^{t} \exp\left(-u^2/2\right) du$$

The convolution integral in eqn. (8) is easily evaluated by computer, using a polynomial approximation to G (Davies, 1971). The lower limit of integration is then the maximum depth magnitude.

Bias in depth references

Assume a sinusoidal fluctuation of water level, with fixed amplitude A. In this case, the mean and median water levels coincide. Time-averaged depth $D(z)$ now equals the magnitude of z for $z \leqslant -A$, and is true zero for $z \geqslant A$. However, in the intermediate range $|z| < A$, the solution of eqn. (2) with an appropriate pdf $p_s(z)$ (Bendat and Piersol, 1966, p. 62)

208

$$p_s(z) = \begin{cases} 1/\pi(A^2 - z^2)^{-1/2} & |z| < A \\ 0 & \text{otherwise} \end{cases}$$

yields the time-averaged depth in this region as

$$D(z) = 1/\pi(A^2 - z^2)^{1/2} - z(1 - P_s(z)) \tag{10}$$

where $P_s(z) = 1/\pi(\pi/2 + \text{Arcsin } z/A)$

Thus, appreciable bias in magnitude exists when elevation is used in lieu of the time-averaged depth $D(z)$, as evident from Fig. 3. From eqn. (10), the maximum deviation is A/π at $z = 0$.
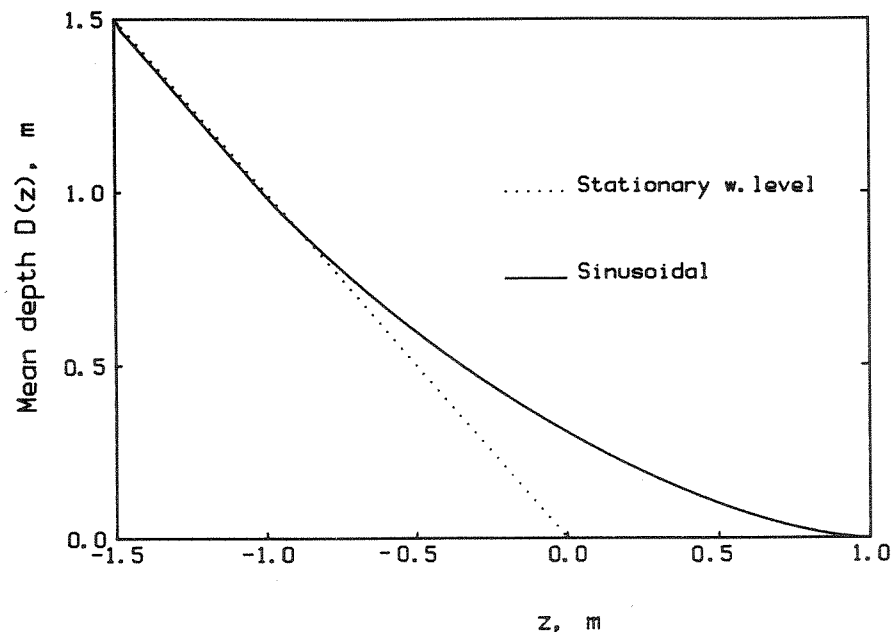
Fig. 3. Bias in depth vs. relative elevation. Sinusoidal water level variation with amplitude $A = 1$ m.

By definition, $d = D(z)$ is a monotone decreasing function with domain $z \leqslant z_{max}$ and range 0—D_{max}; hence there exists an inverse $D^{-1}(d) = z$. Thus, both time-averaged depth and z-scale (within the domain of D) theoretically have the same information content as vegetation distribution parameters. However, depth $D(z)$ is a measure of central tendency (mean), not of time and duration, on which the z-scale is based.

Towards the lower limit of $D(z)$, a substantial part of the z-domain maps into a restricted range of $D(z)$. This implies that the inverse $D^{-1}(d)$ may be difficult to compute accurately in this range.

RESULTS AND DISCUSSION

Regulation impact on environmental factors

The impact of regulations are now considered for the investigated lakes. The vertical distribution of environmental factors in the z-scale is estimated from eqn. (2) and the actual pdf $p_v(z)$. Regulation impact is then assessed by recalculating eqn. (2) with a Dirac-spike pdf centered at $z = 0$. In the following, the statistical treatment applies to no year in particular, but reflects the long-time properties of each lake.

Water-level statistics

The cumulative probability of water levels are shown in Fig. 4 in dimensionless form by scaling the abscissa as $(z - z_{min})/(z_{max} - z_{min})$; thus allowing for easy comparison between lakes.
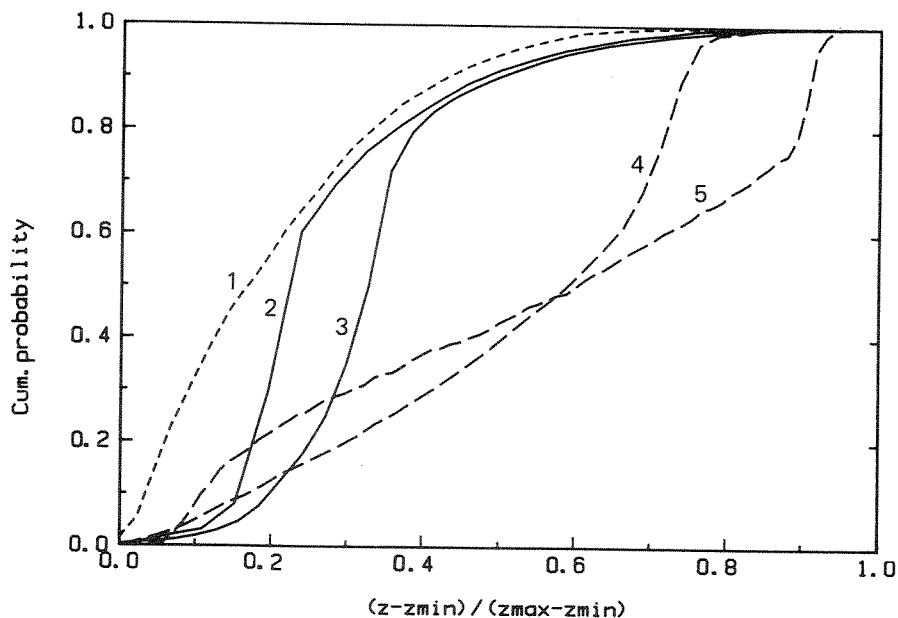
Fig. 4. Water level cumulative probability distribution for selected lakes. Abscissa scaled according to maximum range of water level variation. 1, Vangsvatn; 2, Kilefjord; 3, Tyrifjord; 4, Randsfjord; 5, Hartevatn.

Most regulated lakes in Norway are storage reservoirs, with water level draw-down at winter time. This results in a concave upwards cdf, as exemplified by Lakes Randsfjord and Hartevatn in Fig. 4, due to the uniformly distributed low water levels. The unregulated Lake Vangsvatn shows a strongly upwards convex cdf, indicating that no particular level is prominent. The short-time regulated Kilefjord, and the large Tyrifjord with strong hydraulic damping, show intermediate cdf's, indicating the prominence of water levels close to the median.

210

The actual mean depth of water overlaying the submerged vegetation, $D(z)$, may be computed from eqns. (2) and (4). Since the water levels in the investigated lakes show significant variations throughout time, the $D(z)$-values are computed separately for the growth season (ice-free period) and the winter (ice-covered period).
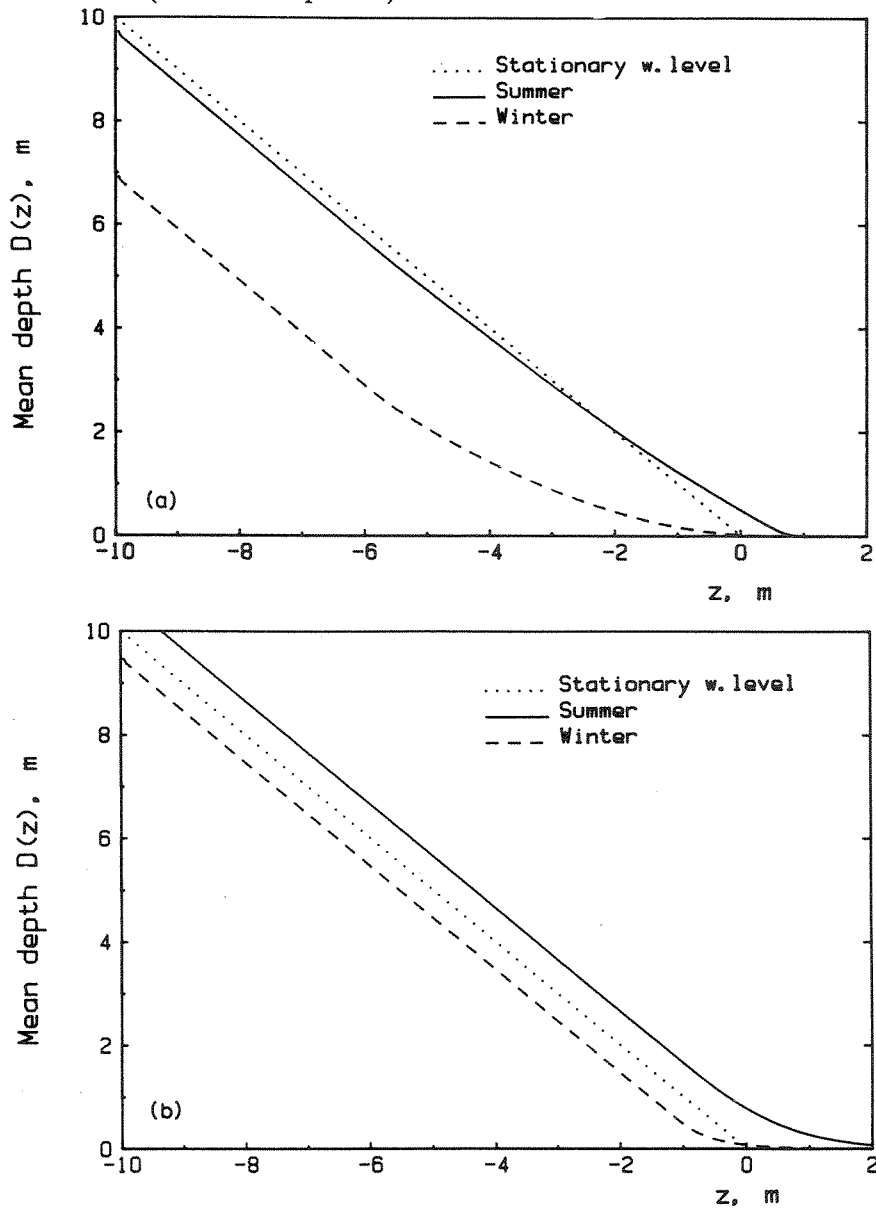
Fig. 5. Time-averaged mean depth $D(z)$ vs. z-level, summer and winter situation in Lakes Hartevatn (a) and Vangsvatn (b).

Figure 5a shows the pronounced difference of summer vs. winter $D(z)$-values for the strongly regulated Lake Hartevatn. In this lake, summer $D(z)$-values closely follow the vertical levels up to the -3 m level. At higher elevations, $D(z)$ exceeds the magnitude of z. The winter $D(z)$-values are far lower, approaching the magnitude of z at higher z-levels.

The unregulated Lake Vangsvatn has a maximal water-level amplitude almost equal to Hartevatn (Table I). Summer $D(z)$-values in Vangsvatn exceed the magnitude of z at all levels (Fig. 5b), whereas the winter situation is reversed. $D(z)$ is nearly linear below the -1 m z-level, but is strongly non-linear in z at higher levels.

Vertical level thus is a heavily biased estimate of depth in its time-averaged sense in these lakes, at least in the intermittently inundated zone. This could be expected from eqn. (10). Below the datum, i.e. the median water level, the bias magnitude is <0.5 m for lakes with annual water-level variation less than 2 m.

Impact on the extent of ice-scour

The normalized ice-scour stress $IS(z)$ was computed from eqn. (6) with ice thickness data from field measurements. Examples of $IS(z)$ are shown in Fig. 6.

In general, ice-scour extent positively correlated to the mean annual range of water level variation. However, the vertical scour distribution clearly differs in detail between lakes with similar ranges of water fluctuations (cf. Fig. 6). Storage lakes with regular draw-down patterns, e.g. Hartevatn (and Breidvatn), display a pronounced 2-peaked distribution of $IS(z)$, corresponding to the high water level at freeze-up time, and the prevailing low winter-time water level. At intermediate z-levels, ice-scour might be less intense (Fig. 6a). A large lake, Byglandsfjord, features an irregular winter draw-down, which is clearly reflected by the scour pattern (Fig. 6b).

Lake Kilefjord is dominated by short-time regulation (Rørslett, 1983), and ice-scour in this lake is strongly concentrated at the 0, -0.5 m z-range. Tyrifjord has a closely similar scour pattern. The estimated scour activity, however, extends to somewhat lower z-levels in this lake (-1, -1.6 m).

Light intensity and threshold distribution

Based upon eqn. (7b), the relative light intensity in each lake was estimated for the ice-free growth season. Water level fluctuations influenced the estimate significantly in shallow waters, resulting in up to 40% deviation either way compared to a stationary water level. This effect ceased rapidly below the -2 m z-level in all lakes except Hartevatn, in which an increase in average intensity could still be demonstrated at the -4 m level.

Regulation impact is severe, however, when the probability distribution of threshold intensities is considered. Contrary to the direct intensity distribution, impact in this case is most adverse towards deeper waters. Based upon eqn. (9), the regulation impact on threshold probability distribution is

212
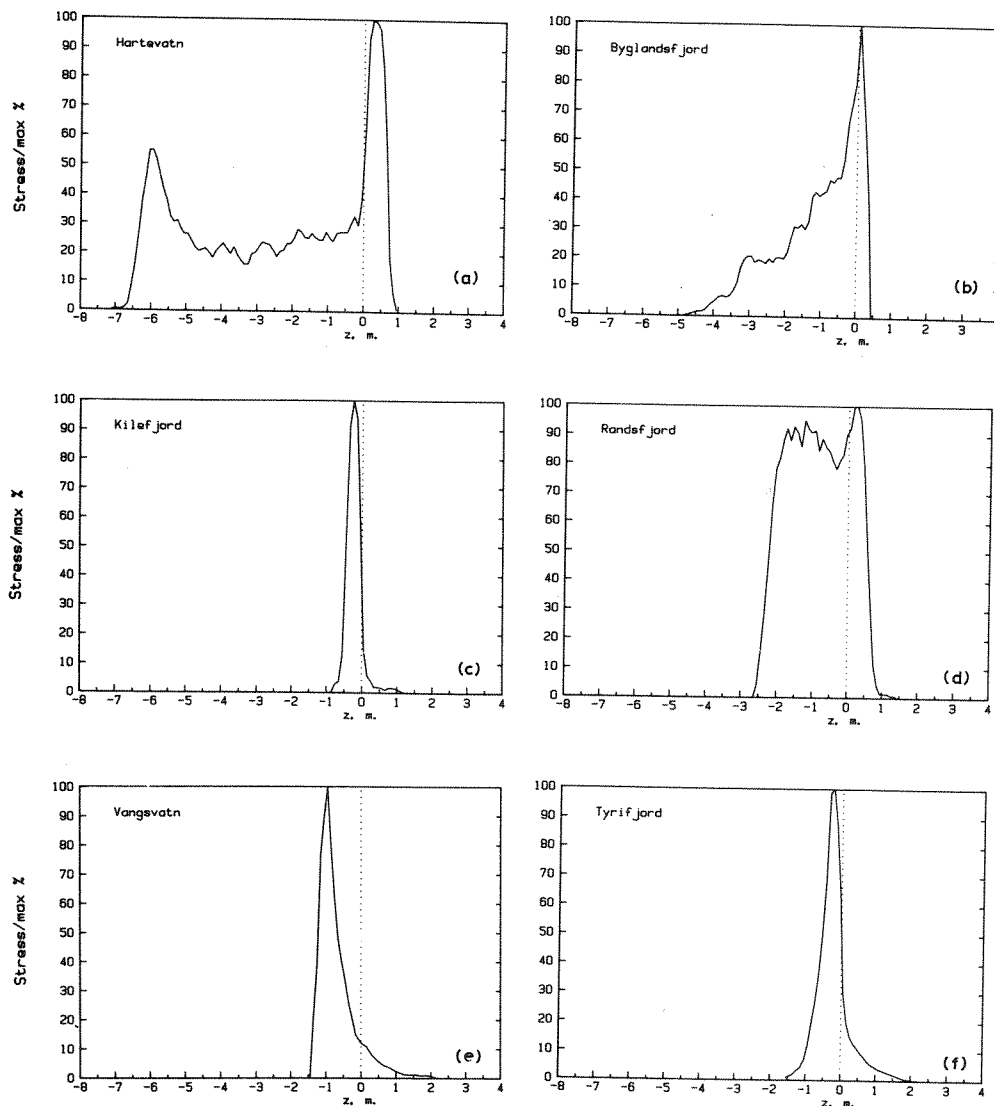
Fig. 6. Estimated vertical distribution of ice-scour stress IS(z). Stress function scaled relative to maximum value for each lake.

illustrated for Lake Tyrifjord (Fig. 7). The vertical threshold probability distribution is shifted into shallower waters (i.e. higher z-levels) when due attention is paid to the varying extent of water overlaying each z-level.

The threshold distributions for thresholds between 1 and 50% relative light intensity in the heavily regulated Lake Hartevatn are shown in Fig. 8. The inflection point of each threshold probability distribution coincides with the time-averaged mean relative light intensity curve, as would be expected from eqn. (9), since the vertical attenuation coefficient K of eqn. (8) is statistically independent of the water level probability distribution.

213
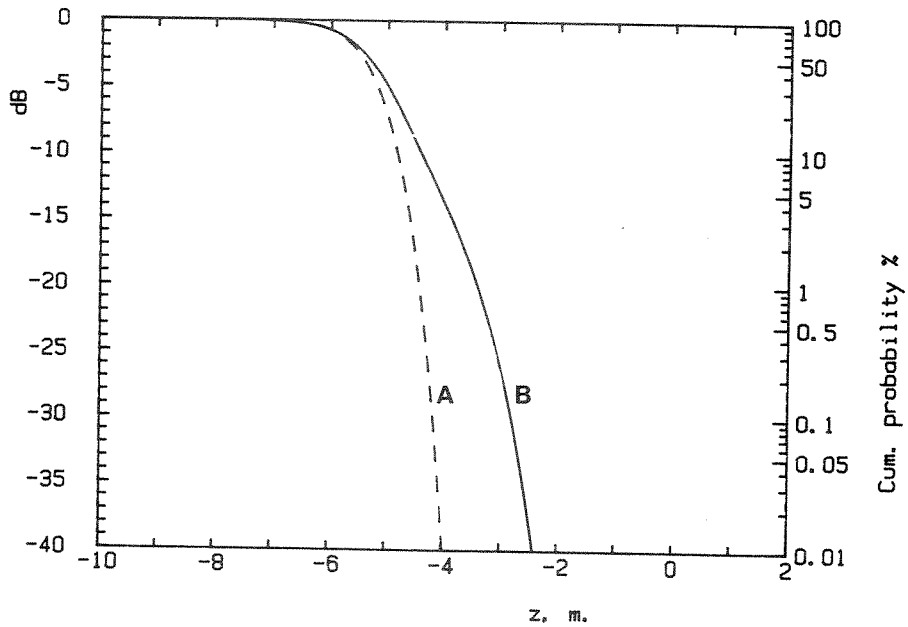
Fig. 7. Estimated vertical cumulative probability distribution for relative subsurface irradiation less than a threshold. A, stationary water level; B, actual pdf $p_v(z)$. Lake Tyrifjord, ice-free period, threshold $r = 6\%$.
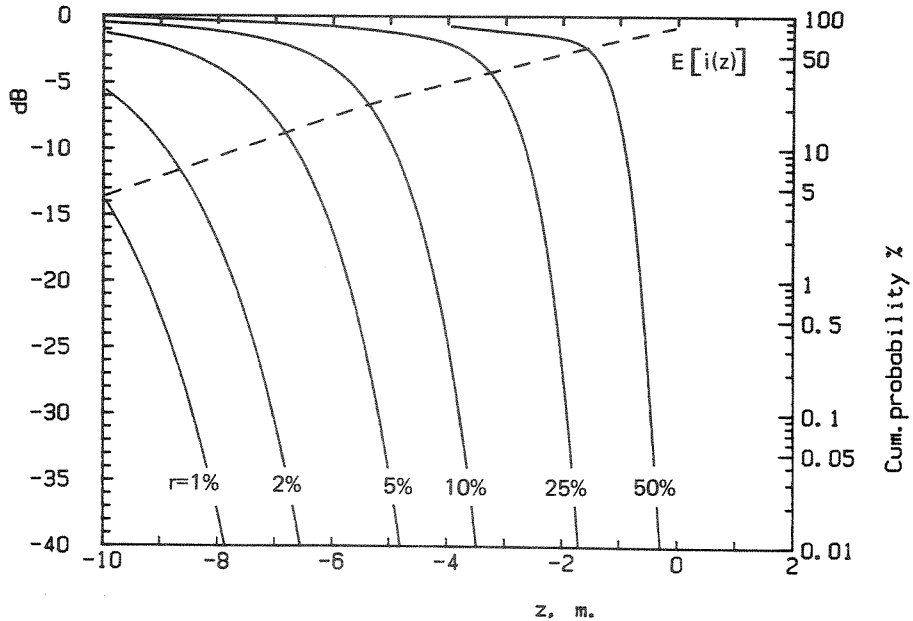
Fig. 8. Estimated vertical cumulative probability distribution for relative light thresholds 1—50%. Dashed line indicates expected relative light intensity $E(i(z))$ (use scale at right, as percentage of intensity). Lake Hartevatn, ice-free period.

214

Regulation impact on submerged macrophyte communities

The macrophyte communities in the investigated lakes are mostly dominated by isoetids (mainly *Isoetes lacustris* L.). In the less extremely oligotrophic lakes (Tyrifjord, Randsfjord), some elodeids (e.g. *Myriophyllum alterniflorum* DC., *Elodea canadensis* Michx) are abundant. Deep-water communities with stoneworts (*Nitella* spp.), bryophytes (*Sphagnum* spp.) and freshwater sponges (*Spongilla* cf. *lacustris* (L.)) are characteristic of all lakes. Helophytes have negligible abundance in these lakes.

The distribution patterns of macrophytes in the investigated lakes could not be statistically correlated to water chemistry, lake altitude, temperature or location of the thermocline (Rørslett, 1983, 1984). Site exposure affected significantly the lower depth limits reached by some species, e.g. *Isoetes lacustris* (Rørslett, 1983). However, community statistics such as upper vertical limits or mean (biomass-weighted) depth were not significantly correlated to site exposure within the extensively investigated Lake Tyrifjord (Rørslett, 1983).

Qualitative vegetation response to regulation

The submerged macrophyte communities, in general, respond to increasing extent of regulation, i.e. larger annual water-level variation, along two response pathways:

(1) A reduction in community diversity and organization pattern. The *r*-strategy species (e.g. *Nitella*) gain in relative importance, compared to the *K*-strategy species (e.g. *Isoetes*). The mean number of aquatics reduces from typically 10—25 in lakes with regulation heights less than 3 m (Kilefjord, Breidvatn, Tyrifjord, Randsfjord), to 1—3 species in the more heavily regulated lakes (e.g. Hartevatn). Vegetation patchiness increases concurrently.

(2) The peak community performance is shifted into deeper waters.

These responses are illustrated in Fig. 9, based upon the available vegetation data from the lakes investigated. The vertical location of the prevailing submerged community is indicated by the characteristic (biomass-weighted mean) depth D_c (Rørslett, 1983). Time-averaged depth is applied in order to facilitate between-lake comparisons. The characteristic depth increases significantly with the mean annual range of water level variation (log D_c = $0.28 + 0.12$ Range; $P < 0.01$).

The gradual break-down of community structure reflects the increasing environmental stress and instability brought about by the regulation schemes. The mainly *Isoetes lacustris*-dominated communities survive to at least 5 m annual range of water-level variation. However, in some lakes with less annual fluctuation of water level, e.g. Randsfjord, *Isoetes* is conspicuously absent from many potential sites. This furnishes an "empty" niche which, in the case of Randsfjord, was recently invaded by *Elodea canadensis*.

Perennial submerged macrophytes in general are confined to *z*-levels below

215
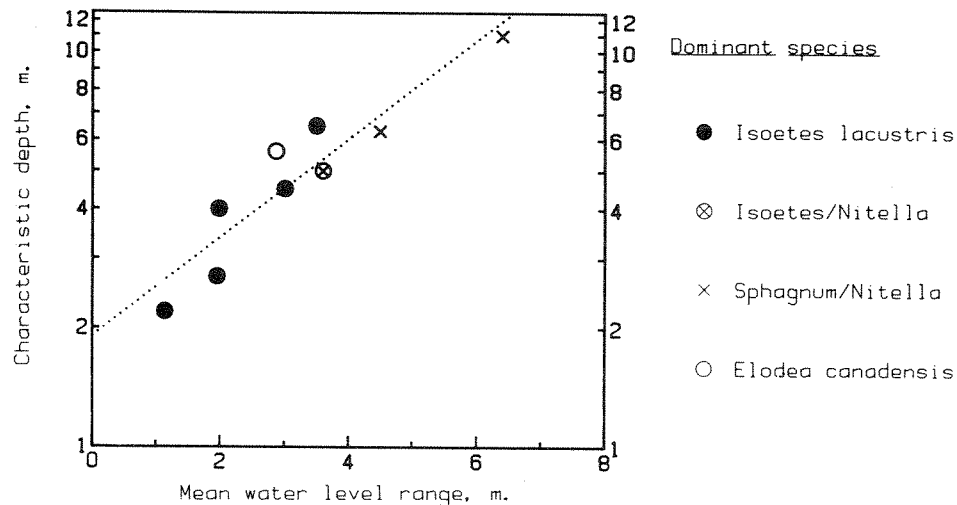
Fig. 9. Characteristic (biomass-weighted mean) depth D_c of the prevailing submerged community in each lake, against the mean annual range of water level fluctuations. Each lake is represented by its most exposed site. Note that *depth* is applied in its time-averaged sense, in order to compare lakes with widely differing water level schedules.

the ice-scour region, whereas some annuals (e.g. *Eleocharis acicularis* (L.) R.&S., *Subularia aquatica* L.) manage to survive at the intermediate scour region found at e.g. Lakes Hartevatn and Breidvatn. The generally increased extent of ice-scour, however, means that a large part of the vertical *z*-domain remains hostile to submerged aquatics in the strongly regulated lakes. The vertical displacement towards deeper water reflects the truncation of the upper potential niche. Concurrently, typical shallow-water species such as *Lobelia dortmann* L., *Littorella uniflora* (L.) Aschers., and many elodeids, are eliminated.

The paucity of data on submerged communities in regulated Scandinavian lakes does not permit a generalization of the trend indicated in Fig. 9. Nilsson (1981) reports a sparse submerged community (*Nitella, Callitriche* and *Ranunculus peltatus* Schrank) from the North Swedish lake Övra Björkvattnet, which has a 5.9 m nominal regulation height. No depth data were given, but the community apparently occurred at more than 6 m below the maximum water level. Nilsson's observations could fit well into the trend shown by Fig. 9. Whether strongly regulated lakes with regulation heights in excess of 10 m are devoid of submerged vegetation or not, remains an open question.

Regulation impact on the extent of the vertical niche

The general pattern shown in Fig. 9 focusses on the extent and possible displacement of the vertical niche due to regulation impact.

The vertical niche could be defined in probabilistic terms by the joint cumulative probability distribution of the ambient factors which constitute

216
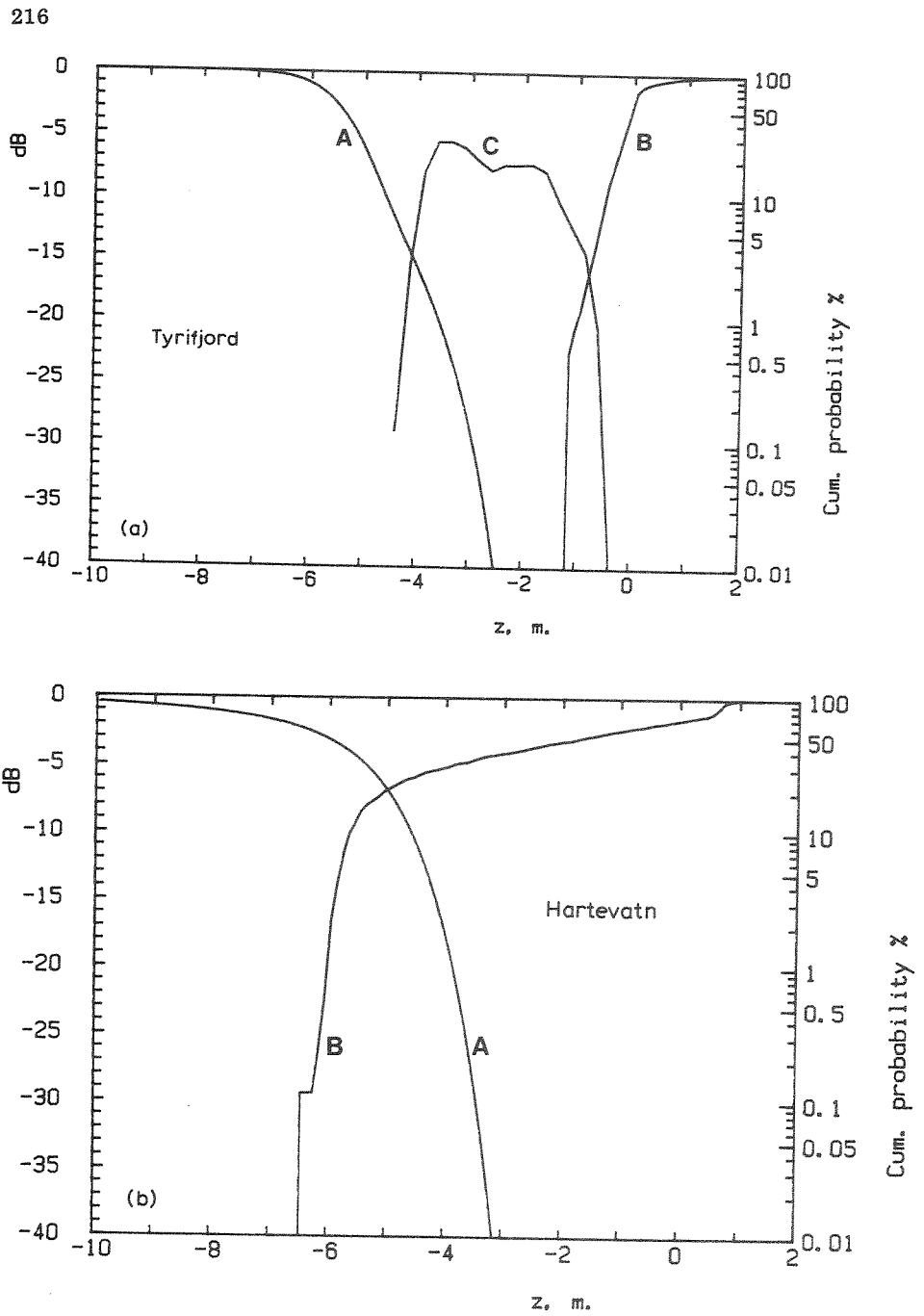
Fig. 10. Vertical cumulative probability distribution of threshold light occurrence (A, $r =$ 6%) and ice-scour stress $IS(z)$ (B). *Isoetes lacustris* coverage is plotted as curve C, using dB-scale with 0 dB = 100% cover. Lake Tyrifjord, abundant *Isoetes lacustris*. Lake Hartevatn, *Isoetes lacustris* absent.

217

the niche hyperspace, when these factors are functionally related to the vertical gradient. With statistically uncorrelated factors, the niche probability space is given by the set of individual cdf's. Derived cdf's might be computed for factors operating through cumulative or threshold effects.

Deep-water penetration of isoetids correlates with light-induced thresholds (Rørslett, 1983). The actual vertical distribution of subsurface thresholds was computed from eqn. (9), with $r = 6\%$. This value correlates significantly with the lower limit of depth extension for *Isoetes lacustris* in Lake Tyrifjord (Rørslett, 1983).

Compared to the case of a stationary water level, regulation tends to shift the threshold distribution into shallower waters (cf. Fig. 8), thus the spatial extent of potential niches is reduced. The computed distributions clearly differ between lakes, depending both on the actual pdf $p_v(z)$ and the probability distribution parameters of the random variable K in eqn. (7b).

The z-domain cumulative distribution of threshold light and ice-scour probability is given in Fig. 10 for two contrasting lakes (Tyrifjord, abundant *Isoetes lacustris*, and Hartevatn, *Isoetes lacustris* completely lacking). Hartevatn is situated downstream of the less regulated Lake Breidvatn, in which *Isoetes* is abundant. The actual depth distribution of *Isoetes lacustris* is clearly bounded within the niche space defined by ice-scour and threshold underwater light climate (Fig. 10a,b).

By transforming the niche axes spanned by these two factors into the equivalent probability space, the realized vertical niche of *Isoetes lacustris* in all the investigated lakes is represented in Fig. 11 in a much condensed form.
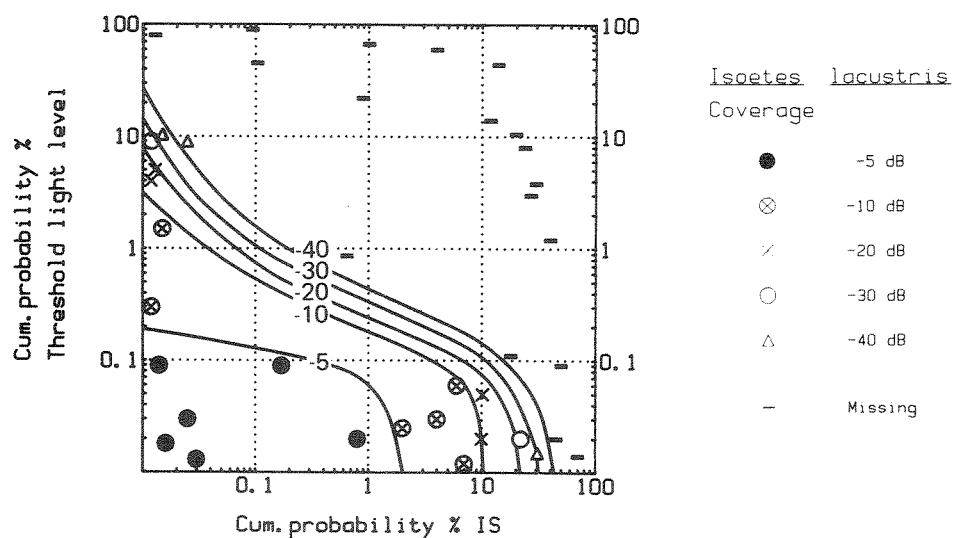
Fig. 11. Niche probability space for *Isoetes lacustris*, defined by threshold light occurrence ($r = 6\%$) and ice-scour stress. Data from all lakes.

218

Ice-scour is clearly an "all or none" factor, thus *Isoetes* performance declines abruptly when ice-scour cumulative probability exceeds some 20% (cf. Fig. 11). Threshold light probability acts more gradually, as shown in Fig. 11. The synergistic effect of combined threshold light and ice-scour probability is evident, leading to the complete absence of *Isoetes lacustris* in central areas of the probability space.

The probability space representation suggests a 10% threshold light occurrence probability and about 20% ice-scour probability as niche limits, if *Isoetes* performance should exceed 1% (-20 dB) cover. With these limits, the vertical niche extents for all investigated lakes are given in Fig. 12.
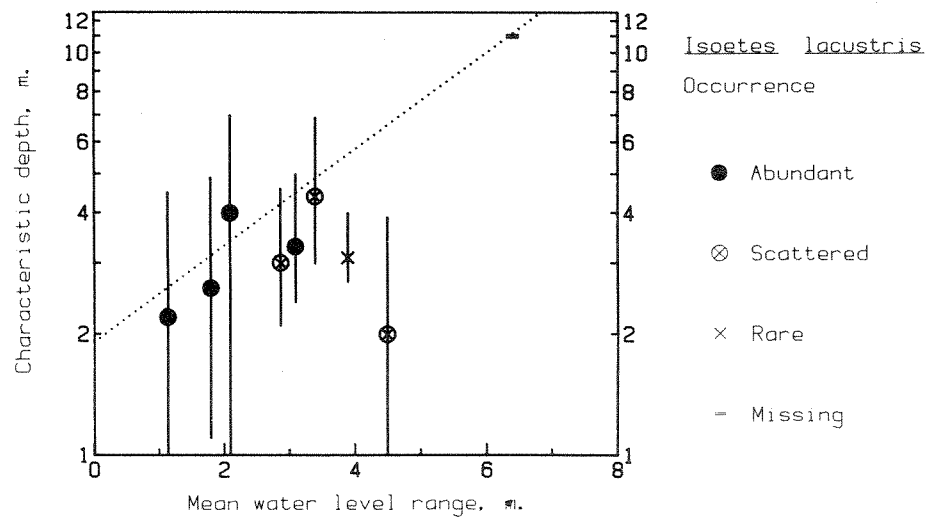
Fig. 12. Niche limits for *Isoetes lacustris*, superimposed on the characteristic depth D_c for the prevailing submerged community in each investigated lake.

The vertical niche extent declines in the more strongly regulated lakes, mostly due to the unfavourable underwater light regime towards the deeper waters. The absence of *Isoetes lacustris* from the heavily regulated Lake Hartevatn could be explained by the fact that the niche extent is nil in this lake. Marginal *Isoetes* lakes, such as Randsfjord and Byglandsfjord, have a much reduced vertical niche extent compared to the *Isoetes lacustris*-dominated Lakes Kilefjord and Tyrifjord. The extension of the vertical niche into shallower waters are fairly well correlated to the mean annual range of water-level variations (Fig. 12). However, the very different probability distributions of water levels in these lakes result in large deviations from the general trend. Lake Vangsvatn, with a wide natural fluctuation of water level, is an evident example. Thus, it is necessary to consider the total probability distribution of water level fluctuations, and not just the mean depths and fluctuation ranges.

219

CONCLUSIONS

Clearly, the concepts of depth and relative elevation need to be carefully distinguished. This is essential when a regulated lake with appreciable fluctuation of water level is considered. Even by relating the vertical position of a plant site to the median water level as datum, site depth in its time-averaged sense is not equivalent to the relative elevation of this point. Furthermore, the magnitude discrepancies, in general, are large in shallow waters where many species attain their peak performance.

Recasting the vertical distribution of submerged macrophytes in terms of the time-averaged depth $D(z)$ resolves ambiguity. Between-lake comparisons of depth distributions are then facilitated. However, much of the information value residing in the pdf $p_v(z)$ is lost.

Ambient factors are easily evaluated as functions of the z-scale, i.e. relative elevation. This approach caters for the time-probability associated with a fluctuating water level, and by definition includes instantaneous depths. Thus, the probability distributions of the ambient factors at any elevation are available, in addition to the expected (time-averaged) values. Between-lake comparisons, however, are no more easy to perform with z-domain representation than with time-averaged depth, unless the data are transformed into the equivalent probability space.

The prevailing winter-time draw-down of Norwegian regulated lakes results in extensive ice-scour along the vertical gradient. The extent of ice-scour governs the upper limits of perennial submerged species. Annual species might occur within the scour region; their quantitative performance, however, are reduced.

The vertical niche of the dominant species in the lakes studied, *Isoetes lacustris*, is in general displaced towards lower z-levels, i.e. deeper waters, due to the regulation impact. In general, the vertical extent of the niche is reduced concurrently with an increased regulation height. Niche limits derived from the niche probability space representation fit the observed data well. Communities dominated by *Isoetes lacustris* survive to an annual water-level range in excess of 5 m. However, the light conditions combined with the water level schedule determine the probability of *Isoetes* survival.

ACKNOWLEDGEMENTS

220

REFERENCES

Bendat, J.S. and Piersol, A.G., 1966. Measurement and Analysis of Random Data. Wiley, New York, 390 pp.

Davies, R.G., 1971. Computer Programming in Quantitative Biology. Academic Press, London, 492 pp.

Hutchinson, G.E., 1975. A Treatise On Limnology. Vol. 3. Limnological Botany. Wiley, New York, 1075 pp.

Nilsson, C., 1981. Dynamics of the shore vegetation of a North Swedish hydro-electric reservoir during a 5-year period. Acta Phytogeogr. Suec., 69: 1—94.

Quennerstedt, N., 1958. Effects of water level fluctuation on lake vegetation. Verh. Int. Verein. Limnol., 13: 901—906.

Rørslett, B., 1983. Tyrifjord og Steinsfjord. Undersøkelse av vannvegetasjon 1977—82. (Lakes Tyrifjord and Steinsfjord. Investigations on the aquatic vegetation 1977—82. In Norwegian). Norwegian Institute for Water Research, Report 0-7800604, 300 pp.

Rørslett, B., 1984. Regulation impact on the submerged macrophytes in the oligotrophic lakes of Setesdal (S. Norway). Verh. Int. Verein. Limnol., 22: in press.

Rørslett, B., Green, N.W. and Kvalvågnæs, K., 1978. Stereophotography as a tool in aquatic biology. Aquat. Bot., 4: 73—81.

Sculthorpe, C.D., 1967. The Biology of Aquatic Vascular Plants. Arnold, London, 610 pp.

Stanley, R.A., Shackelford, E., Wade, D. and Warren, C., 1976. Effects of season and water depth on Eurasian watermilfoil. J. Aquat. Plant Manage., 14: 32—36.

Statistisk Sentralbyrå, 1983. Naturressurser 1982. (Norwegian nature resources 1982. In Norwegian). Central Bureau of Statistics of Norway, Report 83/1: 1—62.

Wassén, G., 1966. Gardiken. Vegetation und Flora eines lappländischen Seeufers. K. Sven. Vetenskapsakad. Skr. Naturskyddsärenden, 22, 142 pp.

Statistics of the underwater light field

Bjørn Rørslett

Norwegian Institute for Water Research
P.O.B. 333 Blindern, N-0314 Oslo 3, Norway.

ABSTRACT

The underwater light field is described as a stochastic process, with the vertical attenuation as a random variable. It is shown that the vertical attenuation integral is well described as a Normal process with uncorrelated increments. The attenuation processes within a water bodyare found to be independent of the incoming irradiance. Thus, the relative light intensity at any depth can be approximated by a Lognormal random variable.

The stochastic description enables the definition of derived functions, e.g., the expected duration and intensity of the underwater light field below any selected threshold value. The impact of a fluctuating water level can be assessed as well.

Measurements of underwater light intensity from a number of lakes in Southern Norway fitted the model with no statistically significant deviations. The studied lakes were mainly oligotrophic. The two productive lakes included did not violate the model, however.

INTRODUCTION

Downwelling subsurface irradiance is a major environmental factor influencing the submerged macrophyte communities in freshwater lakes (SPENCE 1982). Commonly, the waveband 350-700 nm (photosynthetic active radiation, "PAR") is roughly equated with visible light (KIRK 1977).

The underwater light field is highly variable in space and time (KIRK 1977). The inherent variability of the light field renders the statistical analysis of potential macrophyte-light relations difficult. However, once a statistical description of the light field is established, hypotheses of macrophyte response to the light factor can be formulated and tested. It should be stressed that statistical analysis of such responses do not need the resolution of light field features into the physical mechanisms causing attenuation per se. Thus, this approach clearly deviates from recent research on underwater light fields (JERLOV 1976, KIRK 1981a, 1981b). Put simply, any statistical description which enables a good prediction of the light field encountered by a submerged macrophyte, would be sufficient.

Based on data from a number of mainly oligotrophic Norwegian lakes, I propose a stochastic model of the underwater light field. The model relies on the Central Limit Theorem, which states that the sum of partly independent variables tends to a Normal distribution. Light attenuation in water is caused by scattering and absorption by several sources, such as living and non-living particulate suspended matter, dissolved coloured substances, and so on (SPENCE 1982). The measurement errors contribute to the observed variability. This would imply that the apparent attenuation might follow a Normal probability law.

The model is developed for the ideal case of a stationary water level. However, the impact of a fluctuating water level should also be addressed, since many lakes and reservoirs show significant annual variations of their water level. To discriminate between these aspects the symbol 'v' is used throughout to indicate instantaneous depth as the downwards distance from the current water surface, whereas the symbol 'z' is applied only for functions of relative elevations, cf. RØRSLETT (1984a).

MATERIAL AND FIELD METHODS

Measurements of downwelling PAR irradiance from a number of sites in South Norway, encompassing mainly low to medium altitude, soft-water lakes were available for statistical analysis. The geographical locations of the lakes are shown in Fig.1. Pertinent data on morphometry, hydrology, and hydrochemistry are given by FAAFENG et al. (1981, 1982), and RØRSLETT (1984a). The lakes range from ultra-oligotrophic (Secchi transparency 10-23m) to distinctly eutrophic (Secchi transparency 1.2-4m).

In the years 1978-1984, lake PAR data were obtained with a Li-COR quantum meter, type 185A, equipped with a Li-COR 192S underwater sensor. The data base included N=160 observation series from 18 sites in 12 lakes, comprising some 1500 data items. Measurements within each lake were performed intermittently from early spring to late autumn, covering a wide range of weather situations. Collected data were processed by proprietary computer programs, mainly written in Extended BASIC for Hewlett-Packard series 80 microcomputers.

Continuous readings of PAR were acquired from one lake (Maridalsvatn) for periods up to 14 days. Data were obtained at subsurface level and at 3m depth. The data collecting buoy was moored at 4.5m depth, at a fairly wind-exposed site. Thus, the underwater sensor was situated some 1.2-1.5m above the lake floor, when water-level fluctuations within the sampling period were taken into account. Sampling interval was 5 minutes, and the digitized data were stored on an Aanderaa Instruments data logger. Due to instrumentation incompatibility, the full range of the Aanderaa A/D converter could not be utilized, thus some digitizing noise was evident. Hence, the computer analysis of the data was restricted to samples with less than 10% digitizing noise present.

No.	Name (# sites)	Type
1	Venneslafjord (1)	O
2	Kilefjord (1)	O
3	Byglandsfjord (2)	U
4	Åraksfjord (1)	U
5	Bykil (1)	O
6	Hartevatn (1)	O
7	Breidvatn (1)	U
8	Jarenvatn (1)	E
9	Randsfjord (3)	O
10	Tyrifjord (4)	O
11	Steinsfjord (1)	M-E
12	Maridalsvatn (1)	O
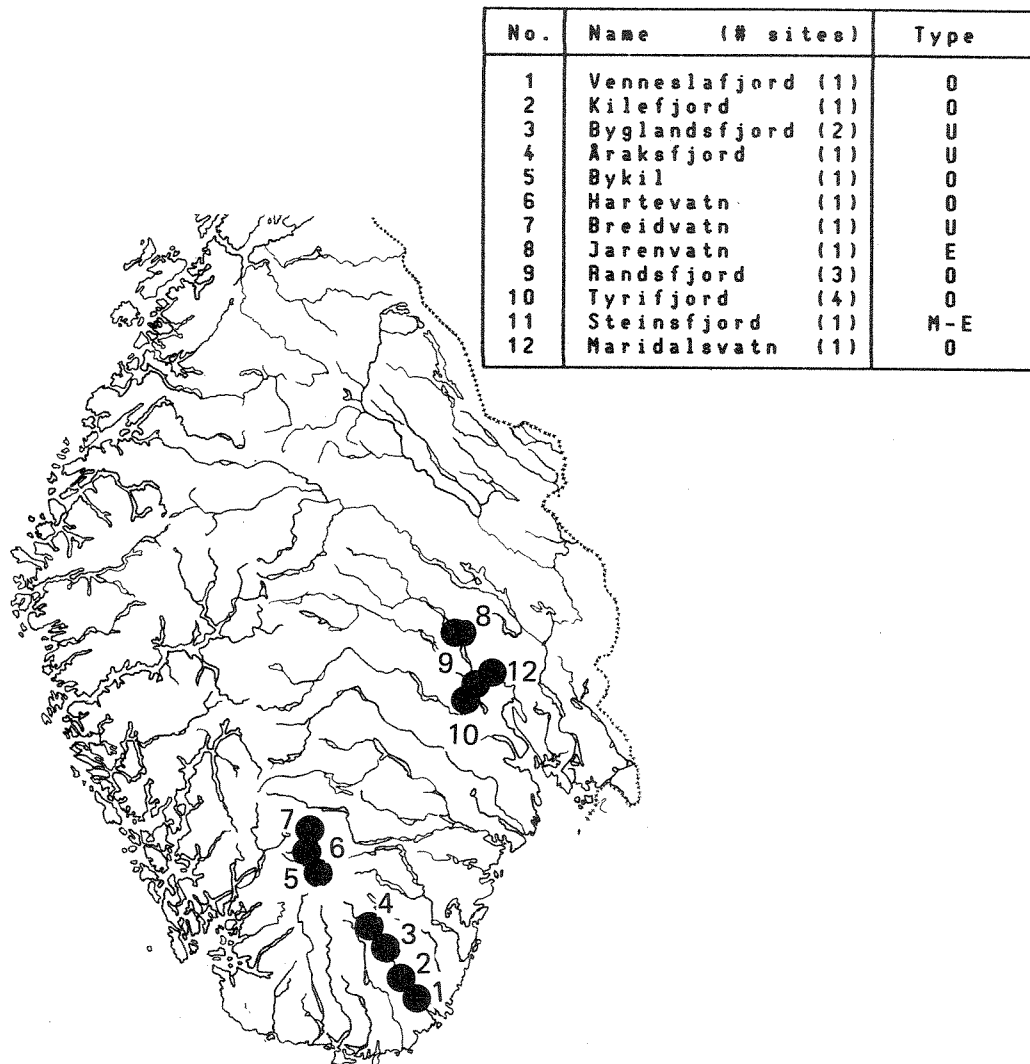
Fig. 1. Geographical location of the studied lakes in Southern Norway. Tabular insert: Lake classification, codes used are

U = ultra oligotrophic , O = oligotrophic
M = mesotrophic,   E = eutrophic

STOCHASTIC DESCRIPTION OF THE UNDERWATER LIGHT FIELD

The vertical attenuation vs. depth

Vertical attenuation of subsurface irradiance follows a generalized Beer-Lambert law. For any wavelength λ, the remaining irradiance at depth v is (BAKER & SMITH, 1982):

(1) $\quad I(\lambda,v) = I(0^+,\lambda) \exp\{ - \int_0^v k(\lambda,u) \, du\}$

where $I(0^+,\lambda)$ = irradiance just below the surface (approaching depth=0 from below).
$k(\lambda,v)$ = vertical attenuation coefficient, m^{-1}.

For the broad-band PAR spectrum (λ=400-700 nm), the remaining averaged irradiance at depth v is (starred items denote PAR quantities) :

(2) $\quad I_*(v) = I_*(0^+) \exp\{- K_*(v)\}$

where $K_*(v) = \int_0^v k_*(u) \, du = \zeta_*$

$k_*(v) = $ vertical attenuation coefficient, m^{-1}.

The parameter $\zeta_*/\ln 2$ is the PAR equivalent to the concept optical depth [1] . To emphasize the functional relationship between attenuation and depth, the notation $K_*(v)$ is preferred to ζ_*. Furthermore, the PAR annotation is dropped, since only PAR quantities will be considered from now on.

Eqn. (2) is more conveniently written in logarithmic form, thus;

(3a) $\quad \ln I(v) = \ln I(0^+) - K(v)$

or as the corresponding normalized (relative) intensity,

(3b) $\quad \ln i(v) = - K(v)$

i.e., $\quad \ln i(v) = \ln I(v) - \ln I(0^+)$

----

[1]   The optical depth, ζ, is defined by the relation:

$I(\zeta) = I(0^+) \, 2^{-\zeta}$.

For example, ζ=3 corresponds to 1/8 of the subsurface intensity (TALLING, 1957).

Provided that incident irradiance is statistically independent from the attenuation processes within that water body, eqns. (3a,b) show that the expectation of $I(v)$, i.e., $E[I(v)]$, is given by:

(4) $E[I(v)] = E[I(0^+)] \ E[i(v)]$

Thus, to ascertain the statistics of the underwater light field, only a knowledge of the stochastical properties of $K(v)$ is necessary, since $I(0^+)$ and its probability distribution can be derived from known metereological data.

Functional models for total attenuation, K(v)

Three alternative functional models for $K(v)$ are now discussed. Afterwards, their stochastical descriptions are outlined.

Model A assumes the attenuation to be constant within the water column under study, thus;

(5) $K_A(v) = k_A v$

From a physical point of view, model A clearly is an over-simplification. However, this does not invalidate its potential for a statistical description of the attenuation phenomena.

A more realistic model would include a depth-varying attenuation coefficient, e.g.;

(6) $K_B(v) = k_w v + K_n(v)$

where k_w is a background attenuation level and the depth-varying attenuation is given as:

(7) $K_n(v) = \int_0^v k_n(u) \ du$

The spectral composition of the underwater light field changes markedly with depth, the light field approaching the background attenuation of some $0.034 \ m^{-1}$ in very clear oceanic waters (JERLOV, 1976). Far higher background levels would be expected in freshwater, however. The averaging effect of quantum sensors mask the spectral composition changes to some extent (HØJERSLEV, 1979).

Now, assume the depth-varying attenuation, k_n, is described by an exponential decline, e.g.;

(8) $k_n(v) = k_0 \exp(- \kappa v)$

thus, its depth-integral K_n is given by:

(9) $K_n(v) = \lambda [1-\exp(- \kappa v)]$

 where $\lambda = k_0/\kappa$

Recently published data (KLEPPER et al., 1984) support this general shape of the vertical attenuation coefficient-depth relation.

Obviously, model A is a special case of the model B, since:

(10) $\lim_{\kappa \to 0} \lambda [1-\exp(- \kappa v)] = k_0 v$

The third model, C, is derived from model B as another special case, where the background attenuation level is zero :

(11) $K_C(v) = K_n(v)$

Finally, I introduce the depth-averaged attenuation coefficient;

(12) $\bar{k} = \langle K(V) \rangle$

 where the carets denote averaging over the water column,
 and $K(V)$ is the appropriate model (A-C).

The differential equations for the models are given by:

(13) $d \ln I/dv = - k_A$ { model A }

(14) $d \ln I/dv = - k_w - k_n(v)$ { model B }

(15) $d \ln I/dv = - k_n(v)$ { model C }

Thus, the potential models can be evaluated by plots of the log-derivative against depth.

Parameter estimation

In the model A case, parameter estimation is straightforward. A linear regression of ln I vs. depth provides for estimates of ln $I(0^+)$ and K, as the Y-intercept and slope of the regression line, respectively.

Model B has four parameters, i.e. $x = \{$ ln $I(0^+)$, λ, κ, k_w $\}$. Writing the eqn.(6) in functional form for N observations;

$$f_i = x_1 - x_2 (1 - \exp(-x_3 v_i)) - x_4 v_i - \ln I_i = 0$$

$$i = 1, \ldots, N$$

This is a condition equation for a generalized least squares adjustment problem (MIKHAIL, 1976). Assuming uncorrelated observations of equal precision, the solution is obtained by solving the matrix equation:

$$V + B\Delta = F$$

where V = residual vector to be minimalized
   B = coefficent matrix
   F = constant term vector
   Δ = vector of unknown parameters

The condition equation is linearized by Taylor series expansion, retaining only terms up to the first degree. The coefficient matrix B of partial derivatives, $B = [\partial f / \partial x]$, and the constant term vector F are given by:

$$B = \left. \begin{bmatrix} 1 \\ -1 + \exp(-x_3 v) \\ -v\ x_2\ \exp(-x_3 v) \\ -v \end{bmatrix} \right|_{\substack{x = x^0 \\ v = v_i}}$$

$$F = \left[\ln I - x_1 + x_2 \{1 - \exp(-x_3 v)\} + x_4 v \right] \left.\right|_{\substack{x = x^0 \\ v = v_i}}$$

where x^0 is a vector of first approximations

The parameter vector is given by:

$$\Delta = (B^tB)^{-1} (B^tF)$$

For this non-linear adjustment, iteration is continued until Δ is practically a null vector. The final estimate of x is:

$$x = x^0 + \Sigma\Delta$$

The model C is estimated analogously, by constraining the parameter x_4 to zero.
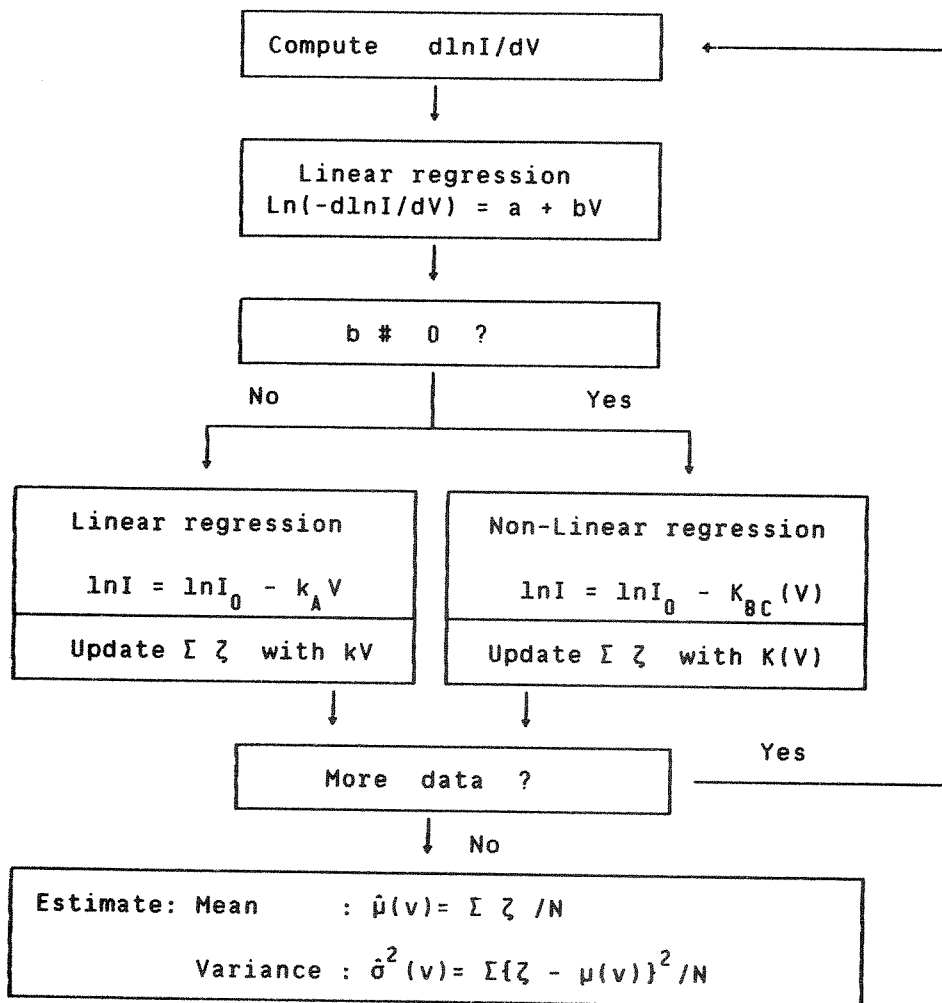
Fig. 2. Flowchart for computer estimation of underwater light field parameters.

Stochastic properties of the attenuation depth function, K(v)

So far, the stochastic nature of K(v) has been left undefined. The total attenuation within a water column is generally considered to consist of additive components (BAKER & SMITH, 1982). This makes the Normal process an excellent candidate for the attenuation process.

As a stochastic process, K(v,t) is described by its mean value function and covariance kernel (PARZEN, 1962). It should be noted that K(.,.) has a doubly defined sample space, i.e., depth and time.

The mean value function of the K(v) process, **in the depth domain**, would be:

$$(16a) \quad m(v;T) = 1/T \int_0^T K(v,t)\, dt$$

$$\lim T \to \infty$$

or

$$(16b) \quad m(v;T) = 1/T \int_0^T \int_0^v k(u,t)\, du\, dt$$

$$\lim T \to \infty$$

From eqn. (16), it follows that K(v,.) would tend to a Normal process if the attenuation changes within the water column show uncorrelated increments however small. Also, uncorrelated time increments of the K(.,t) process would produce a Normal process. Even when some correlation of K(v,t) with time existed or attenuation within the water column was largely constant, the Central Limit theorem ensures that K(v) would asymptotically tend to a Normal process under fairly wide conditions, when K(v) shows weakly time stationarity. The assertion of (partially) independent time increments would result in a covariance kernel:

$$(17) \quad C(s,t) = \sigma^2(v)\, \delta(|s-t|)$$
$$\lim T \to \infty$$

where $\delta()$ is the Dirac delta function

Assuming eqn. (17) to hold, the expectation of K(v) would be independent of time, thus;

(18) $E[K(v)] = E[m(v;t)] = \mu(v)$

Then, the stochastic process K(v) is completely specified as a sequence of random variables, each distributed Normal $\{\mu(v), \sigma^2(v)\}$.

The significance of this assertion is as follows : <u>if K(v) tends to a Normal process, then i(v) would tend to a Lognormal process</u>. This follows directly from eqn. (18), noting that ln i(v) equals -K(v).

The expectation and variance of this Lognormal process is given by:

(19) $E[i(v)] = \exp\{-\mu + \sigma^2/2\}$

(20) $Var[i(v)] = \{\exp(\sigma^2)-1\} \exp\{-2\mu + \sigma^2\}$

where $\mu = \mu(v)$

$\sigma^2 = \sigma^2(v)$

The vertical attenuation integral, K(v), is strictly positive. Under the Normality hypothesis, the probability of negative K(v) values is non-zero, but will ordinarily be vanishingly small. However, the eqns. (19-20) can easily cater for this situation by considering K(v) to be a truncated Normal process. Then i(v) would follow a truncated Lognormal law. For a truncation point at zero, the expectation and variance are given by :

(21) $E[i(v)] = \theta \exp\{-\mu + \sigma^2/2\}$

(22) $Var[i(v)] = \{\exp(\sigma^2)-\omega\} \exp\{-2\mu + \sigma^2\}$

where $\theta = \phi(\mu/\sigma-\sigma)/\phi(\mu/\sigma)$

$\omega = [\phi(\mu/\sigma-2\sigma)/\phi(\mu/\sigma)- \theta^2]$

and the Gaussian integral $\phi()$ is

$$\phi(x) = (2\pi)^{-1/2} \int_{-\infty}^{x} \exp(-u^2/2)\, du$$

INFLUENCE OF FLUCTUATING WATER LEVELS

The water level of many Scandinavian lakes fluctuates considerably, either due to seasonal run-off (mainly snow-melt) or man-made regulations carried out for hydro-electric power production. Statistics of water levels are important in order to describe the vertical gradient for e.g. benthic macrophytes (RØRSLETT, 1984a,b) in such lakes. Since the plant sites are spatially fixed, an Eulerian approach to water level statistics is selected. I have earlier (RØRSLETT, 1984a) shown that the appropriate statistics can be derived from the probability density function (pdf) of water column heights above an elevation point. The pdf are derived from the corresponding cdf:

(23a) $P_v(z)$ = Pr { water level $\leqslant$ level 'z' }

(23b) $p_v(z)$ = $dP_v(z)/dz$

This pdf represents the distribution of $v = v(z)$ at $z = 0$, such that v positive implies the actual water column heights. The z-scale datum is the median water level, and the scale is oriented negative downwards from the datum. The mapping of the Lagrangian depth coordinate v into the Eulerian coordinate $v(z)$ is through the conditional pdf :

(24) $p(v;z)$ = $p_v(v+z)$ = $p_v(u)$

where $v = v(z) = u-z$, $u = v+z$ (cf. Fig.3)

The variable v now represents instantaneous depth at elevation z. The magnitude of z-scale and depth coincides only for a truly stationary water level (RØRSLETT 1984a). In this case, the pdf degenerates into a Dirac delta function centered on $z = 0$. For a <u>stationary water level</u>, Lagrangian (v) and Eulerian (z) coordinate functions, $h(v)$ and $H(z)$ respectively, are related by:

$h(v)$ = $H(-v)$

due to the opposing scale orientations. The rationale for this choice of orientations is expressed by eqn.(24), since the conditional pdf of v given z is directly obtainable from the main pdf $p_v(z)$, and the Lagrangian coordinate then coincide with the common concept of 'depth'.
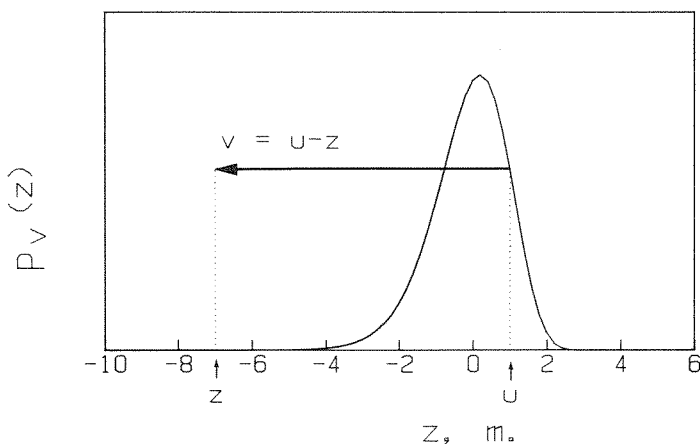
Fig. 3. Hypothetical probability density function $p_v(z)$ of water levels. The instantaneous depths $v=v(z)$ and their pdf $p(v;z)$ are derived by translations, as exemplified on the Figure ($v=u-z$, $u=1$, $z=-7$). Please note that z-axis relates to vertical levels, i.e. Eulerian coordinates. See text for further discussion.

The impact of a fluctuating water level on any (weakly) time-stationary function $H(z)$ is directly obtained by a convolution (RØRSLETT 1984a):

$$(25) \quad E[H(z)] = \int_{-\infty}^{+\infty} H(u) \, p_v(z-u) \, du$$

$$= \int_{-\infty}^{+\infty} h(u-z) \, p_v(u)$$

By this mapping, the eqns. (19, 21) for $i(v)$ can be recast into the corresponding equations for $i(z)$. Thus, noting the restricted domain of $v(z)$, and using the auxilliary $x=K(v)$, the expectation of $i(z)$ in the case of a fluctuating water level is :

$$(26) \quad E[i(z)] = \int_{0}^{+\infty} \int_{-\infty}^{+\infty} \exp(-x) \, p_v(v+z) \, f(x) \, dv \, dx$$

$$= \int_{0}^{+\infty} E[i(v)] \, p_v(v+z) \, dv$$

where $f(x) = (2\pi)^{-1/2} \, \sigma^{-1} \, \exp\{-(x-\mu)^2/2\sigma^2\}$
and the v-subscripts are dropped from μ, σ

Here, the independence of $K(v)$ from the water-level distribution is assumed (cf. RØRSLETT, 1984a). For a truncated Lognormal distribution, eqn. (21), the pdf $f(x)$ is increased by the correction factor $\theta(v)$. The corresponding variances are intractable expressions when the actual pdf $p_v(z)$ is unknown, and would have to be estimated by numerical approximations to the variance integrals, i.e.;

$$(27) \quad Var[i(z)] = \int_0^{+\infty} E^2[i(v)] \, p_v(v+z) \, dv - E[i(z)]^2$$

THRESHOLD DISTRIBUTIONS

Critical light intensities relate to the photosynthetic compensation point of the macrophytes (cf. RØRSLETT, 1984a). Given a relative threshold R, statistics of light intensity below the threshold now are investigated. The probability of the event "$i(v) \leqslant R$" is from eqn.(3b) clearly:

$$(28) \quad Pr\{ i(v) \leqslant R \} = Pr\{ K(v) \geqslant |\ln R| \}$$

Under the Normality hypothesis, this probability (28) equals $\phi(L)$, where $\phi(.)$ is the normal cumulative Gaussian integral, and $L=L(v)$ is the standardized threshold:

$$(29) \quad L(v) = \{\mu(v)-|\ln R|\}/\sigma(v)$$

For a fluctuating water level, eqn. (29) is conveniently expressed as:

$$(30) \quad Pr\{ i(z) \leqslant R \} = \int_0^{+\infty} \phi\{L(v)\} \, p_v(v+z) \, dv$$

which is equal to the expression used by RØRSLETT (1984a), apart from some slight changes of notation.

RESULTS AND DISCUSSION

The goodness of fit of a Normal process

I used the continuous data series from lake Maridalsvatn to illustrate
the main features of the underwater light field as a time series. The
data were acquired for two weeks early October, 1984. During these two
weeks, the weather changed rapidly from heavy overcast and pouring
rain to bright sun. The sunny days were windy in the morning and
afternoon, otherwise calm.

It should be stressed that the measurements represented a realistic
situation for submerged macrophytes, and decidedly were not
representative for deeper waters. The measuring site was close to the
lower depth limit for the isoetid species, Isoetes lacustris, the
predominant macrophyte in lake Maridalsvatn. This species penetrated
to 4.2m depth (time-averaged) at the site. Underwater stereo-
photography clearly demonstrated signs of erosional activity at the
lake floor, these increased sharply beyond the Isoetes beds.

The daily peak $I(0^+)$ ranged from 36 to 870 μE m^{-2} s^{-1}, and at 3m depth
the peak $I(3)$ varied from 12 to 160 μE m^{-2} s^{-1}. The 3m irradiance
tracked the subsurface irradiance rather closely (Fig. 4.), although
with significant point scatter. Thus, the vertical attenuation
evidently fluctuated throughout time.
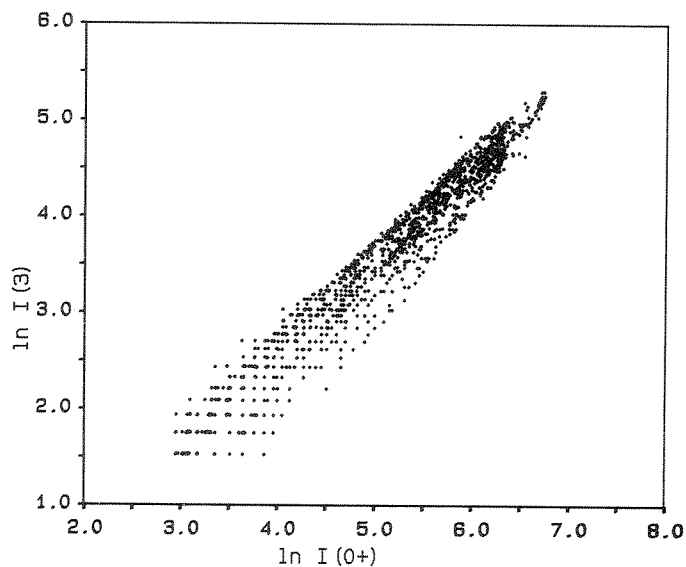
Fig. 4. Measured downwelling quantum irradiance at
subsurface level, $I(0^+)$, and at 3m depth, $I(3)$. Data from
lake Maridalsvatn, 1-14. October, 1984, sampled at 5
minute intervals.

The available data allowed only instantaneous estimates of a depth-averaged attenuation coefficent, i.e.;

$$\tilde{k}(t) = \langle K(v) \rangle = \{ \ln I(0^+, t) - \ln I(3, t) \} / 3 \qquad (m^{-1})$$

Please note that $\tilde{k}$ is referred to Lagrangian depth coordinates, since the sensor position was fixed relative to the current water surface.

The $\tilde{k}$ time series did not relate significantly to incident irradiance (cf. Fig. 5, next page). Thus attenuation within the water column at the site was quite independent from incoming irradiance, as postulated earlier (p. 58).

Some covariation of $\tilde{k}$ with time within each day existed, however, as shown by Fig. 6 (overleaf). Thus, point spread increased somewhat early morning and late evening. This pattern partly is fortuitous, since lowered data resolution and hence enhanced digitizing noise occurred simultaneously due to low levels of incident irradiance. However, very low sun altitudes would augment the red end of the incoming irradiance spectrum. Thus, the apparent attenuation concurrently would increase. This effect could not always be discerned from wind-driven resuspension of the sediments, since wind activity at the site concentrated in early morning and late in the day.

Analysis of the $\tilde{k}$ data demonstrated that periods of calm weather lowered $\tilde{k}$, i.e., increased water transparency, whereas rough weather had the opposite effect. This could be expected under the measurement conditions, since erosion activity due to wind-generated waves would influence the lake floor immediately beneath the submersed sensor. The statistical distribution of $\tilde{k}$ clearly demonstrated these effects. Thus, the distribution was bimodal with peaks at $\tilde{k}=.42$ and $\tilde{k}=.51$ for the calm and rough weather, respectively. The general shape of this distribution curve, however, indicated that a Normal distribution was not unlikely, if a sufficient long observation period included a random mixture of weather situations. However, the present short observation period covered mainly extreme weather, either calm or rough. Also, the necessity to threshold the data in order to increase the signal-to-noise ratio, meant that sunny calm periods were over-represented in the final data series.
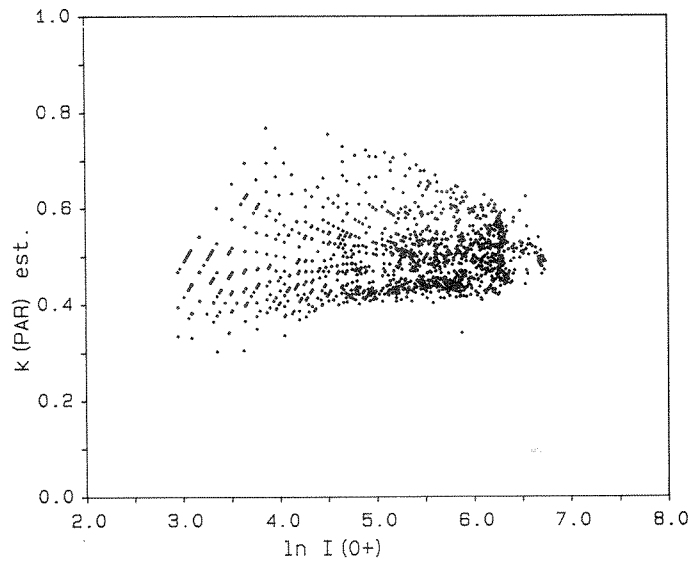
Fig. 5. Instantaneous estimated $\bar{k}$ (0-3m depth) vs. subsurface irradiance $I(0^+)$, sampled at 5 minute intervals. Lake Maridalsvatn, 1-14. October, 1984.
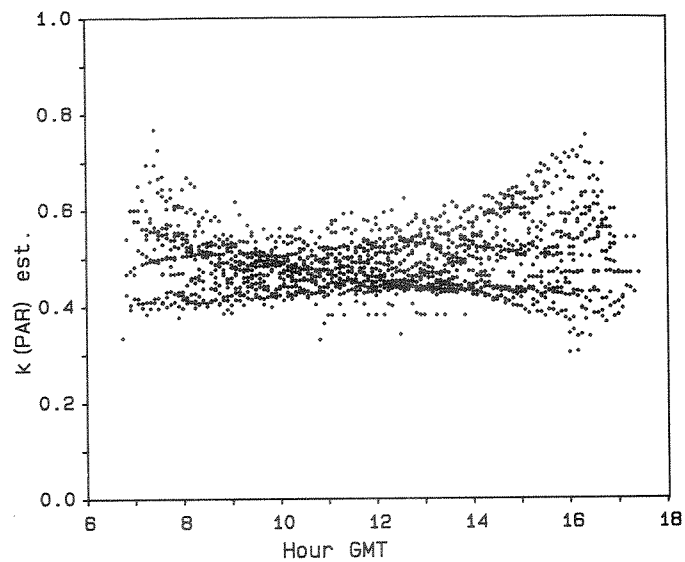

Fig. 6. Instantaneous estimated $\bar{k}$ (0-3m depth) vs. sample time within each day. See text for details and discussion.

To illustrate this point, I "resampled" the raw data with a coarser time resolution (Δt increased from 5 to 15 minutes). The frequency distribution of this series assumed more a Normal shape than did the original series (Fig. 7), and the presence of individual peaks scarcely was noticeable. The Kolmogorov-Smirnov statistic (D_{417}=0.069) was significant at the 5% but not the 1% level, thus, confirming the near-Normal shape of this distribution.

A

B
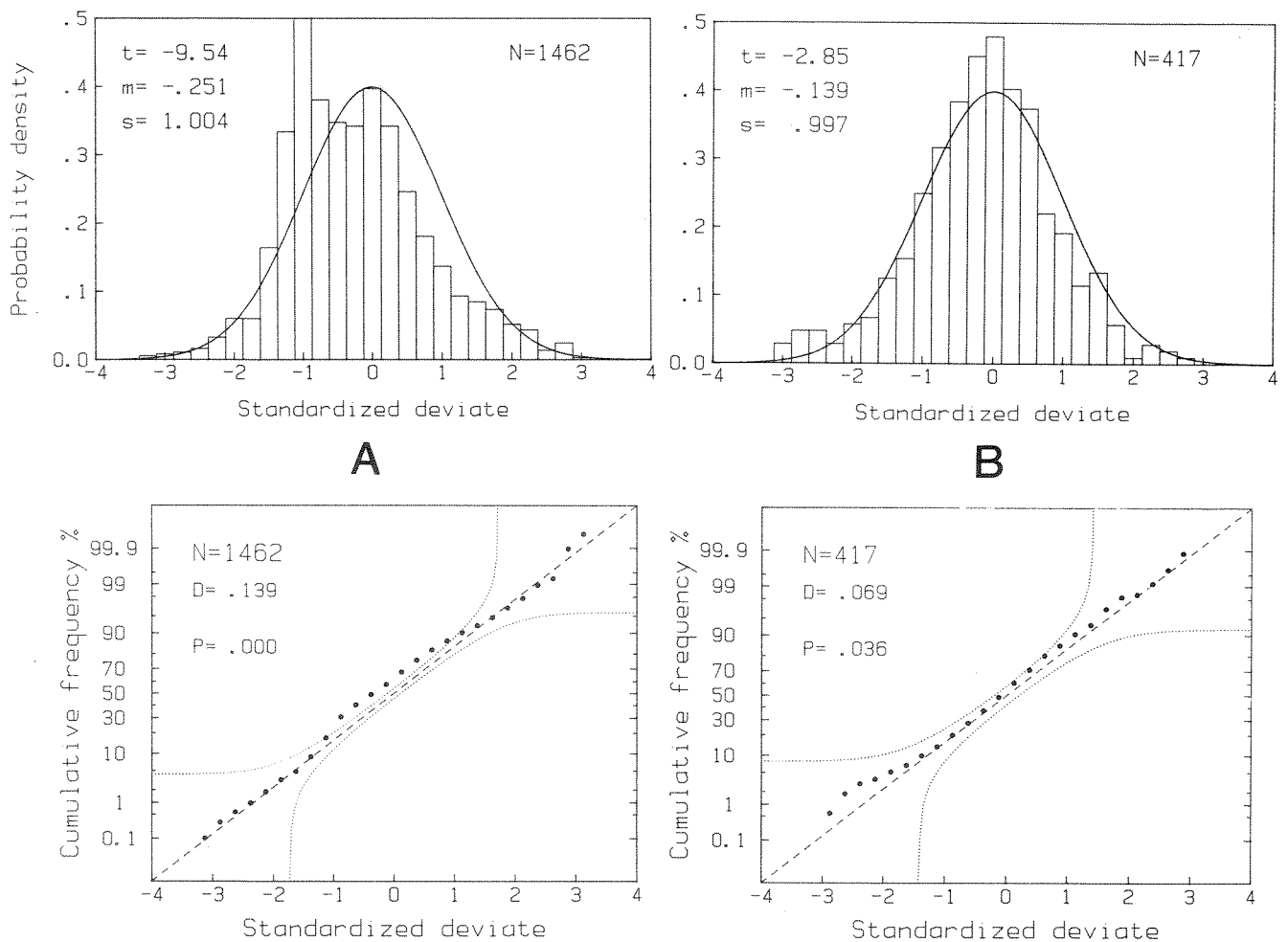
Fig. 7. The frequency distribution of standardized $\bar{k}$ data; (A) sampled with Δt=5 min.,(B) "resampled" with Δt increased to 15 min. See text for discussion.

Upper panel: Frequency distributions, lower panel: Plots of the cumulative distributions, with 95% CI limits derived from the Kolmogorov-Smirnov test indicated (dotted lines). Dashed line show the theoretical N(0,1) cumulative distribution.

The time-structure of the Maridalsvatn data series

The stochastic nature of the $\bar{k}$ time series should ideally be investigated by spectral analysis, to test if the assertion of a white-noise, i.e., Normal process, could be sustained. However, data were lacking at night times, so more indirect approaches had to be taken.

I selected the autocorrelation as indicative of the time-distribution of $\bar{k}$. For the ideal case of a white-noise process, the autocorrelation would approach unity at zero lag, and be zero elsewhere. The autocorrelation function (acf) was computed for 1152 lags, i.e., spanning time steps up to 96 hours. Due to the night situation, data were missing for some nine hours within each 24-hour cycle. The computer program automatically corrected for this when calculating the acf. Hence, segments of the acf (lags 98-180, and so on) are missing. The general shape of the acf indicated that no serious loss of information occurred, though.

The acf of the $\bar{k}$ time series damped quickly out (Fig. 8), indicating the virtual statistical independence of $\bar{k}$ estimates obtained more than three hours apart. Very slight 24-hour periodicity was evident on the acf plot (Fig. 8).

The acf of the coarser-resolved $\bar{k}$ series ($\Delta t = 15$ min., Fig. 9) demonstrated exactly the same features as did the full-resolution ($\Delta t = 5$ min.) series. Additionally, the shape of the acf indicated that the time series closely related to a low-pass random noise process. The acf of the one-step differenced time series, ie.;

$$\Delta \bar{k}(t) = \bar{k}(t) - \bar{k}(t+1)$$

indeed demonstrated the independence of the time increments of $\bar{k}$ (cf. Fig. 10). This acf was clearly representing a white-noise process with zero mean (actually, the observed mean $\Delta \bar{k}$ was 0.0003).

The crosscorrelation function (ccf) between incident irradiance and the 3m irradiance confirmed this (Fig. 11), being merely a convolution of two random-noise processes with zero time delay. The ccf of $\bar{k}$ and $\ln I(0^+)$ demonstrated again the virtual independence of estimated attenuation and incoming irradiance (Fig. 12).
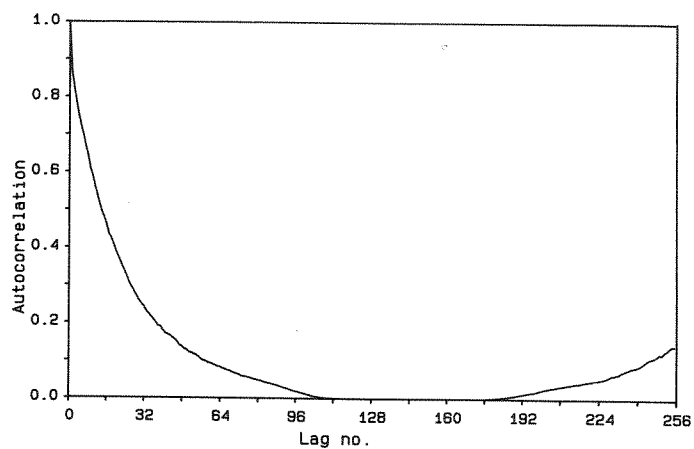
Fig. 8. Autocorrelation function of the $\bar{k}$ time estimates, lake Maridalsvatn. Only first 256 lags shown. Please note that lags 98-180 are undefined, due to missing data (cf. the text). Time step $\Delta t = 5$ minutes.
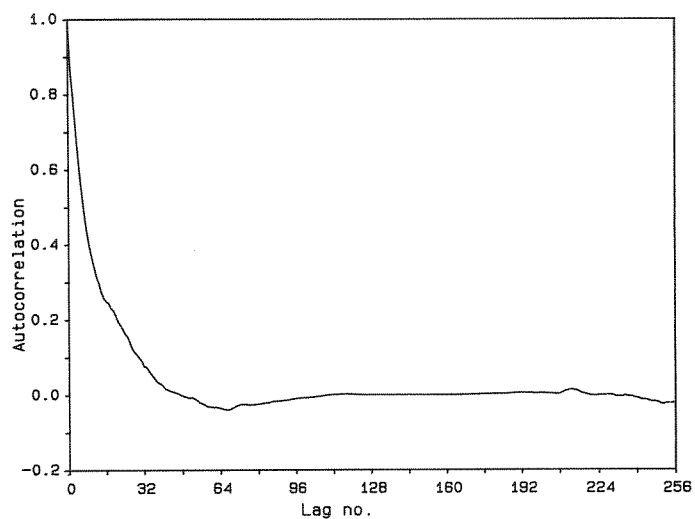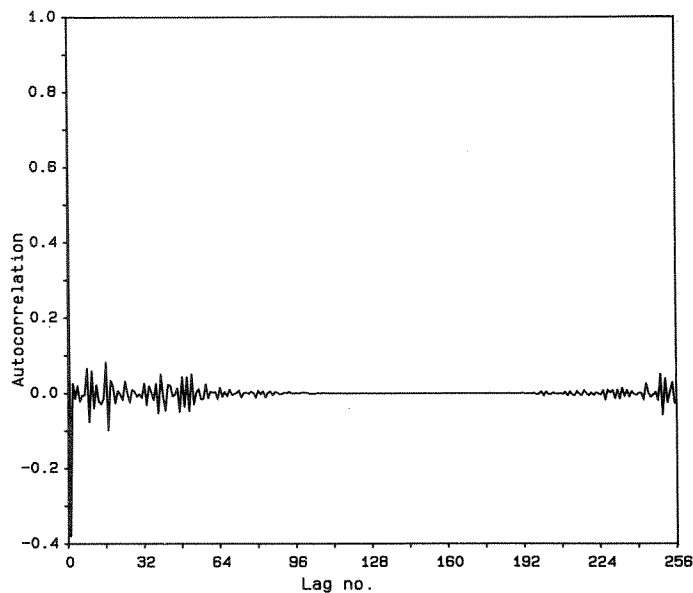

Fig. 9. Autocorrelation function of the $\bar{k}$ time estimates, lake Maridalsvatn. Only first 256 lags shown. Please note that lags 125-160 are undefined, due to missing data (cf. the text). Time step $\Delta t = 15$ minutes.

Fig. 10. Autocorrelation function of differenced k̄ time series, cf. also Fig. 8.
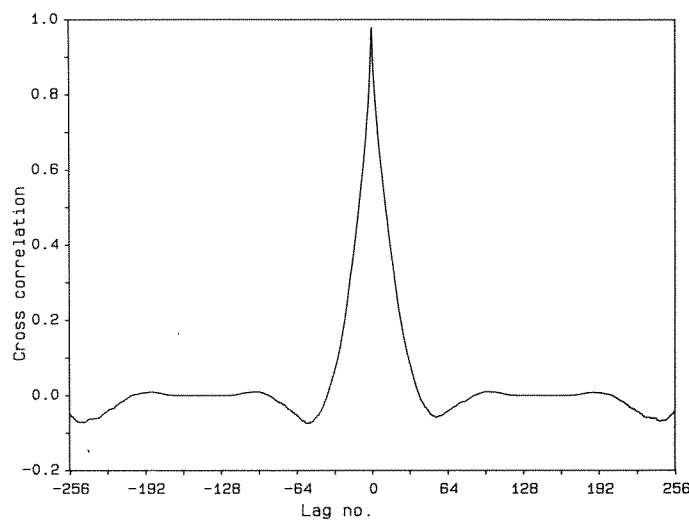
Fig. 11. Crosscorrelation function of incident irradiance, X=I(0⁺), and irradiance at 3m depth, Y. The crosscorrelation C_{xy} shown up to 256 lags leading (-) or lagging (+).

The data were log-transformed before computing the ccf. Time step $\Delta t = 5$ minutes.
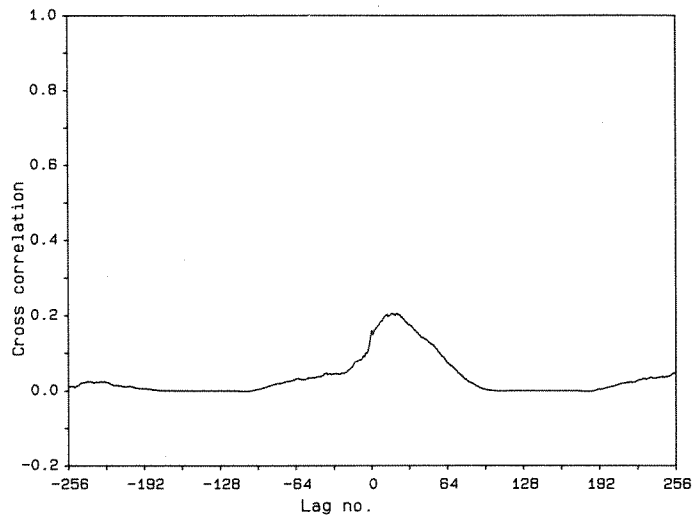
Fig. 12. Crosscorrelation function of incident irradiance, $X = \ln I(0^+)$, and estimated PAR attenuation, $Y = \bar{k}$. The crosscorrelation C_{xy} shown up to 256 lags leading (-) or lagging (+).

The digitizing noise from the A/D converter, determined by Monte Carlo simulation, would result in an root-mean-square (rms) error of 0.007 for the $\bar{k}$ estimates, or an relative error of some 1.4 %. The expected rms error of the differenced time series, due to digitizing noise, would be 0.01, which is much less than the observed standard deviation (0.031). Thus, the noise process of Fig. 10 would not likely be caused by the instrumentation used to acquire the data.

Hence, I conclude that the observed $\bar{k}$ time series represents an approximately stationary process, with some digitizing noise and short-time sudden changes overlaid a slowly oscillating time-pattern. The sudden changes evidently related to wind-driven sediment resuspension occurring mainly late in the evenings.

For the two-week data series, the mean $\bar{k}$ was 0.48 with standard deviation 0.062. This mean was clearly not significantly different from the previous mean $\bar{k}$ estimate, 0.46, obtained by averaging over observation series ($t_7 = 0.32$, NS).

Model fits: The lake data base

A total of 160 observation series was statistically analysed by the models A , B, and C. Using the residual mean square as criterion, the linear model A generally resulted in equal or better fits than did the non-linear models (B, C) in the majority of cases, 57.5% and 42.5%, respectively (Tab. 1). The best-fitting model in all cases had coefficients of determination, R^2, well exceeding 90%. When the simple model A did not apply , however, the more sophisticated model B often spectacularly improved the regression fit, reducing the residual mean square 14.7 times on the average. Not surprisingly, the model B clearly was more adequate for the two productive lakes Steinsfjord (60% best fit) and Jarenvatn (57% best fit). The model C ranked best in 18.8% of the observation series, the improvement with respect to the other models was generally slight, however. Interestingly, the model C, when appropriate, mostly had the linear model A as the major contender.

Model	Percentage of rank			model failed
	#1	#2	#3	
A	57.5	33.1	9.4	–
B	23.8	7.5	–	68.8
C	18.8	13.1	0.6	67.5

Tab. 1. Performance of the models A, B, and C, ranked by residual mean square. N=160 data series, totalling some 1500 observations.

In an earlier paper (RØRSLETT, 1984a), I suggested that the vertical attenuation coefficient could be considered a Normal deviate. This assertion equals Model A of the present paper. As shown in Tab. 1, many light situations would be satisfactorily explained by this model. However, the access to a larger data base has convinced me that this simple model could lead to serious bias in some circumstances. Indeed the regression residuals for the N=160 data series, when analysis is restricted to the model A only, indicated that such bias was present (Fig. 13). In contrast to this, the residuals of the best-fit models from the total data base clearly had a Normal shape (cf. Fig.13).
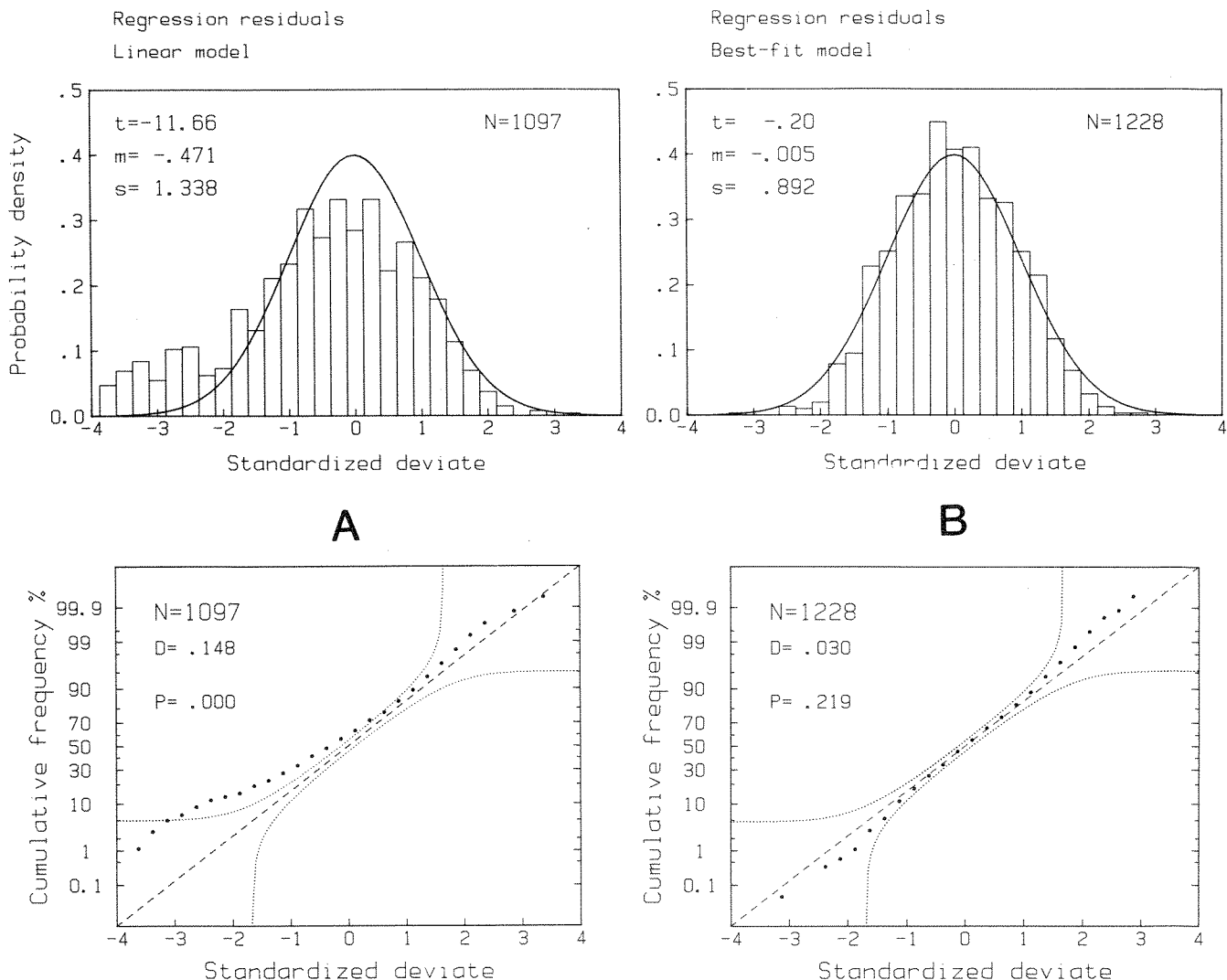
Regression residuals
Linear model

Regression residuals
Best-fit model

t=-11.66   N=1097
m= -.471
s= 1.338

t= -.20   N=1228
m= -.005
s= .892

A

B

N=1097
D= .148
P= .000

N=1228
D= .030
P= .219

Fig. 13. Frequency distribution of standardized regression residuals, N=160 data series.

(A): Model A exclusively , (B): Best-fit model each case

Upper panel: Frequency distributions, lower panel: Plots of the cumulative frequency distributions, with 95% CI limits derived from the Kolmogorov-Smirnov test indicated (dotted lines). Dashed line show the theoretical   N(0,1) cumulative distribution.

Model implications

As shown by Fig. 13, the distribution of the residual errors have a Normal shape when the appropriate model is selected. In other words, estimation of the K(v) parameters by the least-squares method would coincide with the maximum likelihood solution (MIKHAIL, 1976).

Finally, the basic assertion of the stochastic model should be tested. Earlier (p. 62), it is implicitly assumed that the distribution of K(v) converges to a Normal shape whatever the underlying models of the attenuation-depth relationships might be, i.e.:

$$(31) \qquad 1/T \int_0^T K(v;t)dt = E[K(v)] = \mu(v)$$
$$\lim T \to \infty$$

Clearly, the eqn. (31) imposes two separate conditions on the field data, viz.

a) The individual K(v)'s should follow a Normal distribution with site specific mean and standard deviation,

b) Within each site, all data points over depth should follow a Normal distribution with parameters given by (a).

The condition (a) implies the random variable:

$$(32) \qquad Y = \{ \langle K_j(v) \rangle - \langle \mu_j(v) \rangle \}/\langle \sigma_j(v) \rangle$$

$$j = \text{data series index}$$

to be distributed Normal (0,1). Replacing $(\mu(v),\sigma(v))$ with their sampling estimates $(\hat{\mu},\hat{\sigma})$, $\hat{Y}$ would follow the t-distribution with the appropriate degrees of freedom.

The actual estimates of Y did not significantly deviate from the expected distribution, thus, $t_{118}=-0.76$, P>0.4. Hence, the site mean depth-averaged attenuation did not violate the asserted Normal distribution.

The appropriate test of condition (b) would be the observed distribution of the random variable:

$$(33) \qquad X = \{\ln i + \mu(v)\}/\sigma(v)$$

which by virtue of eqn.(3b) should be distributed Normal (0,1). Replacing the parameters (v,μ,σ) by the observed depth $\hat{v}$ and the

sampling estimates $(\hat{\mu}, \hat{\sigma})$, $\hat{X}$ would be asymptotically distributed Normal (0,1) for large N. The actual distribution of the standardized deviate $\hat{X}$ is shown in Fig. 14, with mean 0.0015 and standard deviation 1.020. The mean was clearly not significantly different from zero $(t_{1162} = 0.051$, P>0.9). The cumulative distribution of $\hat{X}$ was tested against the Normal hypothesis by the Kolmogorov-Smirnov test (Fig.14). The Kolmogorov-Smirnov D-statistic was 0.035 with 1164 degrees of freedom (P>0.15), thus, confirming that the cumulative distribution of $\hat{X}$ was not significantly different from a Normal distribution.
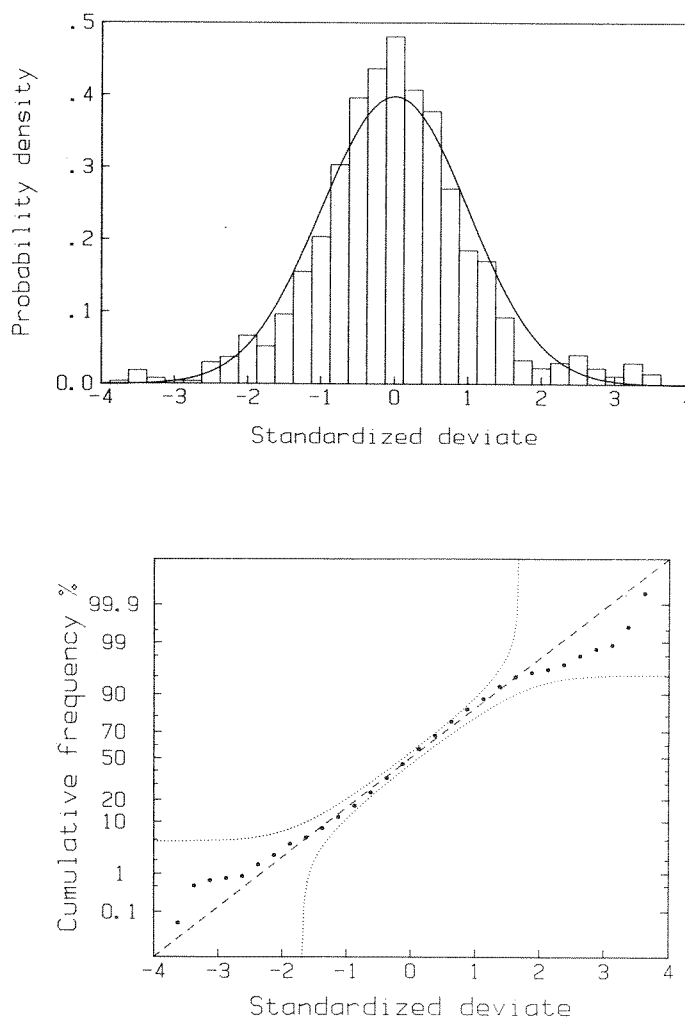
Fig. 14 The frequency distribution of the standardized deviate $\hat{X}$, upper panel, and the cumulative distribution (lower panel). $\hat{X}$ is expected to follow a Normal (0,1) distribution, see text for discussion.

Fig. 15 shows the distribution of single PAR measurements for two representative sites, with expected i(v) and 95% confidence limits indicated. The fit to the stochastic model is clearly acceptable. Test runs with data from the other, less frequently sampled lakes showed similar goodness of fit. The individual $\bar{k}$-values of all observation series ranged from 0.29 to 1.08 ln-units m^{-1}. The coefficient of variation (CV) ranged from 9 to 22%, the higher CV's mainly occurring in the more productive lakes.

Lake : Randsfjord   Years : 1978-1981

Stn.ref./name : RANDS-1 / Jevnaker

Lake : Steinsfjord   Years : 1981-1984

Stn.ref./name : STFJ / Hovedstasjon
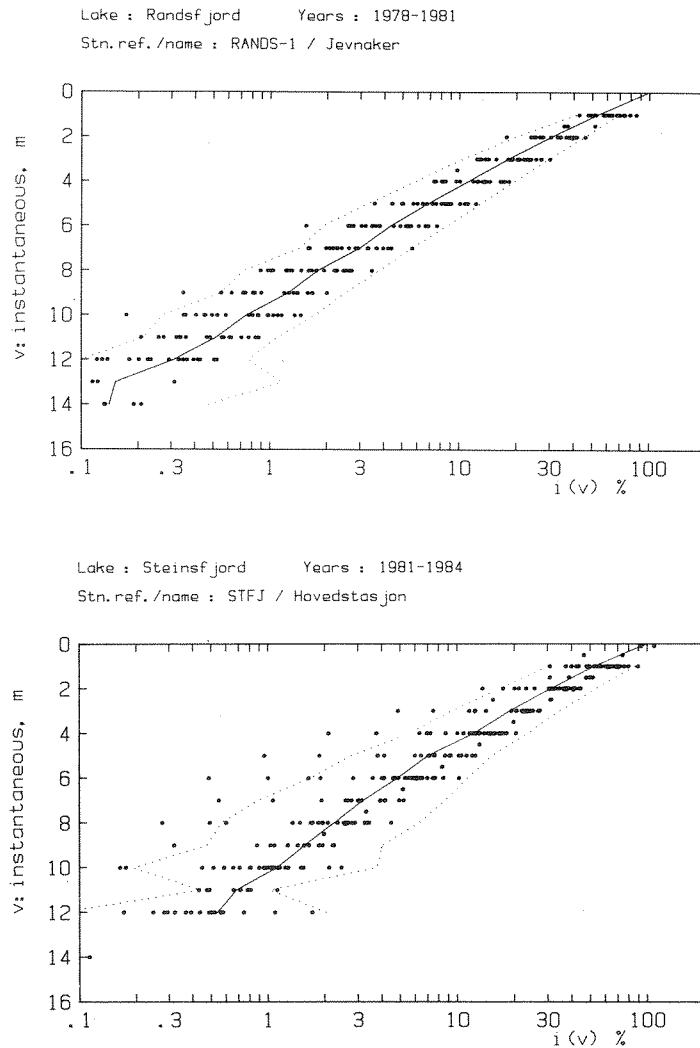
Fig. 15 PAR observations from the oligotrophic lake Randsfjord (upper panel) and the meso-eutrophic lake Steinsfjord (lower panel). The estimated E[i(v)] shown by solid lines, and the 95% CI limits indicated by dashed lines. Estimated depth-averaged parameters :

Randsfjord: $\tilde{\mu}=0.54$, $\tilde{\sigma}=0.063$ (N=22 series, n=260 points)
Steinsfjord: $\tilde{\mu}=0.54$, $\tilde{\sigma}=0.102$ (N=30 series, n=289 points)

Model bias in $I(0^+)$ estimates

In general, the non-linear models B,C, tended to give higher estimates of the subsurface irradiance, $I(0^+)$, than did the linear model A. This was hardly surprising, taking the rapid wave-length selective attenuation in the topmost water layer into account (cf. KIRK, 1977).

When the model A was inferior to the non-linear models, the regression of model B against the model A estimates of $I(0^+)$ was:

$$\ln I_B(0^+) = 0.9928 + 0.9238 \, I_A(0^+)$$

with coefficient of determination of 92.6% (P<0.001). The regression slope was not significantly different from unity ($t_{40} = -1.84$, P >0.05), however. Thus, the bias introduced by model A would likely be less than anticipated from physical theory. Additionally, the regression relationship above indicates the bias to be lower at high, than at very low surface intensities.

Relation of $I(0^+)$ to within-lake variation of attenuation

The estimates of $I(0^+)$ obtained by the best-fits model then were regressed on depth-averaged $K(v)$ estimates, in order to test the basic hypothesis of statistical independence between incident irradiance and attenuation within each water body, cf. eqn. (3a). No statistical significance of the $\ln I(0^+)$ vs. $\bar{k}$ (from best-fitting model) relationship could be demonstrated. The coefficient of determination, R^2, was well below 2% in all cases (P>0.95). Additionally, from the detailed time series from Maridalsvatn, instantaneous estimates of $\bar{k}$ was regressed on simultaneously measured $\ln I(0^+)$. No evidence of significant relation was found (cf. Fig. 5). Thus, the validity of the $I(v)$ expectation eqn. (4) is strongly corroborated.

Relation to Secchi disc transparency

The Secchi disc is widely used to assess water transparency to light. It is often assumed that the Secchi depth represents some fixed percentage of the surface light intensity, values ranging from 1 to 15% are found in the literature (cf. WETZEL, 1975).

Secchi disc readings were regressed against estimates of the vertical attenuation integral, K(S), at the Secchi depth S. A linear regression proved highly significant ($R^2 = 44.0\%$,P<0.001), the point scattering was considerable, however. Curvi-linear regressions improved the co-efficient of determination to a small extent. The best-fit regression (Fig. 16) was:

$$K(S) = \exp (1.423 - 1.826/S)$$

with an R^2 of 48.1 %, thus, indicating a limiting light intensity at the Secchi depth of some 1.7% of the surface value.

Linear regression was not satisfactory when depth-averaged attenuation coefficients, i.e., k_A or K_B(S)/S, were regressed against Secchi depth S. The best-fit curvi-linear regression (Fig. 17) had R^2 of 48.4% (P<0.001), and was:

$$k = \exp (-1.028 + 1.841/S)$$

These results indicate the attenuance to be predictable from Secchi disc reading, although precision of the estimates is likely to be low.
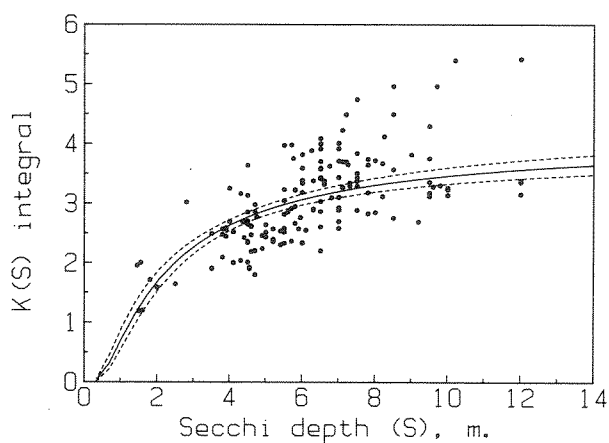
Fig. 16. Vertical attenuation integral, K(S), obtained from the best-fit regression for each observation series, vs. Secchi disc reading, S.   N=160 data series.

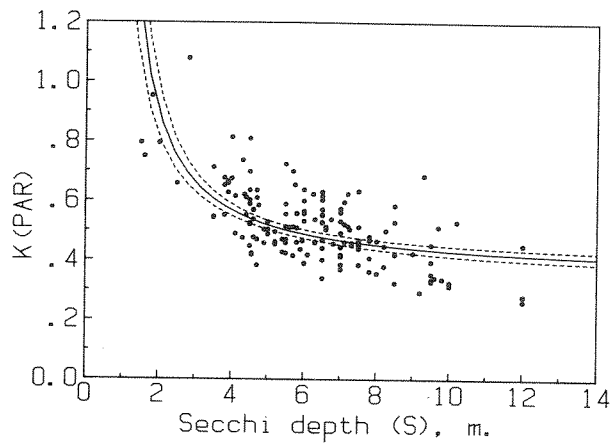Best-fit curvi-linear regression line indicated, with 95% CI limits for that line indicated (dashed).

Fig. 17. Depth-averaged k̄ attenuation coefficient, from the best-fit regression of each observation series, vs. Secchi disc reading, S.   N=160 data series.

Best-fit regression line and the 95% CI limits for that line indicated (dashed).

CONCLUDING REMARKS

I conclude from my observations that the Normality assumption for the vertical attenuation integral describes the underwater light field surprisingly well. The concept should be applicable to most non-productive lakes. However, the two productive lakes included in this study deviated little from the general trend.

The Normal distribution model describes a time-stationary stochastic process. Hence, the attenuation integral follows a white-noise process with non-zero mean. In lakes with seasonal-induced light attenuation, e.g., from phytoplankton blooms, the time-stationarity of this noise process is questionable, unless the distribution parameter μ is adjusted to include a periodic seasonal term, i.e., $\mu(t)=\mu+s(\cos(t))$.

ACKNOWLEDGEMENTS

LITERATURE

BAKER, K.S. & SMITH, R.C. 1982: Bio-optical classification of
    natural waters. 2. <u>Limnol.Oceanogr.</u> 27: 500-509.

FAAFENG, B., BRETTUM, P., GULBRANDSEN, T., LØVIK, J.-E., RØRSLETT, B.
    & SAHLQVIST, E.Ø. 1981: Randsfjorden. Vurdering av innsjøens
    status 1978-80 og betydningen av planlagte reguleringer i
    Etna og Dokka. (In Norwegian). <u>Norwegian Institute for Water
    Research</u>, Report 0-78014 VI, 138 pp.

FAAFENG, B., BRABRAND, Å., GULBRANDSEN, T., LIND, O., LØVIK, J.-E.,
    LØVSTAD, Ø. & RØRSLETT, B. 1982: Jarenvatnet. (In Norwegian).
    <u>Norwegian Institute for Water Research</u>, Report 0-78014 VII,62 pp.

HØJERSLEV, N.K. 1979: Daylight measurements appropriate for photo-
    synthetic studies in natural sea waters.
    <u>J. Cons. int. Explor. Mer.</u> 38(2): 131-146.

HUTCHINSON, G.E. 1957: <u>A Treatise on Limnology</u>. Vol. 1:1: Geography,
    and Physics of Lakes. Wiley, New York, 672 pp.

JERLOV, N.G. 1976: <u>Marine Optics.</u> Elsevier Oceanography Series, 14.
    Elsevier, Amsterdam, 231 pp.

KIRK, J.T.O. 1977: Attenuation of light in natural waters.
    <u>Aust.J.Mar.Freshwater Res.</u> 28: 497-508.

KIRK, J.T.O. 1981a: Monte Carlo study of the nature of the under-
    water light field in, and the relationships between optical
    properties of, turbid yellow waters.
    <u>Aust.J.Mar.Freshwater Res.</u> 32: 517-532.

KIRK, J.T.O. 1981b: Estimation of the scattering coefficient of
    natural waters using underwater irradiance measurements.
    <u>Aust.J.Mar.Freshwater Res.</u> 32: 533-540.

KLEPPER, O., VERMIJ, S.G. & LINGEMAN, R. 1984: The influence of light
    scattering on vertical extinction in Lake Maarseveen.
    <u>Verh. Intern. Verein. Limnol.</u> 22: 82-86.

MIKHAIL, E.M. 1976: <u>Observations and Least Squares.</u> IEP Series in
    Civil Engineering, Dun-Donnelley, New York, 497 pp.

PARZEN, E. 1962: Stochastic Processes. Holden-Day, San Francisco,
324 pp.

RØRSLETT, B. 1984a: Environmental factors and aquatic macrophyte
response - a statistical approach. Aquat. Bot. 19:199-220.

RØRSLETT, B. 1984b: Regulation impact on submerged macrophytes in the
oligotrophic lakes of Setesdal, South Norway.
Verh.Int.Verein.Limnol. 22 (in press)

SPENCE, D.H.N. 1982: The zonation of plants in freshwater lakes.
Adv.Ecol.Res. 12: 37-125.

TALLING, J.F. 1957: The phytoplankton population as a compound photo-
synthetic system. New Phytologist 56: 133-149.

WETZEL, R.G. 1975: Limnology. W.B. Saunders, Philadelphia, 743 pp.

Death of submerged macrophytes - actual field observations and some implications <1>

Bjørn Rørslett

Norwegian Institute for Water Research
P.O.B. 333 Blindern, N-0314 Oslo 3, Norway.

ABSTRACT

Using a photographic sampling method, the spatial distribution of dead submerged macrophytes was investigated in the lakes Tyrifjord and Steinsfjord, South Norway. Death incidents were observed in less than 5% of the samples (N=3257). Disturbed sites with unstable sediments had dead plants occurring at all depths, whereas the normal sites had death incidents mainly towards deeper waters. In this case, the estimated mortality rate rose sharply close to the lower limits of depth extension for the annual _Najas flexilis_ (Willd.)R.&S. and the perennial _Isoëtes lacustris_ L..

The statistical analysis of death incidents for the predominant macrophyte _Isoëtes lacustris_ showed that neither depth or light intensity did adequately account for the observed deep-water mortality increase. However, probit-transformed mortality correlated significantly ($p<0.001$) to a hazard function, derived from light threshold statistics. Mortality magnitude was sufficient to explain the observed steep deep-water decline of _I. lacustris_. It is concluded that the commonly-observed double-exponential depth decline of submerged macrophytes could well be invoked by light-induced mortality.

INTRODUCTION

Sudden death of a plant differs from the normal seasonal growth-senescence pattern. Whenever the mortality rate exceeds the regeneration capacity, population performance and dynamics are adversely affected.

Submerged macrophytes inhabit a hostile environment (HUTCHINSON, 1975), and might easily succumb to prolonged periods of unfavorable conditions. I hypothetize that (1) environmental-induced mortality potentially can regulate the spatial performance of many submerged species, and (2) that a species' susceptibility increases with the life-span length.

During an extensive survey of the aquatic vegetation in two Norwegian lakes, I made observations on the frequency and abundance of dead macrophytes _in situ_. Using photographic sampling, the occurrence of recently dead individuals could be determined with some confidence. The photographic data could be divided into dead rooted plants, and non-rooted vegetative fragments either alive or moribund. The sampling method ensured that my observations relate to sudden death incidents, and not to seasonally induced senescence and die-back.

Direct observations of dead aquatic macrophytes are rarely encountered of in the literature. Information pertaining to _in situ_ death of submerged aquatics in particular, seems to be largely non-existent. This could well be due to the sampling methods applied. The probability of observing plants at the low densities common to deep-water vegetation is vanishingly small, unless quadrat size is increased an order of magnitude compared to grab samplers (RØRSLETT et al., 1978).

STUDY AREA AND VEGETATION

The investigated lakes, Steinsfjord and Tyrifjord, form the Tyrifjord lake complex (Fig.1) in Southeastern Norway. Steinsfjord is a mesotrophic, shallow lake (13.9km^2, mean depth 10.2m), whereas the larger Tyrifjord (121.9km^2) is much deeper (mean depth 114m) and oligotrophic. The lakes are connected through a short and narrow sound. The waters of Steinsfjord are somewhat richer than those of Tyrifjord. Thus the Steinsfjord conductivity (K_{20}) is nearly three times that of Tyrifjord, 9.0 and 3.2 mS m^{-1}, respectively. The mean annual water level fluctuation is 2.0m.
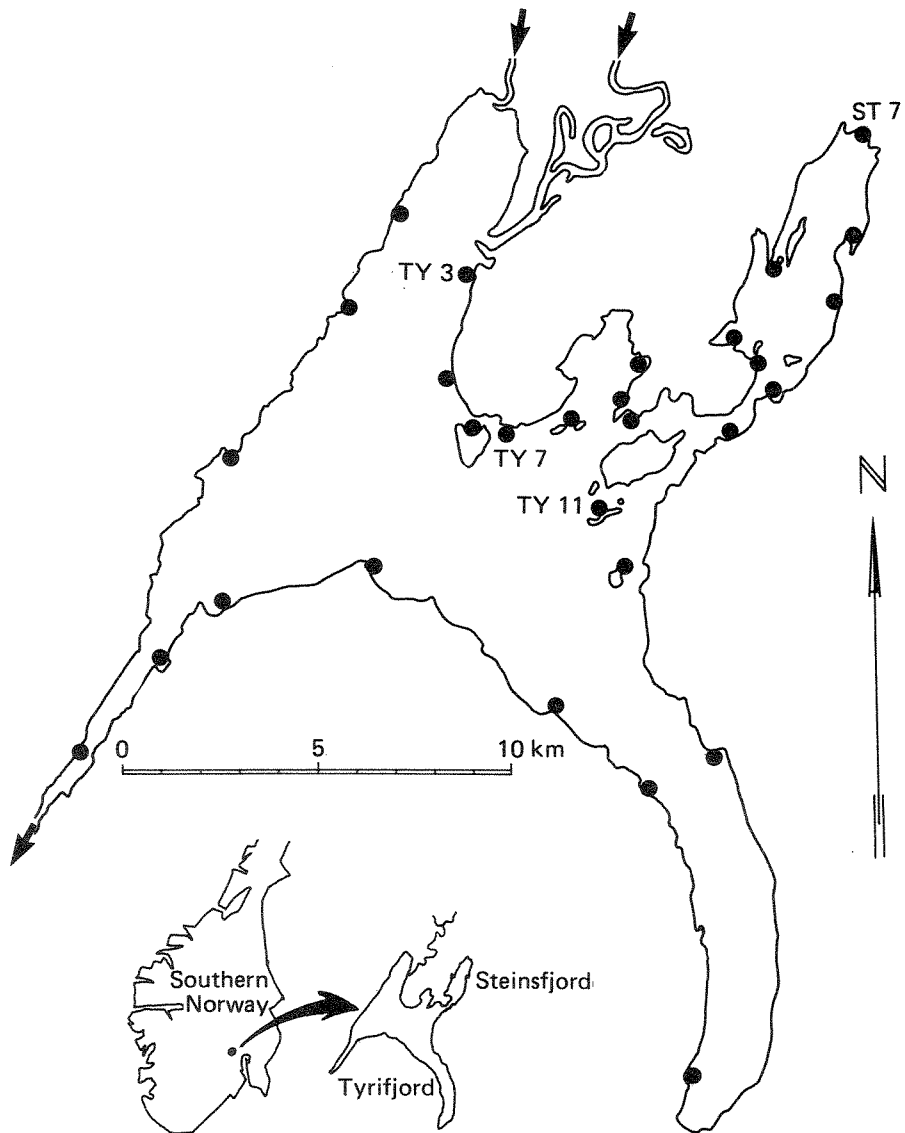
Fig. 1

Geographic location of the studied lakes (insert) and sampling sites.
Sites referred to in the text are indicated by their site codes.

The aquatic macrophytes of Tyrifjord and Steinsfjord are detailed by RØRSLETT (1983). The two lakes had nearly 90% of the species in common. The prevailing communities, however, differed significantly.

Tyrifjord had mainly species-poor submerged communities dominated by the isoetids Isoëtes lacustris L. and Littorella uniflora (L.)Asch., and the elodeid Myriophyllum alterniflorum DC. These three species accounted for two-thirds of all species observations. Lake Steinsfjord had a much more diversified vegetation, and here the submerged vegetation consisted mainly of elodeids (Najas flexilis (Willd.)R.&S., Elodea canadensis Michx., Potamogeton spp., Chara and Nitella spp.).

MATERIAL AND METHODS

I used exclusively underwater stereophotographic sampling in the lakes Tyrifjord (21 sites, N=2612 samples) and Steinsfjord (7 sites, N=645 samples). The technical details are described elsewhere (RØRSLETT et al., 1978). A quadrat size of $0.25m^2$ was used throughout and sampling was depth stratified randomly along transects in the field. SCUBA diving progressed to at least 2 vertical m below observed vegetation. The vertical sampling intensity within the vegetated zone was some 400 samples m^{-1} on a total lake basis in Tyrifjord, and about 100 samples m^{-1} in Steinsfjord. Field work was done May to late October 1978-1981.

Coverage of species was determined from the stereopairs, using either a nested grid approach (RØRSLETT, 1983) or randomized point sampling (GREEN, 1981). Photographic analysis included all vegetation states, encompassing actively growing plants, non-rooted shoots, moribund and dead plants. Photographic evidence used to classify observed plants into the 'dead' category was:

- shoots blackened or shrivelled,

- no visual turgor,

- shoot apices not in the normal upright position,

- shoots visually in a decaying state.

Some isoetid species, mainly <u>Isoëtes lacustris</u>, left a visual 'fingerprint' of their dead individuals. Such 'fingerprints' appeared as starshaped streaks in the recently deposited surface sediment layer. Sometimes remnants of leaves or rhizomes could also be detected.

Observed instantaneous depth of each photographic sample was mapped into relative elevations (z-levels) with datum at median water level, according to RØRSLETT (1984). The data then were assembled into the vertical cover function C(z), estimated by convolution of the raw data $c_{obs}(z)$ with a Hanning weight function (JENKINS & WATTS, 1968) in order to reduce the inherently large statistical variance. Spanning several orders of magnitude, cover C(z) preferably should be expressed on a logarithmic scale. The dB-scale is appropriate when proportional changes in the cover-elevation function are of interest:

$$(1) \qquad dB \ \{C(z)\} = 10 \ \log_{10} \ \{C(z) - C_{ref}\}$$

where $C_{ref} = 100\%$ cover

I selected a subset of the data base, covering the months July and August, for further analysis of death incidents. The cover of dead individuals can be converted into an estimate of the mortality probability :

$$(2) \qquad P_{dead}(z)dz = Pr(Dead;z+dz) \approx C_{dead}(z)/C_{live}(z)$$

where dz = z-scale resolution

From the probability density (pdf) estimates, the corresponding cumulative distribution function (cdf) is easily calculated. Vertical resolution ranged from 0.05m to 0.25m, depending on the numbers of samples available. If dead plants occur outside the colonized range, the cumulative distribution is estimated first, then the pdf is derived from the cdf. In this case, the cdf is arbitrary scaled.

Measurements of subsurface PAR irradiance (400-700 nm) were made with a Li-COR quantum meter, equipped with a Li-COR 192S underwater sensor (Lamda Instruments Inc.). PAR was observed biweekly from May to late October. Vertical attenuation coefficients were estimated by a proprietary computer program, using non-linear least squares regression. Data from four sites in Tyrifjord and one in Steinsfjord were available.

RESULTS AND DISCUSSION

Light climate and submerged macrophytes

Vertical attenuation coefficients k_{PAR} ranged from 0.44 to 0.78 ln-units m^{-1} in Tyrifjord, with a site standard deviation about 0.07. The central lake region had k_{PAR} averaging 0.52 ln-units m^{-1}. Steinsfjord waters were somewhat less transparent, and had mean k_{PAR} at 0.58 ln-units m^{-1} with standard deviation 0.09.

Submerged macrophytes penetrated to time-averaged depths of 5-9m in both lakes. In Tyrifjord, Isoëtes lacustris extended to 5.0m, Myriophyllum alterniflorum to 5.6m, and Nitella opaca (Bruz.)Ag. to 9.0m (one single record at 15.6m, however). Steinsfjord had a species array extending to 5m depth or more. The most important deep-water species were Elodea canadensis (to 7.5m) and Najas flexilis (to 6.1m).

The depth range 1.1-4.2m accounted for 80% or more of macrophyte abundance in both lakes. The abundance-weighted mean depth for the submerged communities was 2.4 and 2.7m in Tyrifjord and Steinsfjord, respectively. RØRSLETT (1984, 1985) demonstrated a general relationship between the mean annual water level range and biomass-weighted mean colonized depths in a number of Norwegian lakes, including Tyrifjord. Thus, the mean colonized depth in the lakes Tyrifjord and Steinsfjord evidently reflected the water level fluctuations. The maximum macrophyte depth extension in these lakes could still be light-limited, however (RØRSLETT, 1983).

Occurrence of dead macrophytes

Dead, rooted macrophytes were observed on 3.8% and 4.3% of the available photographic samples from Tyrifjord and Steinsfjord, respectively. In Tyrifjord, the dominating species Isoëtes lacustris and Myriophyllum alterniflorum made up a major fraction of the 'dead' observations. In Steinsfjord, many species had dead individuals. Here the annual Najas flexilis contributed most to the 'dead' category.

By and large, the abundance of dead plants was low at all investigated sites. Cover values of dead plants hardly ever exceeded -30 dB (0.1%) at any site. The main reasons for this were twofold: (a) the dead individuals evidently decayed rapidly, and (b) most dead plants were observed in deep waters where plant cover itself was very low, -20 dB (1%) or less. The very low abundance of dead plants did tax the photo-

graphic sampling method to its limit, however. Thus, statistical accuracy of the mortality estimates obtained by Eq.2 was not better than $\pm$ 2.7 dB, since individual estimates for cover this low had accuracy only within -1.5 to +1.1 dB.

The investigated sites could be divided into two groups, corresponding to the vertical pattern of vegetative fragments and dead plants. Three sites in lake Tyrifjord, situated in the inflow and outflow areas, were characterized by unstable sediments and variable streamflow. Community heterogeneity was high at these sites (RØRSLETT, 1983). The "disturbed" sites had dead plants occurring irregularily over the vertical gradient (Fig. 2). Furthermore, dead individuals often were observed in a detached, up-rooted state. These observations imply the detrimental impact of physical stress factors, e.g. longshore currents and sediment instability. STANLEY et al. (1976) noted the dis-appearance of young Myriophyllum spicatum L. in the shallows of a Tennessee Valley reservoir, and were unable to explain the eradication of this plant by low water levels only. Tentatively, the elimination was ascribed to shallow-water stress factors.

The other sites in Tyrifjord, and all sites in Steinsfjord, had a clearly different pattern. Here dead plants were concentrated in the deeper regions of the submerged communities (Figs. 3-4). The dead plants at these sites often were in a decaying state.

Spatial distribution of dead plants

There was a clear difference between annual and perennial species, regarding the vertical distribution of dead individuals. I exemplify the contrasting patterns with Najas flexilis (Steinsfjord, annual species) and Isoëtes lacustris (Tyrifjord, perennial species).

Dead Najas flexilis plants were exclusively observed at or below the depth limit of the N.flexilis community (Fig.3). Evidently, these plants had barely passed the seedling stage before death occurred. Lake Steinsfjord carried very dense Najas meadows in the 3.5-5m depth range. Thus, peak density of mature Najas meadows at 4-5m would exceed 5000 shoots m^{-2}. Self-thinning could explain premature death in this case (cf. WESTOBY, 1984). However, this certainly would not apply to the intermittent deep-water stands in the 6 to 7m depth range.
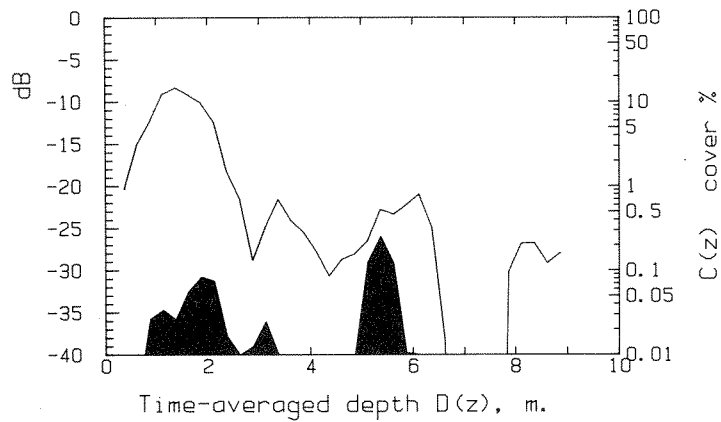
Fig. 2

Vertical distribution of dead plants (shaded) and living macrophytes
(solid line) at the "disturbed" Tyrifjord site TY 3 (cf. Fig.1). All
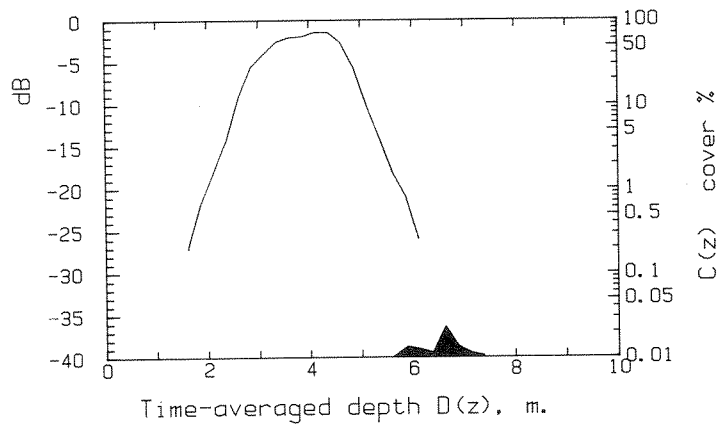species pooled.

Fig. 3

Vertical distribution of *Najas flexilis* at the "normal" Steinsfjord
site ST 7 (cf. Fig.1). Dead plants indicated by shading, living plants
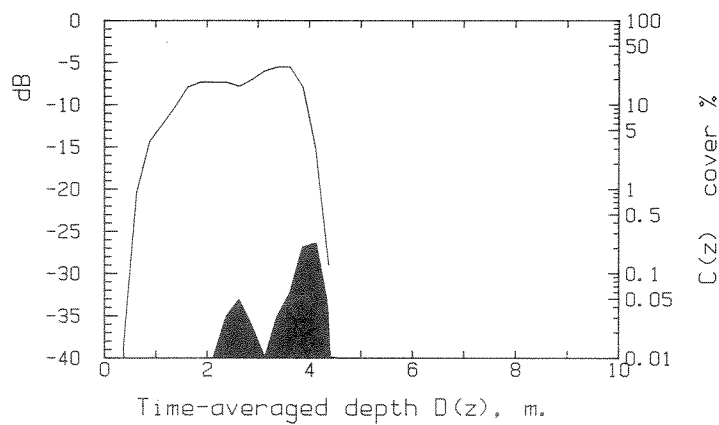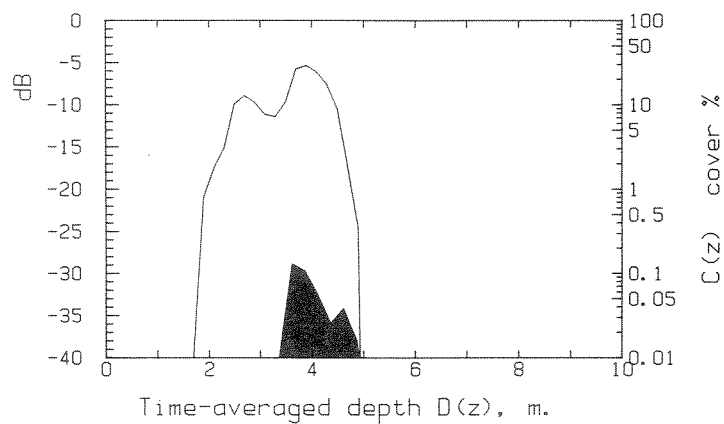shown with a solid line.

Fig. 4

Vertical distribution of Isoetes lacustris at the "normal" Tyrifjord
sites TY 7 (upper panel) and TY 11 (lower panel). Dead plants
indicated by shading, living plants by a solid line.

Contrasting the __Najas__ case, the dead __Isoetes__ plants were always
observed well within the __I.lacustris__ zone. I selected two heavily
exposed sites from Tyrifjord (TY7 and TY11, cf. Fig.1) in order to
reduce interference from sedimentation on the depth performance of
__Isoetes lacustris__ (RØRSLETT, 1983).

Statistical analysis: __Isoetes lacustris__

The two selected __Isoetes__ sites had closely similar $C(z)$-curves
(Fig.4). Sufficient data points enabled a statistical analysis of
__I.lacustris__ depth-death relationships.

Both __Isoetes__ sites featured a sharply increasing abundance of dead
plants close to the lower limit of their depth extension. This would
indicate a control factor with exponential depth distribution, e.g.
subsurface irradiance. Thus, log-transformed mortality estimates
correlated significantly to time-averaged depth at both sites (mean
$R^2 = 0.58$, P<0.001). The regression slopes were not significantly
different ($t_{18} = 0.59$, P>0.5). The mean interpolated depth for 100% dead
plants was 5.3m, within 0.3m of the actually observed depth limit for
__Isoetes lacustris__ in Tyrifjord. Analysis of regression residuals,
however, demonstrated significant curvature. A regression of log
mortality vs. expected light intensity increased R^2 to 0.67 (P<0.001),
but regression residuals still indicated major curvature. Evidently,
mortality was not adequately explained by light intensity.

Earlier (RØRSLETT, 1983, 1984, 1985), critical light thresholds were
assumed for __Isoetes lacustris__. This would imply that mortality could
be described by a dose-response model. I selected the probit model
(FINNEY, 1971). However, any of the other favoured models (e.g. one-
hit, multihit, multistage) would lead to closely similar results
within the observed mortality range for __I.lacustris__ (cf. RAI & VAN
RYZIN, 1981). The dose metameter to use in the analysis is not
trivial, however, since both dose levels and exposure durations in
fact are unknown. The concept of relative doses (MORTON, 1981) would
largely circumvent this problem. In the Appendix, a hazard function
$\lambda(z)$ is derived, relating dose 'intensity' to threshold light
statistics.

A computerized search program then was run on the probit-transformed
mortality data, with available information on light intensity and
threshold values ranging from 1 to 20% in steps of 0.5%. For each
threshold r, the hazard function $\lambda(z;r)$ was estimated by convolution.
A linear regression then was performed for each search step.

Using the coefficient of determination, R^2, as criterion, thresholds in the range 5.5-6.5% fitted the mortality data best, with R^2 exceeding 90%. The maximum R^2 of 95.9% (P<0.001) occurred at the 6% threshold (Fig.5). This regression was

(3) $\phi^{-1}\{Mortality(z)\} = -3.0 + 0.53 \lambda(z)$

where ϕ^{-1} is the inverse Gaussian (probit) transformation

From Eq.(3), a "background" mortality rate of ~0.0014 yr^{-1} is obtained, assuming that the dead plants had succumbed within the last year prior to observation.

The mean annual PAR intensity incident upon the investigated lakes is about 48 W m^{-2} (computed from unpublished data by the Norwegian Metereological Institute, Oslo). Assuming 7% surface loss (HUTCHINSON, 1957) , the actual 6% underwater irradiance threshold thus corresponds to about 2.7 W (PAR) m^{-2}, which is fairly similar to compensation points established by SAND-JENSEN (1978) for Isoëtes lacustris under experimental conditions. Experimentally determined compensation points, however, tended to be lower than the Tyrifjord threshold value in the temperature range 5-15 °C. This is hardly surprising, since the maintenance energy drain from the underground parts was not included in SAND-JENSEN's short-time experiments.

Implications to depth distributions

SPENCE (1976, 1982) postulated the abundance of submerged macrophytes to decline logarithmically below the peak biomass depth, thus implying depth abundance here to be proportional to light intensity. Some graphs presented by SPENCE (1976) allegedly supported this hypothesis. His data were limited, however, and evidently did not include any deep-water stands with their extremely low abundance.

Ample evidence now exists that lake floors are sparsely colonized by macrophytes well below the obvious limit of denser stands (RØRSLETT, 1983, 1984, 1985). In fact, if such scattered stands are taken into account, RØRSLETT (1983) demonstrated macrophyte abundance-depth curves to follow the generalized relation

(4) $C(z) = r_1(z) \; r_2(-z)$

where the "response" functions r_1, r_2 had
the common form

(5) $r(z) \sim \exp \{-a \exp (-bz)\}$

Eq. (4) was validated for several submerged plants, e.g. Iso̤ëtes lacu-
stris, Littorella uniflora, Myriophyllum alterniflorum, and Ranunculus
peltatus Schrank (RØRSLETT, 1983). These species are all perennial.
The vertical abundance of the annual Najas flexilis broadly followed
Eq.(4), the decline towards deeper waters was less than predicted,
however.

Returning to the hypothesis put forward in the introduction, it would
be tempting to associate the characteristic deep-water decline with
observed mortality. If $\Lambda(t,v)$ denotes the hazard function (force of
mortality, instantaneous death-rate) at depth v then for integrable
$\Lambda(t)$ a survivorship time function (PARZEN, 1962) is

(6) $P_s(t,v) = \exp \{ -\int_0^t \Lambda(\tau,v) \; d\tau \}$

This function obviously complies with the second hypothetical
assertion, since with any death-rate $\Lambda(t)$ different from zero a long
life-span (t) enhances susceptibility to death. The Iso̤ëtes lacustris
time-invariant hazard function Λ is derived from Eq.(3) as

(7) $\Lambda(z) = \Lambda(t,z) = -\ln [\; 1-\phi\{-3.0+0.53 \; \lambda(z)\} \;]$

implying an exponential survivorship model (GEHAN & SIDDIQUI, 1973).
Using a mean turnover time of 1.75 years (estimated from SAND-JENSEN &
SØNDERGAARD, 1978), Eq.(6) reproduced the observed Iso̤ëtes decline in
deeper waters (Fig.6). It should be noted that the Iso̤ëtes cover
values in Fig.6 are quite independent from the mortality estimates,
hence the goodness of fit is even more striking. Thus mortality
magnitude would be sufficient to control the deep-water performance,
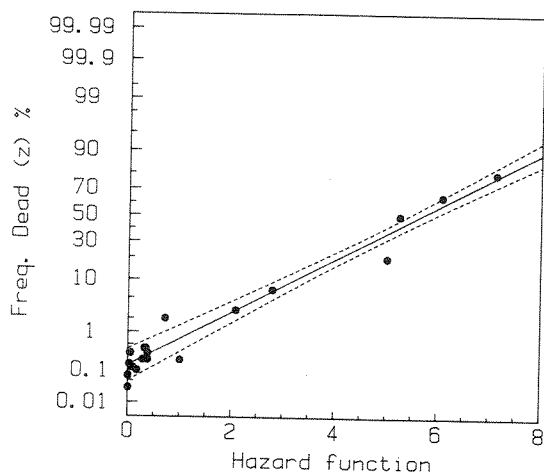at least for the evergreen, slow-growing isoetid species.

Fig. 5

Relation between frequency of dead Isoetes lacustris (probit scale)
and the hazard function λ(z), based on data from Fig. 4. Dashed lines
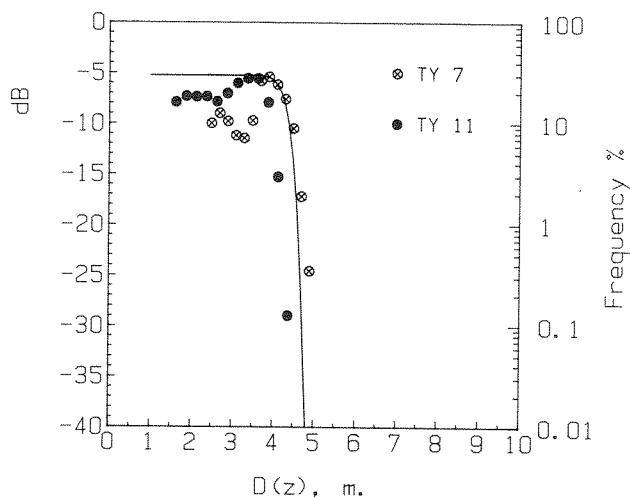indicate 95% confidence limits. See text for details.

Fig. 6

Survivorship depth function P_s for Isoetes lacustris, based on
the mortality relation from Fig.5, and 1.75 years mean turnover (Solid
line : estimated population survival percentage). The survivorship
model is exponential with time-invariant hazard function.

Observed Isoetes abundance from two sites (TY7 and TY11) indicated;
mortality data from these sites were used to establish the hazard
function.

Ordinate is survival frequency / cover on logarithmic dB-scale,
abscissa D(z) is time-averaged depth at vertical level z.

SPENCE (1982) extended his abundance/depth control hypothesis to include wave action and sediment/plant interactions. I would endorse SPENCE's opinions regarding the importance of wave action, which itself influences sediment composition and texture. However, the impact of mortality supported by my results would directly lead to depth distributions of the double-exponential type, thus subsurface light evidently overrides any other environmental factor when the lower depth limits are concerned. Such single-factor impact could well be modified, however, when the species only are partially affected throughout their life cycles. This would apply to submerged annuals and perennial species with seasonal die-back.

CONCLUSIONS

Several patterns emerge from the present study. Firstly, sudden death of submerged macrophytes is likely caused by more than one single environmental factor. Shallow-water macrophytes are strongly influenced by the environmental instability, whereas plants rooted in deeper waters face extended periods of critically low light levels. Secondly, the mortality rate in fringe habitats is high. This indicates the transient nature of plant colonization in such regions.

ACKNOWLEDGEMENTS

APPENDIX: Statistics of the threshold

Within a lake, light statistics might be expressed in terms of relative intensities, $i \in [0,1]$, when the attenuation processes within that water body is independent of the statistical distribution of light entering the lake, I_0. The probability that a randomly selected individual at depth v would be at or below its compensation point $R \in [0,1]$, or equivalently that v is its compensation depth, equals the probability that light intensity $i(v)$ is below the specific threshold for that individual. Assuming that the tolerance R follows a Lognormal law such that $Y = \ln R$ is $Normal(\mu_y, \sigma_y^2)$, the probability of the event "$i(v) \leqslant r$" averaged over all R is:

(A1) $Pr[v_{comp.} \leqslant v] = Pr[i(v) \leqslant r \in R]$

$$= \psi \int_0^1 \phi\{(\ln x + \mu_k v)/\sigma_k v\} \, f_R(x) \, dx$$

where $\phi(.)$ is the Gaussian (Normal) distribution function,

$\ln i(v)$ is distributed truncated Normal $(-\mu_k v, \sigma_k^2 v^2)$ (RØRSLETT, 1984), with correction factor

$$\psi = 1/\phi(\mu_k/\sigma_k) \approx 1$$

and the probability density function f_R is

(A2) $f_R(x) = (2\pi)^{-1/2} (x\sigma_y)^{-1} \exp\{-(\ln x - \mu_y)^2/2\sigma_y^2\}$

(A3) $Pr[v_{comp.} \leqslant v] \approx \psi \, \phi(\theta)$

where $\theta = \theta(v) = (\mu_k + \mu_y/v)/\sigma_k$

The hazard function (cf. PARZEN, 1962) is here defined in the spatial domain as

(A4) $\lambda(v) = \varphi(\theta)/[1-\Phi(\theta)]$

where $\varphi(.)$ is the Normal density function

Thus $\lambda(v)dv$ is the conditional probability of critical light at depth v, given that this has not yet occurred. Equivalently, for a population expanding into deeper waters, $\lambda(v)$ measures the risk of encountering the compensation depth. I consider the hazard function to be the appropriate dose metameter for the dose-response analysis.

Since the water levels fluctuate, the time-averaged hazard function $\lambda(z)$ is obtained by convolution (RØRSLETT, 1984):

(A5) $\lambda(z) = \int_{z}^{+\infty} \lambda(u-z)\, p_v(u)\, du$

where p_v is the probability density function of water level deviations from the median level, and the spatial coordinate z is oriented negative downwards from the median level datum.

This represents a mapping from a Lagrangian, or moving coordinate system, into an Eulerian, or fixed, coordinate system.

LITERATURE

FINNEY, D.J. 1971: <u>Probit analysis</u>. 3rd. ed., Cambridge University
        Press, 333 pp.

GEHAN, E.A. & SIDDIQUI, M.M. 1973: Simple regression methods for
        survival time studies. <u>J. Am. Stat. Ass</u>. 68: 848-856.

GREEN, N.W. 1981: Underwater stereophotography applied in ecological
        monitoring. Report 1: Methods and preliminary evaluation.
        <u>Norwegian Institute for Water Research</u>, Oslo, Report OF-80613.

HUTCHINSON, G.E. 1957: <u>A Treatise on Limnology</u>. 1:1. <u>Geography and
        Physics of Lakes</u>. Wiley, New York, 540 pp.

HUTCHINSON, G.E. 1975: <u>A Treatise on Limnology</u>. 3. <u>Limnological
        Botany</u>. Wiley, New York, 660 pp.

JENKINS, G.M. & WATTS, D.G. 1968: <u>Spectral analysis and its
        applications</u>. Holden-Day, San Francisco, 525 pp.

MORTON, R. 1981: Generalized Spearman estimators of relative dose.
        <u>Biometrics</u> 37: 223-234.

PARZEN, E. 1962: <u>Stochastic processes</u>. Holden-Day, San Francisco,
        324 pp.

RAI, K. & VAN RYZIN, J. 1981: A generalized multihit dose-response
        model for low-dose extrapolation. <u>Biometrics</u> 37: 341-352.

RØRSLETT, B. 1983: Tyrifjord og Steinsfjord. Undersøkelse av vann-
        vegetasjon 1977-1982. (Lake Tyrifjord and Steinsfjord. Investi-
        gations of the aquatic vegetation, 1977-1982. In Norwegian).
        <u>Norwegian Institute for Water Research</u>, Oslo, Report 0-7800604.

RØRSLETT, B. 1984: Environmental factors and aquatic macrophyte
        response in regulated lakes - a statistical approach.
        <u>Aquat. Bot</u>. 19: 199-220.

RØRSLETT, B. 1985: Regulation impact on submerged macrophytes in the
        oligotrophic lakes of Setesdal, South Norway.
        <u>Verh. Internat. Verein. Limnol</u>. 22 (in press)

RØRSLETT, B., GREEN, N.W. & KVALVÅGNÆS, K. 1978: Stereophotography
    as a tool in aquatic biology. Aquat. Bot. 4:73-81.

SAND-JENSEN, K. 1978: Metabolic adaption and vertical zonation of
    Littorella uniflora (L.)Aschers. and Isoetes lacustris L.
    Aquat. Bot. 4:1-10.

SAND-JENSEN, K. & SØNDERGAARD, M. 1978: Growth and production of
    isoetids in oligotrophic Lake Kalgaard, Denmark.
    Verh. Internat. Verein. Limnol. 20: 659-666.

SPENCE, D.H.N. 1976: Light and plant response in fresh water. In
    Evans,G.C.,Bainbridge,R. & Rackham,O. (Eds.): Light as an
    ecological factor, Vol.II, pp. 93-133. 16th Symposium of the
    Brithish Ecological Society, Blackwells, Oxford.

SPENCE, D.H.N. 1982: The zonation of plants in freshwater lakes.
    Adv. Ecol. Res. 12: 37-125.

STANLEY, R.A., SHACKELFORD, E., WADE, D. & WARREN, C. 1976: Effects
    of season and water depth on Eurasian watermilfoil.
    J. Aquat. Pl. Manag. 14: 32-36.

Regulation impact on submerged macrophytes in the oligotrophic lakes
of Setesdal, South Norway <1>

Bjørn Rørslett

Norwegian Institute for Water Research
P.O.B. 333 Blindern, N-0314 Oslo 3, Norway

INTRODUCTION

Some sixty percent of Norway's hydro-electric power potential has been developed so far (STATISTISK SENTRALBYRÅ 1983:12). On an area basis, lake regulations influence a major part of Scandinavian lakes. The regulation height of Norwegian reservoirs is commonly less than 10m. An estimated 23% is regulated less than 5m and some 22% is regulated 5-9.9m (STATISTISK SENTRALBYRÅ 1983:27).

There is a truly remarkable paucity of data on submerged macrophytes in regulated Scandinavian lakes. Based on qualitative field data only, BRAARUD (1928) reported negligible regulation impact on Isoetes lacustris-dominated communities in the Norwegian lake Hurdalssjø (mean annual water level range 3.6m, total range 5.3m). QUENNERSTEDT (1958) related changes in the vertical distribution of e.g. Isoetes lacustris to the annual water level amplitude in North Swedish lakes. The lake Gardiken, then unregulated, but with a wide natural water level range of some 4m annually (5.7m annual maximum) harboured some Isoetes, allegedly with reduced performance and restricted vertical extension. NILSSON (1981) investigated the dynamics of the littoral species in the subsequently regulated Gardiken (a substantial 20m nominal regulation height), and found no traces of the former submerged communities. Submergents survived, however, in the upstream located lake Övra Björkvattnet with a 5.9m nominal regulation height.

According to QUENNERSTEDT (1958), increasing extent of regulation would eventually decrease the vertical distribution of isoetid species. The isoetid communities are the prevailing benthic primary produceres in oligotrophic Scandinavian lakes (LOHAMMAR 1965, SAND-JENSEN 1978). Thus, any changes in isoetid performance due to regulation impact might have negative ecological implications. Regional investigations, however, still are lacking.

To this end, the Otra watercourse in the valley of Setesdal (South Norway) offers a series of regulated lakes with closely similar hydro-chemistry. The approved water level schedules substantially differ, however, thus providing an opportunity to relate vegetational response to the extent of regulation. The intermediate- to high-altitude lakes are storage reservoirs with substantial wintertime draw-down, whereas the low-altitude lakes are operated as damping reservoirs with short-time fluctuations of water level. Regulations for hydro-electric power production date back to the 1950's or even earlier. Thus, any post-regulation transients can be ruled out.

STUDY AREA

The location of the lakes is indicated on Fig.1, and some pertinent data on the water level ranges are given in Tab.1. The lakes are mostly situated on igneous bedrock. The catchment areas are dominated by impediments and conifer forests, with birch replacing spruce and pine at altitudes above some 700 m. The Setesdal valley is sparsely populated and pollutional impact is negligible.

MATERIAL AND METHODS

Hydrochemical investigations were carried out by the Norwegian Institute for Water Research (NIVA, Oslo) from the 1970's onwards. Water analysis followed Norwegian Standard (automatic and manual methods).

Subsurface photosynthetic available radiation (PAR, 350-700 nm) was measured with a Li-Cor LI-1985 Quantum meter and sensor LI-192S (Lambda Instruments, Inc.) intermittently during the summer months. Vertical attenuation coeffients k_{PAR} were estimated by a non-linear least squares technique.

Water level data from the studied lakes were obtained from official gauges monitored by the Norwegian Water Resources and Electricity Board (NVE, Oslo). Daily measurements of water levels were used whenever available. Statistics for water levels were computed for the years 1945 to 1982, and included annual means, maximal annual ranges, total ranges, and cumulative probability distributions using 0.1m vertical resolution. The water level medians could then be computed directly from the cumulative distributions. Spectral analysis of the water level time series was performed with a Fast Fourier Transform (FFT) algorithm, adopted from JENKINS & WATTS (1968). Ice-scour stress in the littoral zone was estimated by convolution with a stress "box" function as outlined by RØRSLETT (1984), using the estimated probability density function of water levels for the ice-covered periods of each lake.

Submerged vegetation was sampled mainly in 1976 by means of underwater stereophotography (RØRSLETT et al. 1978), with quadrat size $0.25m^2$. Coverage of species was determined with a nested grid method (RØRSLETT 1983), with statistical relative accuracy within $\pm$ 20% for cover exceeding 0.1 %, and within $\pm$ 30 % for very low cover in the 0.001 - 0.1 % range. A total of some 800 photographic samples was obtained from 12 sites during the years 1976-83. Photographic analysis included all vegetation states, encompassing moribund and dead plants as well.

However, only data on active growth states were subjected to further analysis.

Observed instantaneous depth of each sample was mapped into relative elevations (z) with datum at median water level, according to RØRSLETT (1984). Vertical cover distribution C(z) was estimated by convolution of raw data c_{obs} (z) with a Hanning weight function (JENKINS & WATTS 1968), in order to reduce the inherently large statistical variance. Spanning several orders of magnitude, cover C(z) preferably should be expressed on a logarithmic scale. The dB-scale is appropriate when proportional changes in the cover-elevation function are of interest.
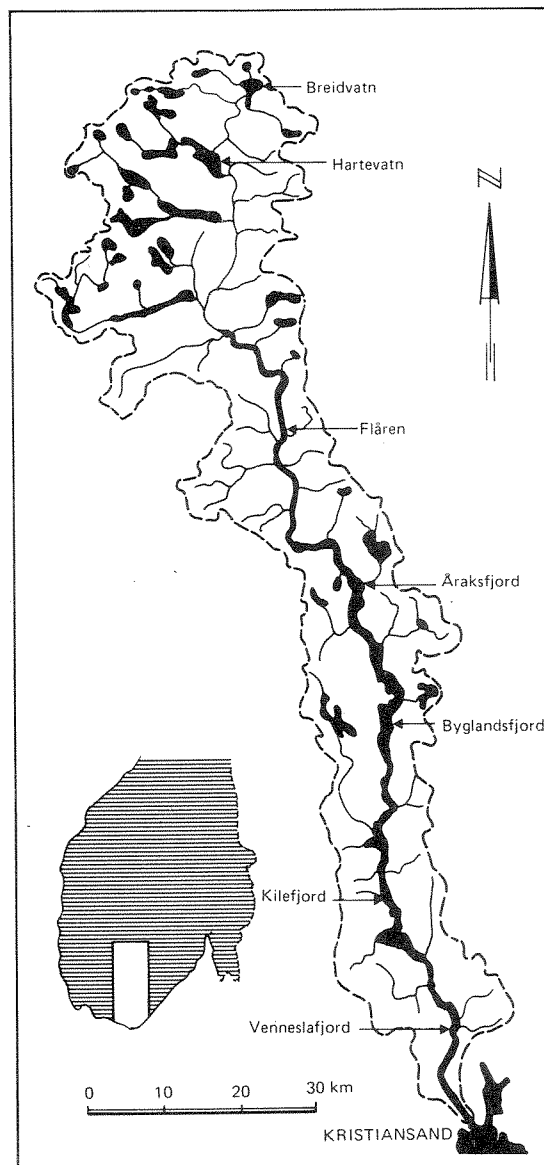

Fig. 1. Location of the Setesdal lakes (South Norway).

RESULTS AND DISCUSSION

Hydrochemistry

Hydrochemical means for 1972-81 are compiled in Tab.2. The waters of the River Otra and its lakes are ultra-oligotrophic. Mean conductivity (k_{20}) ranged from 0.9 to 1.4 mS m^{-1}. The high-altitude lakes Breidvatn and Hartevatn had pH 6.0-6.6, whereas the lower-altitude lakes were somewhat more acidic (pH 5.2-6.0) mainly due to acid precipitation impact. The waters were poor in bicarbonate (40 to 80 mEq HCO_3 m^{-3}). Plant nutrients were low, thus total phosphorus ranged from <2 to 7 mg P m^{-3} and total nitrogen was below 200 mg N m^{-3}.

Optics

The lakes were highly transparent with Secchi-disc readings of 10-23m during the summer season. Spring values were mostly less than 10m due to a rising water level and snow-melt runoff. Mean vertical PAR attenuation coefficients reflected the high Secchi-disc measurements, and ranged from 0.29 in Breidvatn to 0.46 in Hartevatn (k_{PAR} ln-units m^{-1}).

Water level fluctuations

The estimated cumulative probability density functions (cdf's) of water levels are shown on Fig.2. In order to compare the lakes, the distributions are scaled with abscissa as $(z-z_{min})/(z_{max}-z_{min})$.

The cdf's for typical storage reservoirs (the lakes Breidvatn, Hartevatn, Åraksfjord, and Byglandsfjord) were concave upwards and of fairly similar shape, indicating that the low water levels had a rather uniform probability distribution. The lake Kilefjord, operated on a short-time regulation basis, had a rapidly raising cdf close to the median water level.

The mean annual ranges of water level were lower than the nominal regulation heights in the lakes Byglandsfjord, Åraksfjord, and Hartevatn. The lakes Kilefjord and Breidvatn, however, had annual means exceeding the licensed ranges by some 0.5m. The maximal annual range of water levels equalled or exceeded the nominal regulation heights in all lakes. Spectral analysis demonstrated significant periodic variance components, with some 80-90 % of total variance associated to frequencies less than 4 yr^{-1}. The short-time regulated Kilefjord had significant variance components up to 12 yr^{-1}.

The lakes Breidvatn, Hartevatn, Åraksfjord and Byglandsfjord were characterized by draw-down during late autumn and winter, whereas the lake Kilefjord had a high and even water level during wintertime. Ice covers the higher-altitude lakes until mid June, while the lower-altitude lakes are ice-free in April-May. The ice breaks on the lakes Breidvatn, Hartevatn and Byglandsfjord after the rapid spring-time rise of water level.

Ice-scour stress

Estimated vertical scour stress distributions were computed for all lakes with available hydrological data. Examples of stress distributions for the lakes Kilefjord, Byglandsfjord, Hartevatn, and Breidvatn, are shown on Fig.3. Evidently, scour stress differed between these lakes.

Kilefjord featured a sharply peaked stress maximum centered on $z=-0.3m$, reflecting the prevailing high wintertime water levels. Scour stress in Byglandsfjord (and Åraksfjord) peaked at $z=+0.1m$ and was negligible above the $+0.4m$ level. At lower z-levels, estimated scour stress declined exponentially and was virtually zero below $z=-4.5m$. This scour pattern reflects the variable extent of winter draw-down in these lakes.

The storage reservoirs Hartevatn and Breidvatn displayed a two-peaked scour stress pattern (cf. Fig.3), corresponding to the high water levels at freeze-up and the prevailing low draw-down levels. Scour stress at intermediate z-level was much lower, due to the rapid filling-up and draw-down of these lakes. Closely similar vertical patterns are also found in other Norwegian storage reservoirs (Rørslett unpubl.).

Table 1.   Characteristic hydrological data of the Setesdal lakes.
           Annual means computed for the years 1945-1982. The
           water level ranges for Venneslafjord and Flåren are estimates
           based on vegetation physiognomy and zonation (no official
           water gauges present in these two lakes).

Lake	Altitude m	Area km^2	Lake type *	Regulation height ** m	Water level variation, m Annual mean	max.	Total 1945-1982
Venneslafjord	38	1.7	UR	-	1.0		>1.0
Kilefjord	167	5.5	DR	1.5	2.0	2.9	3.2
Byglandsfjord	202	30.7	ST	5.0	3.6	4.9	5.9
Åraksfjord	203	11.2	ST	5.0	3.5	4.9	5.0
Flåren	274	1.4	WB	-	1.5		>1.5
Hartevatn	757	6.0	ST	7.0	6.4	7.3	7.9
Breidvatn	897	3.1	ST	2.5	3.0	3.5	3.5

*)   Reservoir types: UR= nominally unregulated   DR = damping reservoir
                       ST= storage reservoir   WB = weir basin

**) Nominal regulation height as licensed by Norwegian authorities

Table 2.   Optical and hydrochemical data from the Setesdal lakes.
           Mean values and characteristic ranges 1972-1983, compiled
           from data by Norwegian Institute for Water Research.

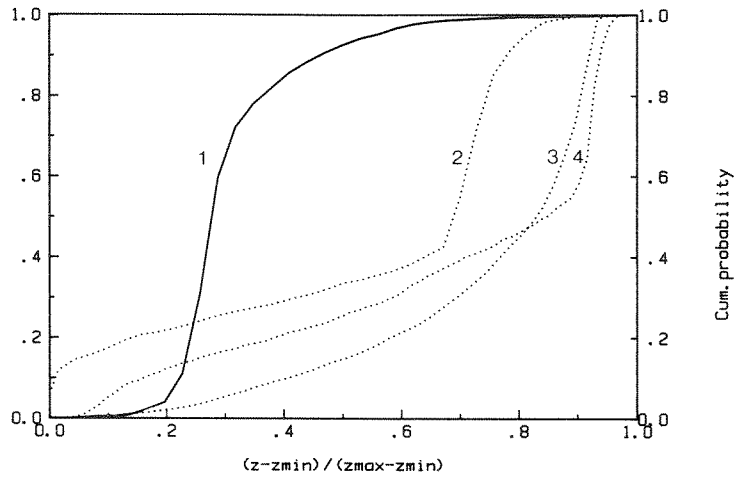| Lake	Vertical attenuat. k_{PAR} m^{-1}	Secchi disc transp. m	pH range	Conduct. $mS\ m^{-1}$	HCO_3 $meq\ m^{-3}$	Tot.P $mg\ P\ m^{-3}$	Tot.N $mg\ N\ m^{-3}$
Venneslafjord	0.36	8-10	5.2-5.8	1.1-2.2	80	6	180
Kilefjord	0.35	9-12	5.2-5.8	1.1-1.7	45	7	190
Byglandsfjord	0.34	9-21	5.8-6.0	1.0-1.2	40	2	130
Åraksfjord	0.32	8-23	5.8-6.1	1.0-1.1	40	<2	140
Flåren	0.60	>4	5.7-6.3	1.1-2.8	50	5	150
Hartevatn	0.46	7-13	6.0-6.4	0.9-1.3	70	4	120
Breidvatn	0.29	10-18	6.2-6.6	0.9-1.1	70	3	140

Fig. 2. Cumulative probability distribution of water levels. Estimated from daily water gauge data 1945-81.

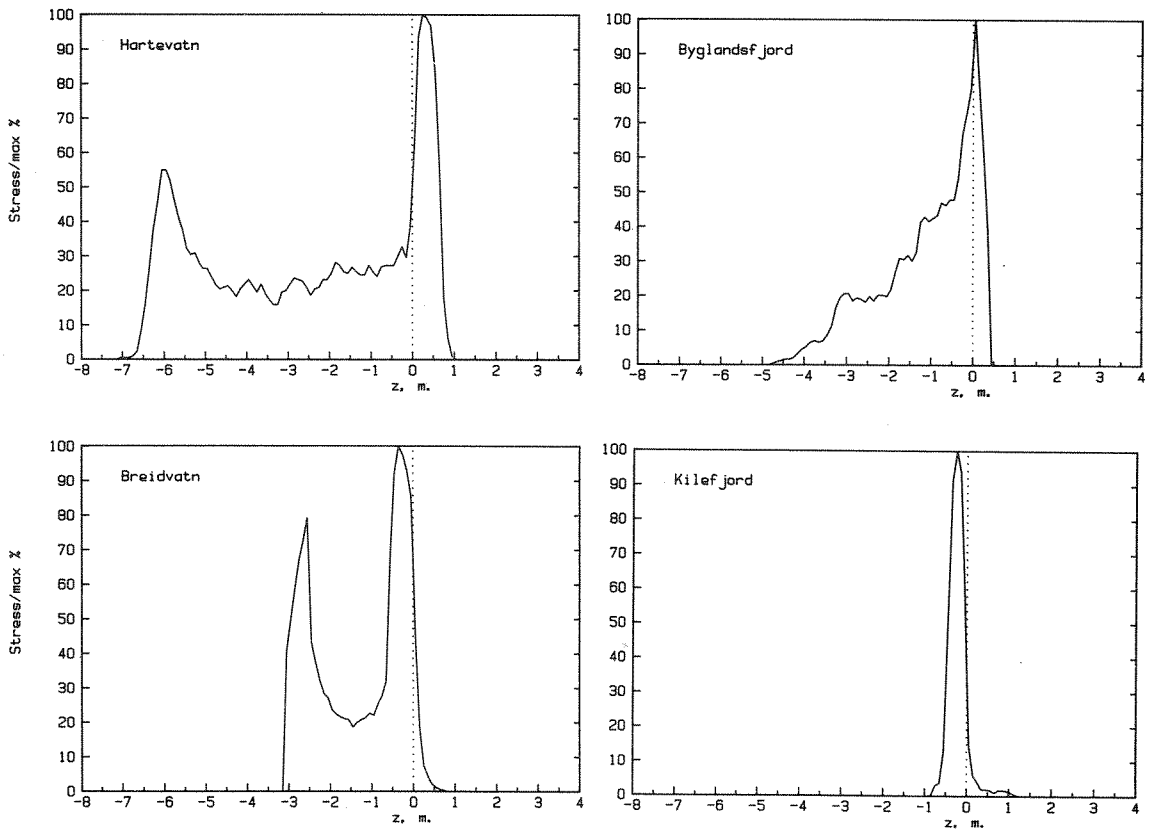1= Kilefjord   2= Breidvatn   3= Byglandsfjord
4= Hartevatn

Fig. 3. Estimated ice-scour stress as function of relative elevation (z-level) for the lakes of Fig.2.

Macrophytes

Helophytes occurred with negligible abundance in five out of the seven
Setesdal lakes. The low-altitude lakes Venneslafjord and Kilefjord
supported mainly <u>Equisetum fluviatile</u>-dominated reedswamp on some
sheltered shores.

The submerged vegetation is summarized in Tab.3. The observed species
were few in number and are typical of Norwegian oligotrophic waters.
The isoetids predominated the species lists. It is well known that
isoetids are unable to use bicarbonate (SAND-JENSEN 1978, SØNDERGAARD
& SAND-JENSEN 1979). The species assemblage of the Setesdal lakes thus
might reflect the low alkalinity of the lake waters.

Excluding helophytes, the number of macrophyte species declined from
16 in the low-altitude lake Venneslafjord to 11 in the high-altitude
lakes Hartevatn and Breidvatn. Using linear regression, the altitude
gradient was statistically significant (P<0.05). COLLINS & LIKENS
(1969) reports a comparable altitude gradient from five New Hampshire
lakes spanning altitudes from 258 to 1542 m, and related the gradient
to temperature effects.

The number of permanently submerged species, i.e. species occurring
below the lowest water level, ranged from 3 to 16 in the Setesdal
lakes. No correlation was found between number of submerged species
and altitude (P>0.2). However, submerged species richness declined
significantly with increasing mean annual range of water level
(P≤0.01).

Table 3.　Submerged macrophytes in the Setesdal lakes, with time-averaged maximum depth limits.　Species denoted with "+" did occur in a lake, but with too low abundance to ascertain its depth limits. Species denoted by "X" occur below median water level, but not permanently submerged.

Species	Lake number						
	1	2	3	4	5	6	7
Vascular plants:							
Callitriche hamulata Kuetz.	+	+	+	+	+	X	+
Eleocharis acicularis (L.)R.&S.	1.9	+	X	X	+	X	+
Isoetes echinospora Dur.	+	+	3.0	+	+	X	1.9
Isoetes lacustris L.	2.8	6.5	4.5	6.0	>4.0		3.7
Juncus bulbosus L.	3.8	5.0	4.5	5.0	>4.0	X	+
Littorella uniflora (L.)Asch.	2.8	1.5					
Lobelia dortmanna L.	2.3	3.5	X	X			
Myriophyllum alterniflorum DC.	2.3	+	+	+	3.0		
Ranunculus reptans L.	X	X	X	X	X	X	X
Sparganium angustifolium Michx.	1.2	5.0	3.2	3.3	2.9	+	2.0
Subularia aquatica L.	X	X	X	X	X	X	X
Utricularia minor L.	8.8	12.0	6.5	13.0	>4.0		
Utricularia ochroleuca R.Hartm.	1.2	4.5					
Utricularia vulgaris L.	3.5	4.5	3.8		>4.0		
Others:							
Fontinalis dalecarlica Br.Eur.		6.0					>5.7
Nitella cf. flexilis (L.)Ag.					18.0	14.5	>5.7
Sphagnum subsecundum Nees							
var. inundatum (Russ.)C.Jens.	8.8	12.0	11.0	13.0	>3.5	16.0	>5.7
Spongilla cf. lacustris (L.)	6.5	7.5	6.8	14.0	>4.0	18.0	>5.7

Lake numbers:　1= Venneslafjord　2= Kilefjord　3= Byglandsfjord
　　　　　　　　4= Åraksfjord　5= Flåren　6= Hartevatn
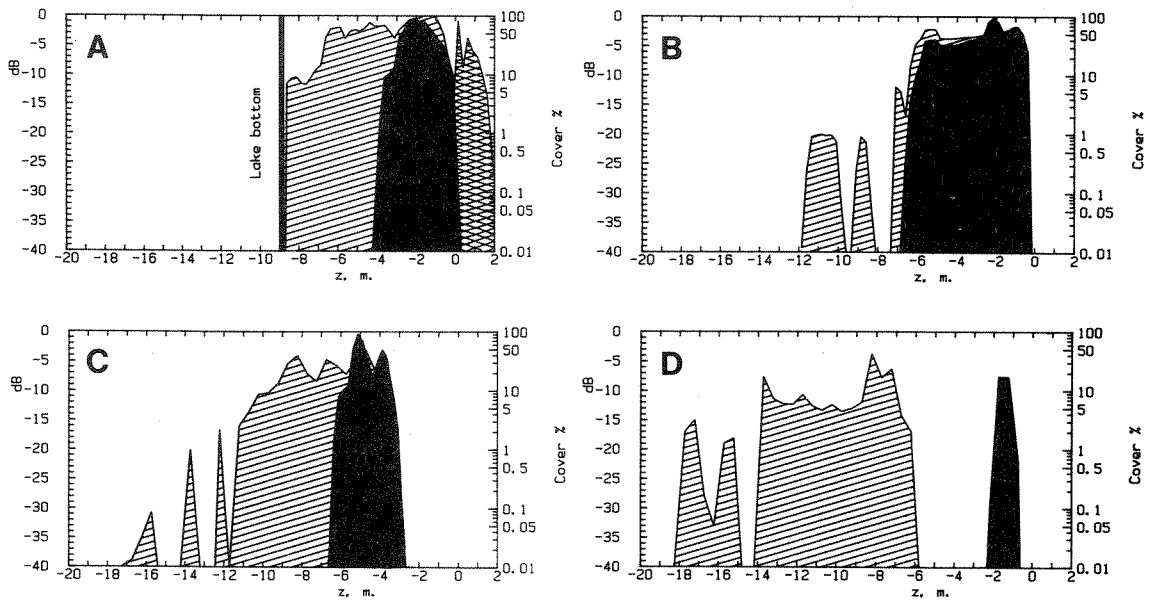　　　　　　　　7= Breidvatn

<u>Fig. 4.</u> Vertical extension of macrophyte communities in some
representative Setesdal lakes. Note vertical scale is
z-level (<u>not</u> depth), with zero at median water level.
Negative z-levels are below, positive above the median
water level.

Estimated cover in dB-scale re 0 dB = 100% cover.
Macrophyte communities grouped into categories:
Helophytes (chequered), isoetids (black), and others
(vertical hatch).

A: Venneslafjord

B: Kilefjord

C: Åraksfjord

D: Hartevatn (note: only annual isoetids in this lake).

Depth extension of the species

The recorded depth extension for all species are given in Tab.3, using time-averaged depth values in order to facilitate between-lake comparison (RØRSLETT 1984).

The species divided into three distinct categories. Typical shallow-water species were e.g. Eleocharis acicularis, Subularia aquatica, Isoetes echinospora, Lobelia dortmanna, and Littorella uniflora. These species penetrated to depths of 2-3m (however, Isoetes echinospora was found at 4.0m in the lake Byglandsfjord). Similar depth ranges for these species are reported in the Scandinavian literature (THUNMARK 1931, BAARDSETH 1942, NYGAARD 1958, SAND-JENSEN 1978).

Another species group occupied intermediate depth ranges, from 4.0 to 6.5m depth. This group included Utricularia vulgaris (to >4.0m), U.ochroleuca (to 4.5m), Sparganium angustifolium and Juncus bulbosus (both to 5.0m), and Isoetes lacustris (to 6.5m).

The true deep-water species group comprised the vascular species Utricularia minor (to 13.0m), and the cryptogams Sphagnum subsecundum var. inundatum (to 16.0m) and Nitella cf. flexilis (to 18.0m). The freshwater sponge Spongilla cf. lacustris (to at least 17.0m) could be included as well. The deep-water occurrences of bryophytes and stone-worts are well documented earlier (cf. HUTCHINSON 1975). More interesting, however, is the deep-water penetration of U.minor. HUTCHINSON (1975:409) doubts the ability of freshwater angiosperms to grow at depths exceeding some 9m, and similar views are put forward by other authors, e.g. SCULTHORPE (1967) and WETZEL (1975). The observations of U.minor and Elodea canadensis (to 12.0m in Lake George, SHELDON & BOYLEN 1977; also at 14.5m in the Norwegian lake Randsfjord, Rørslett unpubl.) clearly indicate that freshwater vascular plants are not confined to the upper 9-10m depth range (also see SPENCE 1982:80). Recently, SINGER et al. (1983) reported the North American Utricularia geminiscapa to a new 18.0m depth record, thus confirming the widespread deep-water occurrence of Utricularia species.

Vertical distribution of submerged communities

In all lakes, community coverage peaked several meters below the median water level (Fig.4). Peak coverage often occurred on subsurface terraces, e.g. in the lakes Venneslafjord, Kilefjord, Byglandsfjord, and Breidvatn. A littoral shelf was missing at the studied sites of Åraksfjord, Flåren, and Hartevatn.

The vertical distribution and zonation of the submerged communities followed a closely similar pattern in all lakes (cf. Fig.4). Excluding helophytes, three predominating community types could be discerned, viz. a shallow-water isoetid community with mainly annual species (Eleocharis acicularis, Subularia aquatica, Ranunculus reptans, and Isoetes echinospora), an intermediate-water type with mainly Isoetes lacustris, and the mainly non-vascular deepwater community with Nitella, Sphagnum and Spongilla. The vertical ranges of these community types, however, did overlap to a significant extent, thus the cover-elevation function C(z) of the integrated community was rather smooth and did not show the waxing and waning of the species involved (cf. Fig.4). Community patchiness increased towards deeper waters and induced heavy rippling of the C(z)-curve in this region. The deep-water patchiness evidently is an intrinsic feature of such communities, thus RØRSLETT (1983) found similar ripple patterns caused by vegetation patchiness in the Norwegian lake Tyrifjord with a photographic mean sampling density of some 400 samples per vertical meter.

Impact from an increasing extent of regulation might be inferred from Fig.4. The spatial overlap within the community types was large at lake Venneslafjord with an annual water level range less than 1m, and nil at Hartevatn with its 6.4m mean annual fluctuation range. Spatial separation between isoetids and helophytes was evident in Kilefjord (2m mean annual range of water level) and amounted to some 1.5m at exposed sites. However, this lake had the same species array as Venneslafjord, and supported helophytes at sheltered sites. The upstream lakes Byglandsfjord and Åraksfjord with annual water levels up to 5.9m (mean 3.5m) harboured an impoverished submerged flora, and the vegetation-free littoral enlarged to more than 3 vertical meters. Perennial isoetids, mainly Isoetes lacustris, were prevailing in these lakes, however. Hartevatn with a maximum water level range of 7.9m had only annual amphibious isoetids present in a narrow band centered around the -2m z-level, and featured an otherwise barren littoral above the -6m level. Although found in the upstreams located Breidvatn with a 3.5m maximum water level range, Isoetes lacustris was certainly missing in lake Hartevatn.
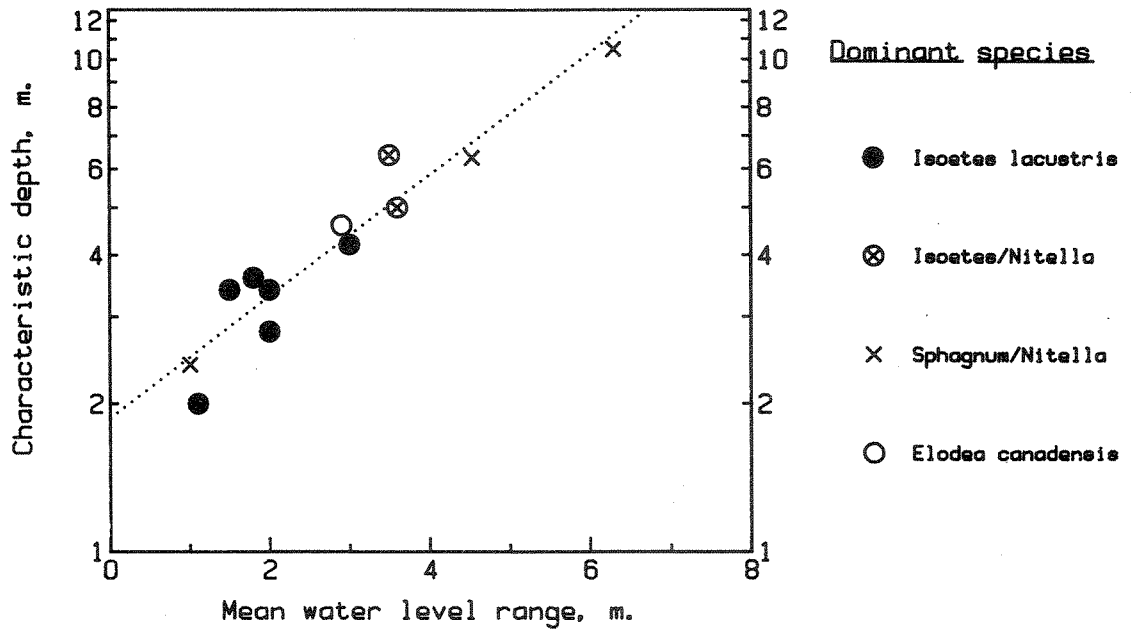
Fig. 5. Characteristic depth (biomass-weighted, time-averaged of
the submerged communities in the Setesdal lakes, against
the mean annual range of water level fluctuations.
Additional data from RØRSLETT (1984) included.

The characteristic (biomass-weighted) time-averaged depth D_c for the
total submerged community was highly correlated (P<0.01) to the mean
annual water level range (cf. Fig.5). Thus, increasing extent of
regulation evidently shifts macrophyte peak performance into deeper
waters. The regression equation was

$$\log D_c = 0.27 + 0.12*(\text{Mean annual water level range})$$

The vertical displacement correlated significantly with extent of ice-
scour (P<0.001). QUENNERSTEDT (1958) related the disappearance of e.g.
Isoetes lacustris in Swedish regulated lakes to the increased
amplitude of annual water levels. According to Quennerstedt, the
vertical extent of the **Isoetes** zone would decrease concurrently. This
hypothesis was not supported by the Setesdal data. Linear regression
of **Isoetes** zone extent against mean annual water level range was not
significant (P>0.3). This indicates that the environmental factors
affecting the upper and lower niche limits, and hence the extent of
the vertical vegetated zone, are statistically uncorrelated.

COLLINS & LIKENS (1969) related within-lake depth gradients of macrophytes to the thermocline position. Thermocline depths in the Setesdal lakes ranged from 10 to 25m (except for the shallow lakes Venneslafjord and Flåren), thus temperature is unlikely to influence the isoetid communities, which ceased at time-averaged depths less than 7m. RØRSLETT (1983) found strong evidence of light controlling the downward limits of macrophytes in the oligotrophic Norwegian lake Tyrifjord, operating through the vertical probability distribution of species-specific irradiance thresholds. Using a 6% relative threshold, the performance of <u>Isoetes lacustris</u> in the Setesdal lakes inversely correlated to estimated threshold probabilities at different z-levels (P<0.001). RØRSLETT (1984) demonstrated that regulation tended to shift light threshold levels into shallower waters. Thus the potential vertical niche of e.g. <u>Isoetes lacustris</u> could be restrained towards deeper waters due to regulation impact on subsurface light climate. Eventually, its actual niche space would vanish whenever ice-scour stress limited the upwards extension of <u>I.lacustris</u>.

ACKNOWLEDGEMENTS

LITERATURE

BAARDSETH, E. 1942: A study of the vegetation of Steinsfjord,
      Ringerike. Nytt Mag.NatVidensk. 83: 9-47.

BRAARUD, T. 1928: Den høiere vegetasjon i Hurdalssjøen.
      Nyt Mag. NatVidensk. 67: 1-53.

COLLINS, L.W. & LIKENS, G.E. 1969: The effects of altitude on the
      distribution of aquatic plants in some lakes of New Hampshire,
      U.S.A. Verh. Internat. Verein. Limnol. 17:154-172.

JENKINS, G.M. & WATTS, D.G. 1968: Spectral analysis and its
      applications. Holden-Day, San Franscisco, 525 pp.

LOHAMMAR, G. 1965: The vegetation of Swedish lakes.
      Acta Phytogeogr. Suec. 50: 28-48.

NILSSON, C. 1981: Dynamics of the shore vegetation of a North Swedish
      hydro-electric reservoir during a 5-year period.
      Acta Phytogeogr. Suec. 69: 1-94.

NYGAARD, G. 1958: On the productivity of the bottom vegetation in
      Lake Grane Langsø. Verh. Internat. Verein. Limnol. 13: 144-155.

QUENNERSTEDT, N. 1958: Effects of water level fluctuations on lake
      vegetation. Verh. Internat. Verein. Limnol. 13: 901-906.

RØRSLETT, B. 1983: Tyrifjord og Steinsfjord. Undersøkelse av vann-
      vegetasjon 1977-82. Norwegian Institute for Water Research,
      Report O-7800604 (In Norwegian).

RØRSLETT, B. 1984: Environmental factors and aquatic macrophyte
      response in regulated lakes - a statistical approach.
      Aquat. Bot. 19: 199-220.

RØRSLETT, B., GREEN, N.W. & KVALVÅGNÆS, K. 1978: Stereophotography as
      a tool in aquatic biology. Aquat. Bot. 4: 73-81.

SAND-JENSEN, K. 1978: Metabolic adaption and vertical zonation of
      Littorella uniflora (L.)Aschers. and Isoetes lacustris L.
      Aquat. Bot. 4: 1-10.

SCULTHORPE, C.D. 1967: The biology of aquatic vascular plants.
    Arnold, London, 610 pp.

SHELDON, R.B. & BOYLEN, C.W. 1977: Maximum depths inhabited by aquatic
    vascular plants. Amer. Midl. Nat. 97: 248-254.

SINGER, R., ROBERTS, D.A. & BOYLEN, C.W. 1983: The macrophytic com-
    munity of an acidic lake in Adironack (New York, U.S.A.): a new
    depth record for aquatic angiosperms.
    Aquat. Bot. 16: 49-58.

SØNDERGAARD, M. & SAND-JENSEN, K. 1979: Carbon uptake by leaves and
    roots of Littorella uniflora (L.)Aschers. Aquat. Bot. 6: 1- 12.

SPENCE, D.H.N. 1982: The zonation of plants in freshwater lakes.
    Adv. Ecol. Res. 12: 37-125.

STATISTISK SENTRALBYRÅ 1983: Naturressurser 1982.
    Central Bureau of Statistics of Norway, Report 83/1, 62 pp.

THUNMARK, S. 1931: Die See Fiolen und seine Vegetation.
    Acta Phytogeogr. Suec. 2: 1-198.

WETZEL, R.G. 1975: Limnology. W.B. Saunders, Philiadelphia, 743 pp.